NASA Technical Paper 1388
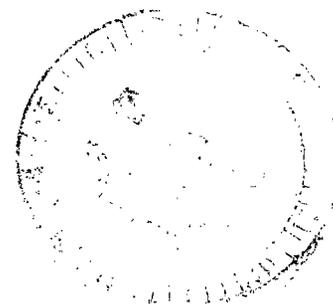
Generation of Linear Dynamic Models
From a Digital Nonlinear Simulation

Carl J. Daniele and Susan M. Krosel

FEBRUARY 1979

NASA

NASA Technical Paper 1388

Generation of Linear Dynamic Models From a Digital Nonlinear Simulation

Carl J. Daniele and Susan M. Krosel
Lewis Research Center
Cleveland, Ohio

CONTENTS

SUMMARY

Presented in this report are the results and methodology used to derive linear models from a nonlinear simulation. It is shown that bias errors in partial derivative calculations using the method of finite differences can cause large enough errors in matrix elements such that eigenvalues of the system can be changed. These errors can be reduced and in some cases eliminated through positive and negative perturbations about the operating point. Linear models developed in this manner can show the same eigenvalues for different finite-difference perturbations within the linear range about the operating point.

It is also shown in this report that positive and negative perturbations in the system inputs can cause the linear model to represent better the nonlinear simulation in both directions about an operating point than when only a single perturbation is used.

As an illustration of these positive and negative perturbation techniques, linear models of the F100 engine were derived from the nonlinear engine simulation. Comparisons of step-response transients run on a nonlinear simulation with those generated using the linear models were very good. It is also shown that, because of the small perturbations required for transient comparisons, great care must be used to insure that there is as little startup transient in the nonlinear simulation as possible. A large startup transient can completely overshadow the effects of a small input.

Finally, techniques to obtain reduced-order linear models from full-state linear models were investigated. The modal- and normal-reduction techniques were applied to the full-state linear models of the F100 engine. Results from transients run on the full-state and reduced-order models compared quite well.

INTRODUCTION

In recent years much work has been done on the application of multivariable (optimal) control theory to the design of controls for many applications; specifically, for aircraft propulsion systems. Emphasis on this type of work has resulted from a desire to obtain improved engine performance over a wider operating envelope. This desire has necessitated the development of increasingly complex engines having more control variables and requiring more engine measurements. A great deal of multivariable control work has been done on turbofan engines. For example, the Pratt & Whitney F100 turbofan engine has variable fan and compressor geometry, engine bleeds, gas-generator

fuel flow, and exhaust-nozzle area. Experience gained from this engine can be used to develop multivariable controls for even more complex variable-cycle engines (VCE). In addition to the controls already mentioned, VCE may have variable turbine geometry, duct-burner fuel flow, and a separate duct nozzle. The proper control of these engines will require the measurement of even more engine parameters.

Work currently done using multivariable (optimal) control theory is given in references 1 to 4. In reference 1 linear quadratic regulator (LQR) theory was used to derive optimal control of the F100 engine. The controls developed in reference 1 were evaluated on a real-time, hybrid simulation of the F100 in reference 2. In reference 3 controls were designed for the F100 engine using output feedback regulator (OFR) theory. Minimum-time acceleration control histories are derived for the F100 engine using nonlinear programming in reference 4.

All the optimal control design techniques described in these references require linear engine models, since no body of optimal control theory has been developed for nonlinear systems. Thus, a good linear representation of the engine system must be obtained. Since most simulations developed to describe these physical systems are nonlinear, linear models that are valid about an operating point must be derived. Also, because of the nonlinear characteristics of the engine system, more than one linear model is necessary, in general, to describe the nonlinear system. For example, for the F100 engine six linear models are needed to represent the engine over its wide operating range.

A method used to linearize the nonlinear system about an operating point is the "offset derivative" method. This technique makes use of the method of finite differences to approximate partial derivatives about an operating point. For the F100 studies previously described, the linear models were derived in reference 5 from the nonlinear F100 digital simulation described in reference 6.

A problem that arises in using the method of finite differences is that small numerical errors (bias errors) can occur in the partial-derivative approximations. This report describes the derivation of linear models from a nonlinear simulation using positive and negative perturbation techniques so that bias errors are minimized. These perturbation techniques were applied to the F100 nonlinear simulation, and new linear models were derived. These models are different from those derived in reference 5 due to the different perturbation technique and due to many changes and updates having been added to the nonlinear simulation.

Once the linear (full state) models of the system have been determined, it may be possible to reduce the order of the linear models while still retaining the important dynamic characteristics of the system. This is desirable for two reasons: First, a lower order system is easier to handle mathematically; second, controls developed using optimal control techniques (such as LQR) require that all specified states of the system be

used to derive the optimal control. However, some of the states are not measurable and thus cannot be used for control purposes. Also, if all the states of a large-order system were measurable, the control derived would be too complex to implement. Two reduction techniques were investigated - modal reduction (ref. 1) and normal reduction (refs. 7 and 8). Both techniques are applied to the F100 full-state linear models derived in this report. Reduction of the original linear models is described in reference 1.

Once the full-state and reduced-order linear models are generated, they should be evaluated as to how well they approximate the dynamics of the nonlinear system about the operating points for which they were generated. As an example, this evaluation is made for the F100 linear models by comparing transients for the full-state and nonlinear engine models and the full-state and reduced engine models. In doing this evaluation the effects of a nonlinear simulation startup transient on small-perturbation input response is discussed.

ENGINE DESCRIPTION

As an example of the linear-model generation technique, a nonlinear engine simulation is used. This simulation is of the Pratt & Whitney F100-PW-100 (3) engine schematically shown in figure 1. The engine is an axial, mixed-flow, augmented, twin-spool, low-bypass-ratio turbofan. A single inlet is used for both the fan and engine core airflows. Airflow leaving the fan is separated into two streams: one passes through the engine core and the other through the annular fan duct. The three-stage fan is connected by a through-shaft to the two-stage, low-pressure turbine. A 10-stage compressor is connected by a hollow shaft to the two-stage, high-pressure turbine. The fan has variable, trailing-edge, inlet guide vanes. The compressor has a variable-inlet guide vane followed by two variable stator vanes. Engine airflow bleed is extracted at the compressor exit and discharged through the fan duct during starting. Compressor-discharge bleed air is also used to cool the high- and low-pressure turbine blades and to power the augmentor turbopump. The main combustor consists of an annular diffuser and a chamber with 16 full nozzles. The engine core and fan duct streams combine in an augmentor and are discharged through a variable, convergent-divergent nozzle. The augmentor consists of a diffuser section and five concentric manifolds.

ENGINE SIMULATION

Nonlinear Model

The nonlinear digital simulation used in this report is Pratt & Whitney's digital simulation CCD 1103-1.0 (ref. 6). The simulation uses overall performance maps to

describe steady-state component performance. Performance maps are provided for the fan, fan duct, compressor, burner, high-pressure turbine, low-pressure turbine, afterburner, and exhaust nozzle. Dynamic relationships, based on the laws of conservation of mass, energy, and momentum are incorporated in the nonlinear simulation. These include rotor inertial effects, volume gas dynamics, and heat-transfer effects. The dynamic elements are modeled with recursion formulas. The digital simulation includes a simulation of the engine control system. The control simulation supplies fuel flow, exhaust-nozzle area, compressor variable-vane position, compressor bleed, and fan-inlet-guide-vane position inputs to the engine simulation. These control inputs are computed as functions of various engine measurements and the pilot-set power level angle (PLA) command.

Nonlinear State-Space Model

As mentioned earlier, the nonlinear dynamic equations in the simulation include rotor inertial effects, volume gas dynamics, and heat-transfer effects. The physical quantities represented by these equations are rotor speeds, volume pressures, and temperatures. The nonlinear equations are described in nonlinear state-space form; that is, they are of the form

$$\dot{\overline{X}} = \overline{f}\left(\overline{X}, \overline{U}, t\right) \tag{1}$$

and

$$\overline{Y} = \overline{g}\left(\overline{X}, \overline{U}, t\right) \tag{2}$$

(All symbols are defined in appendix A.) The state variables $\overline{X}$ cannot change instantaneously with time. The output variables $\overline{Y}$, which are important engine parameters but not necessarily states, can change instantaneously with time. In the nonlinear engine simulation, there are 16 of these nonlinear state equations. The 16 states corresponding to these state equations are

X_1 fan speed, N_L

X_2 compressor speed, N_H

X_3 compressor-discharge pressure, P_{T3}

X_4 interturbine pressure, $P_{T4.5}$

X_5 augmentor pressure, P_{T7M}

X_6 fan-inside-diameter discharge temperature, $T_{T2.5H}$

X_7 duct temperature, $T_{T2.5C}$

X_8 compressor-discharge temperature, T_{T3}

X_9 burner-exit fast-response temperature, T_{T4HI}

X_{10} burner-exit slow-response temperature, T_{T4LO}

X_{11} burner-exit temperature, T_{T4}

X_{12} fan-turbine-inlet fast-response temperature, $T_{T4.5HI}$

X_{13} fan-turbine-inlet slow-response temperature, $T_{T4.5LO}$

X_{14} fan-turbine-exit temperature, T_{T5}

X_{15} duct-exit temperature, T_{T6C}

X_{16} exhaust-nozzle-inlet temperature, T_{T7M}

The five control variables are

U_1 main-burner fuel flow, WFMB

U_2 exhaust-nozzle-jet area, AN

U_3 fan-inlet-guide-vane position, CIVV

U_4 compressor variable-vane position, RCVV

U_5 compressor bleed-flow fraction, BLC

The afterburner fuel flow was not included in these studies. The output variables are

Y_1 engine net thrust, FNMX

Y_2 total engine airflow, WFAN

Y_3 burner-exit temperature, T_{T4}

Y_4 fan stall margin, SMAF

Y_5 compressor stall margin, SMHC

Y_6 empirical fan-exit $\Delta P/P$ parameter, $DP_{2.5QP}$

Y_7 theoretical fan-exit $\Delta P/P$ parameter, $DP_{2.5SC}$

Linear State-Space Models

To derive optimal controls for the F100 engine, a linear engine model is required since no body of optimal control theory has been developed for nonlinear systems. Thus, a linear representation of the engine must be obtained from the nonlinear state and output equations (eqs. (1) and (2)). Also, no single linear model can accurately

represent the engine because of its wide operating range and nonlinear characteristics. Thus, linear models must be derived at various flight conditions and power settings throughout the engine operating envelope. The criteria used to select the various operating points is that a combination of the linear models generated at these operating points must adequately describe the dynamic operation of the engine over the whole envelope. Figure 2 shows a typical engine operating envelope and the flight conditions chosen within the envelope to describe engine operation. Table I gives the reasons for choosing these flight conditions. (Table I and fig. 2 are also found in ref. 9.)

Nonlinear equations (1) and (2) can be linearized to yield the following linear state-space equations

$$\dot{\overline{X}} = \overline{A}\,\overline{X} + \overline{B}\,\overline{U} \tag{3}$$

$$\overline{Y} = \overline{C}\,\overline{X} + \overline{D}\,\overline{U} \tag{4}$$

The mathematics used to derive equations (3) and (4) from (1) and (2) are given in appendix B. The matrices $\overline{A}$, $\overline{B}$, $\overline{C}$, and $\overline{D}$ are constant at an operating point, thus the models are linear and time invariant. The linear model is shown in block diagram form in figure 3.

The "offset derivative" method with forced steady-state balance was used to derive the linear models from the nonlinear engine simulation at the selected engine operating points. The method of finite differences was used to obtain approximations of the system partial derivatives at an operating point (ref. 5).

$\overline{A}$ and $\overline{C}$ matrix generation. - The use of finite differences to approximate partial derivatives requires that each state and input variable be perturbed individually, while all others are held constant. The $\overline{A}$ and $\overline{C}$ matrices are generated by perturbing the states. From appendix B

$$A_{ij} = \frac{\partial \dot{X}_i}{\partial X_j} \tag{5}$$

and

$$C_{ij} = \frac{\partial Y_i}{\partial X_j} \tag{6}$$

Next, the linearity of these matrices must be checked. This is done by first generating an $\overline{A}$ matrix with one perturbation size and then a second $\overline{A}$ matrix $\overline{A}'$ with a different perturbation size. If both $\overline{A}$ and $\overline{A}'$ have the same elements, the perturbation

sizes are in the linear range about the operating point. In practice, however, it is difficult to compare all the elements of the matrices, especially if the system is large. Also, because of iteration tolerances in the simulation, the elements could vary from matrix to matrix but still retain valid information of the linearity of the system. A more practical method of checking for linearity is to calculate the matrix eigenvalues:

$$\left. \begin{array}{c} |\overline{A} - \lambda\overline{I}| = 0 \\[2ex] |\overline{A}' - \lambda'\overline{I}| = 0 \end{array} \right\} \tag{7}$$

If λ approximates λ' within the frequency range of interest, both perturbation sizes are within the linear range about the operating point, and both $\overline{A}$ and $\overline{A}'$ are valid. The choice of which perturbation size to use is arbitrary. The smaller perturbation size may cause numerical problems in calculating the partial derivatives, especially if it is not much larger than the iteration tolerance size specified in the simulation. The larger perturbation size insures easier calculations of the partial derivatives, but it may approach the linearity limit about the operating point. Further restrictions on the perturbation size for the states are given in appendix C.

This procedure was performed on the nonlinear F100 simulation. The perturbation sizes picked were +0.5 and +1 percent of the steady-state values of states, based on work done in reference 5. The operating point selected was at sea-level-static idle, which was one of the six operating points selected for control studies in reference 1. This operating point was selected for evaluation because it results in an unchoked nozzle, which can cause computation difficulties. This aggravates the problem of calculating finite-difference partial-derivative approximations at this condition. Thus, if accurate linear models can be obtained at this operating point, no additional problems should be encountered at the other operating points where the nozzle is choked.

Results for the +0.5 and +1.0 percent perturbations at the sea-level-static-idle operating point are given in table II(a). Note that the eigenvalues are significantly different for the two perturbation sizes. This is shown graphically in figure 4(a) for the five lowest eigenvalues. From this, one real eigenvalue and one complex pair were the same for both perturbation sizes. However, the +1 percent perturbation showed two real eigenvalues at -3.97 and -8.15 radians per second, and the +0.5 percent perturbation showed a complex pair. Other perturbation sizes, both larger and smaller, were investigated; however, no repeatability was found for the eigenvalues.

One cause of this problem is that there are small errors (bias) in the finite-difference calculations. The bias errors are discussed in detail in appendix C. In the F100 nonlinear simulation implicit techniques, which require iteration for solution, are used to calculate the partial derivatives. The bias errors occur when implicit techniques

are used, and the iterations required to derive the partial derivatives converge within the specified tolerance but not at zero.

A method for reducing the effect of this bias error was investigated. First, the states were perturbed in the positive direction from the operating point to generate $\overline{A}$ and $\overline{C}$ matrices $\left(\overline{A}_+ \text{ and } \overline{C}_+\right)$. Then, the states were perturbed in the negative direction from the operating point to generate new $\overline{A}$ and $\overline{C}$ matrices $\left(\overline{A}_- \text{ and } \overline{C}_-\right)$. Finally, the $\overline{A}_+$ and $\overline{A}_-$ matrices and the $\overline{C}_+$ and $\overline{C}_-$ matrices were averaged to obtain the $\overline{A}$ and $\overline{C}$ matrices. The rationale for doing this is explained in appendix C.

Eigenvalues from $\overline{A}$ matrices determined in this manner are shown in table II(b) for the ±0.5 and ±1.0 percent perturbations about the sea-level-static, idle operating point. Note that there is still a shift in the eigenvalues. However, there is much more consistency in the low-frequency range because there is no shifting from complex to real eigenvalues or vice versa. The improved accuracy of the averaged $\overline{A}$ matrix is shown graphically for the lower frequency eigenvalues in figure 4(b). From this figure the biggest shift is a movement of a real eigenvalue from -12.2 to -14.1 radians per second for the ±0.1 and ±0.5 percent perturbations, respectively.

From table II(b), the larger errors in the eigenvalue correspondence are at the high end of the frequency spectrum where an eigenvalue shifted from -422 to -268 radians per second. While this is a large shift, it may be disregarded for most applications (especially controls). Uncertainty about the exact nature of a high-frequency eigenvalue is more acceptable than uncertainty in the low-frequency range.

It is interesting to note here that, as explained in appendix C, the iterative nature of the solution of the partial derivatives for an implicit formulation does not guarantee an exact eigenvalue match, since there is no guarantee that the bias errors introduced by the positive and negative perturbations will cancel when the partial derivatives are averaged. If the method of finite differences are used and the partial derivatives are explicitly calculated, the eigenvalue correspondence would be exact. Results from the ±0.5 percent perturbation were used in subsequent analyses.

$\overline{B}$ and $\overline{D}$ matrix generation. - Digital logic built into the nonlinear simulation derives the $\overline{B}$ and $\overline{D}$ matrices from the supplied $\overline{A}$ and $\overline{C}$ matrices by forcing a steady-state match with the nonlinear simulation results. The mathematics for doing this are presented in appendix B. For a specified control perturbation and given $\overline{A}$ and $\overline{C}$ matrices, the $\overline{B}$ and $\overline{D}$ matrices may be calculated by setting the left side of equation (3) to zero. Equations (3) and (4) thus become

$$\overline{X} = -\overline{A}^{-1}\overline{B}\,\overline{U}\Big|_{\dot{\overline{X}}=0} \tag{8}$$

$$\overline{Y} = \overline{D} - \overline{C}\,\overline{A}^{-1}\overline{B}\,\overline{U}\Big|_{\dot{\overline{X}}=0} \tag{9}$$

As long as the perturbations in the control vector are in the linear range about the operating point, the $\overline{B}$ and $\overline{D}$ matrices are valid. A method of checking the linearity of these matrices comes from their definitions. From appendix B

$$B_{ij} = \frac{\partial \dot{X}_i}{\partial U_j} \tag{10}$$

$$D_{ij} = \frac{\partial Y_i}{\partial U_j} \tag{11}$$

In the linear range about the operating point the $\overline{A}$, $\overline{B}$, $\overline{C}$, and $\overline{D}$ matrices are constant. Thus, for two perturbation sizes in the linear range, the ratio of the steady-state or output vectors should be equal to the ratio of the control-input vectors (eqs. (8) and (9)). For the linear models generated in this report, the perturbation sizes for the controls were supplied in the nonlinear simulation. They were +3 percent for the fuel flow and nozzle area, +5$^{\text{o}}$ for the fan-inlet-guide-vane position (CIVV), +1$^{\text{o}}$ for RCVV, and 0.2 percent for the customer-compressor-bleed-flow fraction (BLC). The reasons for the selection of these perturbation sizes are given in reference 5. However, in using these perturbation sizes it was found that slightly different steady-state values were obtained with the nonlinear simulation when perturbing in the positive and negative directions; that is, for equal positive and negative perturbations, the resulting state and output derivations were slightly different. For example, at the sea-level-static-idle operating point, a +3 percent change in fuel flow in the nonlinear simulation caused a change of 67.2 rpm in compressor speed; a -3 percent change gave a -73.4-rpm change in compressor speed. Thus,

$$R_y = \left| \frac{67.2}{73.4} \right| = 0.916 \tag{12}$$

$$R_u = \left| \frac{+3 \text{ percent (WFMB)}}{-3 \text{ percent (WFMB)}} \right| = 1 \tag{13}$$

Since these differences are considered small compared with the actual compressor speed (9198.1 rpm), the 3-percent perturbation is within the linear range about the operating point. To obtain $\overline{B}$ and $\overline{D}$ matrices that are representative at the operating point, control perturbations were made in the positive direction to generate $\overline{B}_+$ and $\overline{D}_+$ and in the negative direction to generate $\overline{B}_-$ and $\overline{D}_-$. As with the $\overline{A}$ and $\overline{C}$ matrices, the $\overline{B}_+$ and $\overline{B}_-$ and the $\overline{D}_+$ and $\overline{D}_-$ matrices were averaged. The resultant linear model exhibited a 70.3-rpm change in compressor speed for a 3-percent change in fuel flow at

the sea-level-static-idle condition. (Note that $(67.2 + 73.4)/2.0 = 70.3$ rpm.)

It should be noted here that the derivation of the $\overline{B}$ and $\overline{D}$ matrices is application dependent. The averaging technique gives a better overall description of the operating point when the inputs are to be perturbed in both positive and negative directions. However, for some applications the best model may be one that retains exact information about the system in only one direction. An example of this would be using the linear models to determine minimum time acceleration controls (ref. 4). However, in all cases, the $\overline{A}$ matrix should be as accurate as possible so that the actual system dynamics are adequately described.

To summarize, the final method used for generating linear models using the positive and negative perturbation technique was as follows:

(1) Matrices $\overline{A}_+$ and $\overline{C}_+$ were generated by a positive perturbation of the states. (For the F100, +0.5 percent of the states was used.)

(2) Matrices $\overline{A}_-$ and $\overline{C}_-$ were generated by a negative perturbation of the states. (For the F100, -0.5 percent of the states was used.)

(3) The matrices were averaged

$$\overline{A} = \frac{\overline{A}_+ + \overline{A}_-}{2} \tag{14}$$

$$\overline{C} = \frac{\overline{C}_+ + \overline{C}_-}{2} \tag{15}$$

(4) Using $\overline{A}$ and $\overline{C}$, matrices $\overline{B}_+$ and $\overline{D}_+$ were calculated by perturbing the controls in the positive direction. (For the F100, +3 percent WFMB and AN, +5° for CIVV, +1° for RCVV, and +0.2 percent for BLC.)

(5) Using $\overline{A}$ and $\overline{C}$, matrices $\overline{B}_-$ and $\overline{D}_-$ were calculated by perturbing the controls in the negative direction. (For the F100, -3 percent WFMB and AN, -5° for CIVV, -1° for RCVV, and -0.2 percent for BLC.)

(6) The matrices were averaged

$$\overline{B} = \frac{\overline{B}_+ + \overline{B}_-}{2} \tag{16}$$

$$\overline{D} = \frac{\overline{D}_+ + \overline{D}_-}{2} \tag{17}$$

With this technique linear models can be derived from a nonlinear simulation. The models generated for the F100 engine are presented in appendix D for the six operating

points defined in reference 1. For each operating point, the $\overline{A}$, $\overline{B}$, $\overline{C}$, and $\overline{D}$ matrices, the corresponding eigenvalues and eigenvectors, and the matrix of mode shapes are given.

Linear-Model Validation

Once the linear models are generated, they should be evaluated as to how well they approximate the dynamics of the nonlinear system about the operating points from which they were generated. This is accomplished by comparing transients run on both the linear and nonlinear simulations. For a given input the linear model should retain the dynamics of the nonlinear model for all the states and outputs, and the steady-state error between the model responses should be small.

This comparison was done for the F100 full-state models. A +3-percent fuel-flow and nozzle-area step transients were run on both the full-state linear and nonlinear simulations. Figures 5 and 6 compare responses of selected states and outputs with the fuel-flow and nozzle-area steps, respectively. These transients were run at the sea-level-static-idle operating point. Responses of the other states and outputs are compared in appendix E. In figures 5 and 6 as well as those presented in appendix E, the zero time point is the time at which the step input is applied. The nonlinear simulation was run for 0.1 second before the step was applied to eliminate any startup transient. The importance of this will be discussed later.

Figure 5(a) shows the response in fan speed to a +3-percent step in fuel flow. The nonlinear simulation results are denoted by dashed lines, while the solid lines denote the linear simulation results. The agreement between these two fan-speed responses is good. The responses exhibit the same dynamic characteristics and have small steady-state differences. The observed steady-state error (7 rpm at 2 sec) in fan speed was attributed to the averaging done to derive the linear model. The steady-state error would have been negligible (due only to convergence tolerances in the nonlinear simulation) if the $\overline{B}$ and $\overline{D}$ matrices had been derived for only a +3-percent perturbation in the inputs. However, the steady-state error would have been much larger than 7 rpm if transients had been compared for a -3-percent perturbation in fuel flow. The compressor-speed response to a +3-percent fuel-flow step is shown in figure 5(b). Here also, the agreement is good, and the steady-state error is small - about 4 rpm at 2 seconds. Figure 5(c) shows the burner-exit total-temperature response to the fuel-flow step. Here the agreement is excellent with the steady-state error of only 0.2 K at 2 seconds. The response of engine net thrust to a fuel-flow step is shown in figure 5(d). Here also, the agreement is very good. Note that at 0.05 second both responses show the same high-frequency dynamics with the nonlinear model undershoot somewhat larger than the linear-model undershoot. The steady-state error is 0.01 kilonewton at 2 seconds.

Figure 6(a) shows the fan-speed response to a +3-percent step in nozzle area for the nonlinear and linear simulations. In general, the responses are similar; however, the percentage of steady-state error (6 rpm) is somewhat larger than the fuel-flow step. Again, this is due to the averaging technique used to generate the $\overline{B}$ matrix. Note that the nonlinear response does not start at zero rpm at zero time. The small error is due to a startup transient in the nonlinear simulation.

A startup transient is the result of a small error in an engine balance at zero time. In steady-state calculations an engine balance is forced by the simulation logic. However, in transient calculations a different calculation path is generally followed through the simulation. Depending on how the tables are read and on how the quantities are calculated, small errors relative to the steady-state solution may result. Since an engine balance is not forced, the error tends to drive the system to a different operating point to achieve an engine balance (even if no input is applied). One method used to null out the startup transient is to run the simulation for a short time and let the engine balance before applying the desired input. This was done on the nonlinear simulation where it was run for 0.1 second before the step in fuel flow or nozzle area was applied. Thus, in all the figures that show a transient run on the nonlinear simulation, the zero-time point is actually at 0.1 second. For the linear model transients the zero-time point is actually at time zero. In figure 6(a) the offset in fan speed at zero time is thus due to the speed drifting slightly lower than steady state. Although the steady-state value is subtracted in an attempt to use zero as a reference point, the actual reference point is not zero. From figure 6(a) the error was 0.5 rpm, which is considered negligible. It should be noted that the same error also occurs in figure 5(a) but the startup transient effect is not apparent because of the large change in fan speed to a fuel-flow input. In the following comparisons an error at zero time due to a startup transient will be called a startup transient offset.

Figure 6(b) shows the compressor-speed response to a step change in nozzle area. The responses agreed well with a steady-state error of 2 rpm at 2 seconds. The response of burner-exit total temperature to a nozzle-area step is shown in figure 6(c). At zero time the startup transient offset is 0.1 K. In general, both responses show the same dynamics with the linear response overshooting slightly higher and earlier than the nonlinear response. The error at 2 seconds is 0.2 K. Again, this error is due to the averaging technique used to derive the $\overline{B}$ matrix. Comparison of thrust responses from the nonlinear and linear simulations for a +3-percent step in fuel flow is shown in figure 6(d). Thrust is an output variable and can change instantaneously. At zero time the nonlinear simulation shows an immediate response to nozzle-area change. This response was not due to a startup transient offset. The linear model essentially starts at zero thrust. However, the linear model does have the potential of responding instantaneously to a step change in an input (eq. (4)). For an output variable, the $\overline{D}$ matrix

represents the rate of change of that variable to an input. Since equation (4) is algebraic, the output variable can respond instantaneously to an input change. Note that the state variables cannot change instantaneously since they are modeled by a differential equation (eq. (3)). Thus, at zero time the $\overline{C}\,\overline{X}$ contribution is zero in equation (4). For a change in nozzle area the $D(1, 2)$ element, which is multiplied by the change in nozzle area, gives the immediate thrust response. However, the $\overline{D}$ matrix elements are formed from a forced, steady-state match using the nonlinear simulation. Since the transient comparisons agree quite well (0.005 kN error), the $D(1, 2)$ element gives the correct sensitivity of the thrust to a nozzle-area change. Also, if the linear model had predicted the immediate thrust response, the whole transient would have been shifted up, since the system is linear, and the error would have been 0.155 kilonewton. Thus, the thrust response observed in the nonlinear simulation at zero time must be attributed to some effect not described in the linear-model approximation. From the figures shown the linear model does approximate the nonlinear system well at the sea-level-static-idle operating point. The same comparisons were made at the other five operating points. Although not presented, results of these comparisons showed that the linear-model approximations were as good as or better than the sea-level-static-idle case.

These comparisons have shown that the nonlinear simulation has a very small startup transient whose effect is considered negligible. Experience has shown, however, that a large startup transient can completely overshadow the effects of a small input. This can be especially troublesome when trying to run transients to compare with linear models. In general, gross transients requiring large inputs are not affected by the startup transient. Since the problem of startup transients in nonlinear simulations is of general interest, it is discussed in appendix F.

Reduced-Order Models

The results and methodology used to derive linear models from a nonlinear simulation have been presented. These are full-state linear models. Depending on the application of these models, it may be desirable to reduce the order of the model. For example, a problem results when trying to use full-state models for designing multivariable controls that require full-state feedback. A full-state model could require a very complex control as well as a large amount of sensors to measure the states. Some of these states, however, may not be measurable. Thus, it is desirable to reduce the order of the model, keeping the states that are measurable and that contain significant dynamic information for control purposes.

In general, all model reduction techniques assume the system can be partitioned into two subsystems — one having fast dynamics (high-frequency eigenvalues) and one

having slow dynamics (low-frequency eigenvalues)

$$\overline{X} = \begin{pmatrix} \overline{X}_S \\ \hline \overline{X}_F \end{pmatrix} \qquad (18)$$

The states having fast dynamics are approximated by their steady-state values by assuming

$$\dot{\overline{X}}_F = 0 \qquad (19)$$

In essence, this says that the high-frequency eigenvalues can be neglected and the dynamics of the whole system can be adequately represented by the low-frequency eigenvalues. If the eigenvalues of the system separate well, a good reduced-order model will result. Usually, a 10 to 1 separation of eigenvalues is acceptable, but in most physical systems the eigenvalues cannot be easily separated, and generally there is coupling between the states resulting in complex pairs of eigenvalues. Also, the identification of states with specific eigenvalues is difficult. However, in general, for a particular application specific states must be included in the reduced-order model. Thus, the states that are retained specifically in the reduced-order model are based on intuition, engine controls experience, and engine protective requirements. The states that are not retained must be reconstructed from the reduced-order model from a linear combination of the retained states and outputs.

Generally, a conflict arises when trying to determine how to reduce the full-state model. If all states are measurable, then the dynamic accuracy of the reduced-order can be assured by using the modal-reduction technique. In this technique the desired eigenvalues are specified, and the full-state model is transformed in such a manner that the states with eigenvalues that are not desired are approximated by their steady-state values.

In most cases, however, all the states are not measurable. Therefore, the model must be reduced so that implementation of a control is possible. Yet the model must retain as much dynamic accuracy as possible. Once the states are specified, the normal-reduction technique is used. The full-state model is permuted and then partitioned into desired and undesired states

$$\overline{X} = \begin{pmatrix} \overline{X}_D \\ \hline \overline{X}_{UD} \end{pmatrix} \qquad (20)$$

Those states that are not retained (undesired) are approximated by

$$\dot{\overline{X}}_{UD} = 0 \qquad\qquad (21)$$

In general, problems can arise in using either method, depending upon the circumstances. If the states to be retained are specified and the modal-reduction technique desired so that dynamic accuracy is retained, the eigenvalue-state relation must be determined. This can be difficult. If the states to be retained are not specified, a problem similar to the one presented in using the modal technique also arises when using the normal-reduction technique. In general, many measurable states are available but not all can be used for control purposes. Also, one subset of states may provide a better control than another. Thus, an eigenvalue-state relation may have to be determined to pick the best subset of states.

The choice of reduction method is not clear when the states to be retained for control purposes are specified. For example, for the F100 engine, the states that must be retained are compressor speed, fan speed, burner pressure, and augmentor pressure (from ref. 1). Thus, a fourth-order, reduced-order model is desired, and the use of both reduction techniques is explored.

Modal reduction. - The modal-reduction technique requires that the eigenvalues of the retained states be specified. If the eigenvalue associated with each state can be identified, the reduced-order model will be dynamically accurate for the states that are retained since the reduced-order model will contain the specified eigenvalues exactly. However, it is difficult in practice to identify the eigenvalue associated with each state.

One method used to determine the eigenvalue-state correspondence is to first form the eigenvectors associated with the system eigenvalues. The equation describing this is

$$\overline{A}\,\overline{e} = \lambda\overline{e}$$

The eigenvector for an eigenvalue in a 16th-order system contains 16 elements; each element gives the weight of the corresponding state on the eigenvector. The eigenvectors can then be converted into mode shapes (magnitude and angle). Then the elements are ratioed to the largest element so that the relative contribution of each state can be determined.

For example, for the sea-level-static-idle operating point the eigenvalues of the $\overline{A}$ matrix are given in table III, and the corresponding mode shapes in table IV. These were taken from appendix D. From the mode shape the state associated with each eigenvalue is determined. For example, if states 1, 2, 3, and 5 are desired, then for state 1 the vectors with the largest contribution of state 1 on each mode-shape magnitude (largest first real element) are selected. From table IV the vectors selected are 9, 14, and 15 (where 14 and 15 are a complex pair). From table III these vectors correspond to a real

eigenvalue at -2.86 radians per second and a complex pair at -0.744±0.20 radian per second. For state 2 the largest contributions of the second element are found in vectors 14 and 15 from table IV. Note that this state does not contribute strongly to any mode shape. For state 3 the vectors 3, 14, and 15 are selected from table IV. (Although vector 3 contains a 1.00 for element 3, vector 14 contains a 0.9.) Note that complex pairs cannot be broken up. For state 5 vector 2 is selected. Table V(a) shows the state eigenvalue correspondence for a modal reduction at this operating point keeping states 1, 2, 3, and 5. Although there are five different eigenvalues shown, a fourth-order system is desired. Coupling causes this difficulty: The complex pair cannot be broken up. Because the complex pair strongly influences three states, it should be chosen. The eigenvalue at -268.16 radians per second is needed for state 5. The choice between the remaining two eigenvalues is arbitrary. Thus, two models are possible, and they are listed in table V(b). The only way to select one of the two models would be to try each and to compare with the full-state model by comparing similar transients.

Normal reduction. - Another reduction method is to permute the states into two groups - those which are to be retained and those which are to be discarded. This is the normal-reduction method of references 7 and 8. The advantage of this method is its simplicity; the disadvantage is that the resulting model will not, in general, retain exact eigenvalues. For the sea-level-static-idle operating point, a normal reduction which retained states 1, 2, 3, and 5 was performed and the resulting eigenvalues were -0.878, -2.66, -142.8, and -245 radians per second. Comparing these eigenvalues with those selected for the modal reduction shows that essentially all three real roots were retained but that the complex roots were approximated by another real root. While it is true that in the normal-reduction technique some dynamic accuracy is lost for the retained states, it is much simpler to use. Thus, as long as the states that must be kept are specified, the normal-reduction method seems to be the better technique to apply.

Fourth-order models were derived using the normal-reduction technique. The reduced-order matrices $\overline{ABR}$, $\overline{BBR}$, $\overline{CBR}$, and $\overline{DBR}$ and eigenvalues are given for each of the six operating points in appendix G.

Reduced-order model validation. - Once the reduced-order models are derived, they must be evaluated as to how well they approximate the dynamics of the full-state model. This is done by comparing transients run on both simulations. For example, 3 percent steps in fuel flow and nozzle area were input to both linear models. Comparisons of responses of selected states and outputs are shown in figures 7 and 8, respectively. The operating point is at sea-level-static idle. (A discussion of transient responses of other states and outputs is given in appendix H.)

Figure 7(a) shows the fan-speed responses to a +3-percent fuel-flow step. The reduced-order model rises somewhat faster than the full-state model. This is due to the absence of high-frequency information in the model reduction. In general, the

16

transients have the same shape, and the error at 2 seconds is 2 rpm. The agreement should be good since fan speed is a retained state. Figure 7(b) shows the compressor-speed responses to a step in fuel flow. Compressor speed is a retained state and, again, agreement is good. The loss of some high-frequency dynamics model is indicated by the faster initial rise of the reduced-order linear model. The error at 2 seconds is 2 rpm. Figure 7(c) shows the compressor-discharge-pressure responses. This is also a retained state in the reduced-order linear model. Here, again, the reduced-order model response rises more quickly, but, in general, the agreement is good. The error at 2 seconds is 0.25 kilopascal (kilonewtons per square meter). Figure 7(d) shows the interturbine-pressure responses. Interturbine pressure is not a retained state, but it can be reconstructed since it is linearly related to the retained states and the inputs. The immediate response at zero time for the reduced-order model results from the reconstruction (the reason for this is discussed in ref. 8). The transients, however, agree well, and the error at 2 seconds is 0.1 kilopascal. Figure 7(e) shows the augmentor-pressure response. This again is a retained state and again the loss of high-frequency information in the linear model is evidenced by the faster rise time. The transients agree quite well, with the error at 2 seconds being 0.1 kilopascal. Figure 7(f) shows the thrust responses. Thrust is an output variable that can change instantaneously. At zero time the immediate response for the reduced-order model is due to the reconstruction process. At 0.1 second the loss of high-frequency information is evident in the difference in rise times between the two responses. After 0.1 second the responses show the same shape, and the error is 0.005 kilonewton at 2 seconds.

The loss of dynamic information is evident in the transient responses of the reduced-order model (fig. 7). If a state is retained, the reduced-order response rises faster than the full state. If it is a reconstructed state variable, there is an immediate response at zero time. Finally, if it is an output variable there is an immediate response at zero time and a faster rise time in the reduced-order response.

Figure 8(a) shows the fan-speed responses to +3 percent in nozzle area. Here, the agreement is excellent with a 0.5-rpm error at 2 seconds. Figure 8(b) shows the compressor-speed responses. Here, also, the agreement is excellent, although the responses do diverge somewhat, with an error of 0.4 rpm at 2 seconds. Figure 8(c) shows the compressor-discharge-pressure responses. Like the fan and compressor speeds, compressor-discharge pressure is a retained state. However, the loss of high-frequency information is much more evident for this state. The full-state model shows a much larger undershoot and a much faster rise time than the reduced-order model response. After 0.1 second the responses agree quite well, and at 2 seconds the error is 0.1 kilopascal. Figure 8(d) shows the interturbine-pressure responses. The immediate response for the reduced-order model at time zero is due to the fact that this is a reconstructed state. The loss of high-frequency information is evident in the

lower undershoot and slower rise time for the reduced-order model response. The error at 2 seconds is 0.2 kilopascal. The augmentor-pressure responses are shown in figure 8(e). This is a retained state, and the agreement between the two models is excellent. Figure 8(f) shows the thrust responses. There is no obvious immediate response at zero time for this output variable, and the agreement is excellent.

The loss of high-frequency information was not as noticeable for the nozzle-area transients as it was for the fuel-flow transients. The better agreement for the nozzle-area step is due to the negligible high-frequency sensitivity of the discarded states to nozzle area. The only state that seemed affected strongly by the reduction is the compressor-discharge pressure. The results probably would have been worse if augmentor pressure had not been retained.

The reduced-order techniques used to generate the models discarded some of both high- and low-frequency states. Thus, both high- and low-frequency information was lost. Errors that show up in the reduced-order models can be attributed to this loss of information, especially when there is strong coupling between the retained and eliminated states.

Although not shown herein, the full-state models and reduced-order models were compared at other operating points for response to transients in fuel flow and nozzle area. In all cases the results were as good as or better than those presented for the sea-level-static-idle operating point. These results indicate that a fourth-order model adequately represents this system.

CONCLUSIONS

This report presents the methods used to derive and validate linear models from a nonlinear digital simulation. To derive a good linear model at an operating point, good partial derivatives must be obtained. When using the finite-difference method to approximate partial derivatives, small errors in the calculations can occur. These errors are bias errors, which must be minimized or eliminated if possible. This can accomplished by perturbing the states in both positive and negative directions about an operating point and averaging the resulting partials. For simulations in which differential equations are solved explicitly, this method results in repeatability in the system eigenvalues for different perturbation sizes about the operating point. For simulations in which the differential equations are solved implicitly, exact repeatability of system eigenvalues for different perturbation sizes is difficult to obtain because of the iterative nature of the solutions. This is demonstrated by deriving linear models of the F100 engine from an implicit, nonlinear simulation of the engine. Comparison of eigenvalues obtained by the averaging technique for different perturbation sizes about an operating point showed better repeatability of low-frequency eigenvalues, than of high-frequency

eigenvalues. For most applications (controls) the low-frequency eigenvalues are of greater interest.

Using the newly calculated $\overline{A}$ and $\overline{C}$ matrices and assuming a forced steady-state match with the nonlinear simulation, the $\overline{B}$ and $\overline{D}$ matrices were calculated. The accuracy of these matrices was checked by showing that linearity holds for different perturbation sizes in the controls in the nonlinear system. For the models in this report the $\overline{B}$ and $\overline{D}$ matrices were calculated by perturbing the inputs in both positive and negative directions about an operating point and averaging the resulting partial derivatives. Thus, for a given perturbation size the linear model predicts the average steady-state value that the nonlinear simulation would arrive at for the same perturbation size in the plus and minus direction about the operating point.

Once the accuracy of the matrices was assured, the ability of the linear models to approximate the nonlinear system at an operating point was investigated. This was done by comparing similar transients run with the nonlinear and linear simulations. The inputs were +3-percent steps in fuel flow and nozzle area. These comparisons showed that the linear models approximated the nonlinear simulation well and thus the method used to derive the linear models was good. The linear models were derived at six operating points.

In comparing transients from the nonlinear and linear simulations, a startup transient was observed in the nonlinear simulation. A startup transient can occur in a nonlinear simulation as a result of a small error in the engine balance at zero time. In steady-state calculations an engine balance is forced. In transient calculations a different calculation path is made through the simulation and, depending on how quantities are calculated, small errors may result. With no other input applied, the errors tend to drive the system to a different operating point to achieve a balance. In the F100 nonlinear simulation this error is considered to be negligible, but experience has shown that a large startup transient can completely overshadow the effects of a small input. In general, gross transients are not affected by startup transients. A method generally used to null out a small startup transient is to let the simulation run for a short time, with no input applied, to achieve an engine balance.

The models derived from a nonlinear simulation are full-state models. For the F100 engine simulation the linear models are 16th order. Depending on the application of these linear models, it may be desirable to reduce the order of the model. For example, if the 16th-order models are used for multivariable control design studies that make use of optimal control theory, full-state feedback is required. For a 16th-order model this would result in an expensive and possibly impossible control to implement since it may be impossible to measure some of the states. Thus, the full-state models were reduced to fourth-order models. The states that were retained were found from previous studies to be measurable and capable of being used for engine control. The

states are fan and compressor speeds, burner pressure, and augmentor pressure.

Two reduction methods were considered, modal and normal reduction. The modal-reduction technique requires selection of eigenvalues to retain the desired states in the reduced-order model. The eigenvalue-state relation is determined by mode-shape analysis. If this relation is well defined, the reduced-order models are dynamically accurate since the eigenvalues are retained. The problem encountered with this method is that it is, in general, difficult to determine the eigenvalue-state relation because of coupling between the states. And because of this coupling, the set of eigenvalues needed to describe the retained states may not be unique. The normal-reduction technique requires that the states to be retained be specified. The reduced model resulting from the use of this technique does not necessarily retain the eigenvalues associated with the retained states, and in this sense it is not as dynamically accurate as that generated by the modal method. Also, if the states to be retained are not specified, a mode shape would be required to determine which states to keep. However the retained states are specified, the normal-reduction technique was easy to implement and resulted in a unique reduced-order model. The eigenvalues resulting from this reduced-order model should be approximately equal to those that were shown to be important in the mode-shape analysis done for the modal-reduction technique.

Using the normal-reduction technique, fourth-order models were generated at the six engine operating points. To determine how well the fourth-order models approximated the 16th-order models, transients were run on both models for +3 percent steps in fuel flow and nozzle area. In general, the transients for the state variables from the two models agree quite well. The loss in high-frequency dynamics due to the reduction can be observed in the transient response. From the comparisons made at the various operating points, the fourth-order models approximate the full-state models well and can be used for control analysis.

Finally, the methods used in this report to generate linear models from a nonlinear digital simulation are general. The application presented is for the F100 engine, but the method is not restricted to that simulation. The problems of bias errors in finite-difference approximations of partial derivatives and startup transients in nonlinear simulations, again, are not limited to the F100 simulation. They are universal and must be dealt with whenever deriving linear models or comparing transients run with the nonlinear and linear simulations.

Lewis Research Center,
    National Aeronautics and Space Administration,
        Cleveland, Ohio, September 1, 1978,
            505-05.

APPENDIX A

SYMBOLS

$\overline{A}$	state matrix (n×n)
$\overline{ABR}$	reduced-order state matrix
AN	nozzle jet area, m^2
$\overline{B}$	control matrix (n×n)
$\overline{BBR}$	reduced-order control matrix
BLC	customer-compressor-bleed-flow fraction
$\overline{C}$	output matrix (ℓ×n)
$\overline{CBR}$	reduced-order output matrix
CIVV	fan-inlet-guide-vane position, deg
$\overline{D}$	feed-forward matrix (ℓ×m)
$\overline{DBR}$	reduced-order feed-forward matrix
$DP_{2.5QP}$	empirical fan-exit $\Delta P/P$ parameter
$DP_{2.5SC}$	theoretical fan-exit $\Delta P/P$ parameter
d/dt	total derivative, sec^{-1}
e	eigenvector
FNMX	engine net thrust, kN
f	function
g	function
$\overline{I}$	identity matrix
$j\omega$	imaginary part of eigenvalue, rad/sec
K	linear slope
N_H	compressor speed, rpm
N_L	fan speed, rpm
n	index value
ΔP	change in pressure, kPa
P_{T3}	compressor-discharge pressure, kPa

$P_{T4.5}$	interturbine pressure, kPa
P_{T7M}	augmentor pressure, kPa
PLA	power level angle
R	ratio
RCVV	compressor variable vane position, deg
SMAF	fan stall margin
SMHC	compressor stall margin
s	LaPlace operator, sec^{-1}
$T_{T2.5C}$	duct temperature, K
$T_{T2.5H}$	fan inside-diameter discharge temperature, K
T_{T3}	compressor-discharge temperature, K
T_{T4}	burner-exit temperature, K
T_{T4HI}	burner-exit fast-response temperature, K
T_{T4LO}	burner-exit slow-response temperature, K
$T_{T4.5HI}$	fan-turbine-inlet fast-response temperature, K
$T_{T4.5LO}$	fan-turbine-inlet slow-response temperature, K
T_{T5}	fan-turbine-exit temperature, K
T_{T6C}	duct-exit temperature, K
T_{T7M}	exhaust-nozzle-inlet temperature, K
t	time, sec
Δt	change in time, sec
$\overline{U}$	control vector (m)
WFAN	total engine airflow, kg/sec
WFMB	main burner fuel flow, kg/sec
$\overline{X}$	state vector (n)
$\overline{\Delta X}$	change in state

$\overline{\Delta \dot{X}}$ change in state derivative

$\overline{Y}$ output vector (ℓ)

ϵ error tolerance

λ eigenvalue, rad/sec

σ real part of eigenvalue, rad/sec

Superscripts:

$\cdot$ total derivative, $\sec^{-1}$

$-$ vector quantity

-1 matrix inverse

$\sim$ small perturbation

$'$ different quantity

Subscripts:

b   bias

c   calculated

D   desired

F   fast

i   index

j   index

n   true value

o   operating point

S   slow

sum   summed value

UD   undesired

u   input

y   output

+   positive perturbation

−   negative perturbation

APPENDIX B

LINEARIZATION MATHEMATICS

The problem is to linearize nonlinear equations

$$\dot{\overline{X}}_o = \overline{f}\left(\overline{X}_o, \overline{U}_o, t\right) \tag{B1}$$

$$\overline{Y}_o = \overline{g}\left(\overline{X}_o, \overline{U}_o, t\right) \tag{B2}$$

where the subscript o indicates some operating point where the equations are balanced (ref. 10). Let $\overline{X}_o$, $\overline{U}_o$, and $\overline{Y}_o$ be the operating point values of the states, controls, and outputs, respectively. Assume the system is operated close to nominal conditions so that $\overline{X}$ and $\overline{U}$ deviate only slightly from $\overline{X}_o$ and $\overline{U}_o$. Then define $\widetilde{\overline{U}}$ and $\widetilde{\overline{X}}$ such that

$$\left. \begin{array}{l} \widetilde{\overline{U}} = \overline{U} - \overline{U}_o \\[2ex] \widetilde{\overline{X}} = \overline{X} - \overline{X}_o \end{array} \right\} \tag{B3}$$

where $\widetilde{\overline{U}}$ and $\widetilde{\overline{X}}$ are small perturbations about the operating point.

To linearize equation (B1), expand in a Taylor series about $\overline{X}$ and $\overline{U}$, and substitute (B3) into (B1) such that

$$\dot{\widetilde{\overline{X}}} + \dot{\overline{X}}_o = \overline{f}\left(\overline{X}_o, \overline{U}_o, t\right) + \overline{A}\left(\overline{X}_o, \overline{U}_o, t\right)\widetilde{\overline{X}} + B\left(\overline{X}_o, \overline{U}_o, t\right)\widetilde{\overline{U}} + \text{HOT} \tag{B4}$$

Now, assume all the higher order terms (HOT) are small compared with the other terms and subtract (B1) from (B4):

$$\dot{\widetilde{\overline{X}}} = \overline{A}(t)\widetilde{\overline{X}} + \overline{B}(t)\widetilde{\overline{U}} \tag{B5}$$

At an operating point the system is assumed to be time invariant; thus,

$$\dot{\widetilde{\overline{X}}} = \overline{A}\widetilde{\overline{X}} + \overline{B}\widetilde{\overline{U}} \tag{B6}$$

The $\overline{A}$ and $\overline{B}$ matrices are Jacobian matrices defined by

$$A_{ij} = \frac{\partial f_i}{\partial X_j} \quad \begin{array}{l} i = 1, n \\ j = 1, n \end{array}$$

$$B_{ij} = \frac{\partial f_i}{\partial U_j} \quad \begin{array}{l} i = 1, n \\ j = 1, m \end{array} \Bigg\} \tag{B7}$$

Equation (B2) is linearized by again assuming small perturbations about the operating point. Let

$$\overline{\widetilde{Y}} = \overline{Y} - \overline{Y}_0 \tag{B8}$$

where $\overline{\widetilde{Y}}$ is a small perturbation about the operating point. Then expand (B2) in a Taylor series and substitute (B3) and (B8) into (B2):

$$\overline{Y} - \overline{Y}_0 = \overline{g}\left(\overline{X}_0, \overline{U}_0, t\right) + \overline{C}\left(\overline{X}_0, \overline{U}_0, t\right)\overline{\widetilde{X}} + \overline{D}\left(\overline{X}_0, \overline{U}_0, t\right)\overline{\widetilde{U}} + \text{HOT} \tag{B9}$$

Again, assume that the HOT's are negligible, and subtract equation (B2):

$$\overline{\widetilde{Y}} = \overline{C}(t)\overline{\widetilde{X}} + \overline{D}(t)\overline{\widetilde{U}} \tag{B10}$$

where, assuming time to be invariant,

$$\overline{C}(t) = C_{ij} = \frac{\partial Y_i}{\partial X_j} \quad \begin{array}{l} i = 1, \ell \\ j = 1, n \end{array}$$

$$\overline{D}(t) = D_{ij} = \frac{\partial Y_i}{\partial U_j} \quad \begin{array}{l} i = 1, \ell \\ j = 1, m \end{array} \Bigg\} \tag{B11}$$

Equations (B6), (B7), (B10), and (B11) comprise the linearized model.

The approximation of partial derivatives of equations (B7) and (B11) is accomplished by finite differences in the nonlinear simulation. Digital perturbation logic is built into the simulation such that once the desired operating point is reached, the states are varied one at a time while the others are held constant. This is done to derive the $\overline{A}$ and $\overline{C}$ matrices. Once these matrices are derived, the logic in the simulation is set

up so that there is no steady-state error between the linear and the nonlinear models. This is accomplished by forcing

$$\overline{A}\widetilde{\overline{X}} + \overline{B}\widetilde{\overline{U}} = 0$$

Then

$$\widetilde{\overline{X}} = -\overline{A}^{-1}\overline{B}\widetilde{\overline{U}} \tag{B12}$$

This equation is implemented by making small perturbations in the inputs and calculating $-\overline{A}^{-1}\overline{B}$. Once $-\overline{A}^{-1}\overline{B}$ is known and since $\overline{A}$ is known,

$$\overline{B} = -\overline{A}\left(-\overline{A}^{-1}\overline{B}\right) \tag{B13}$$

For the last matrix $\left(\overline{D}\right)$, using equation (B10) yields

$$\widetilde{\overline{Y}} = \overline{C}\widetilde{\overline{X}} + \overline{D}\widetilde{\overline{U}}$$

Rearranging and inserting equation (B12) result in

$$\widetilde{\overline{Y}} - \overline{C}\left(-\overline{A}^{-1}\overline{B}\widetilde{\overline{U}}\right) = \overline{D}\widetilde{\overline{U}} \tag{B14}$$

where $\overline{D}$ is calculated by making small changes in the inputs while holding all the states constant such that equation (B14) is satisfied.

APPENDIX C

THE PROBLEM OF BIAS

In using finite differences to calculate partial derivatives, problems arise when there are small mathematical errors in the calculations. Since the perturbations made are small, changes in the model may also be small, and the resultant mathematical errors can cause significant errors in the partial derivatives. This is termed a bias problem. The discussion of this problem will proceed first with explicit calculations which, although not the case with the simulation here, are easy to understand. Then the effects of this problem on implicit calculations are considered. Finally, the problem of selecting the correct perturbation size is addressed. Some of this material is presented in reference 11.

Explicit Equations

Explicit equations are those in which solutions are obtained without iteration. For example, given

$$\frac{dX}{dt} = f(X) \tag{C1}$$

this equation can be solved on the digital computer by using a difference equation such as

$$X(n + 1) = X(n) + f\left[X(n)\right] \Delta t \tag{C2}$$

This is an open integration method known as Euler's method, wherein $X(n + 1)$ can be calculated explicitly from previous values of $X(n)$. When this method is used in the simulation, the finite-difference scheme is also explicit and is

$$\frac{\partial}{\partial X_j}\left(\frac{d}{dt} X_i\right) = \frac{f_i\Big|_{X_j+d_j} - f_i\Big|_{X_j}}{X_j + d_j - X_j} \tag{C3}$$

where d_j is the perturbation size. In steady state $f_i\Big|_{X_j} = 0$ analytically, but mathematically it may not because of small calculation errors.

If there is a steady-state bias,

$$\dot{X}_c = \dot{X}_b + \dot{X}_n \tag{C4}$$

27

where $\dot{X}_c$ is the calculated derivative, $\dot{X}_b$ is the bias value, and $\dot{X}_n$ is the true derivative.

For a linear system

$$\frac{\Delta \dot{X}_n}{\Delta X} = \text{constant} = K \tag{C5}$$

where K is independent of stepsize or direction of perturbation. Perturbing (C4) by ΔX and dividing by ΔX gives

$$\frac{\Delta \dot{X}_c}{\Delta X} = \frac{\dot{X}_b}{\Delta X} + \frac{\Delta \dot{X}_n}{\Delta X} \tag{C6}$$

Thus, the bias error is a function of the perturbation size and can get large as ΔX gets small.

The bias problem for explicit calculations can be eliminated in two ways. First, the differential equations can be sampled in steady state, and the bias error can be calculated. Then, the method of finite differences can be used to determine the partials, and the bias can be subtracted. Second, the states can be perturbed in the positive and negative directions about the operating point.

For a positive perturbation

$$\left(\frac{\Delta \dot{X}_c}{\Delta X}\right)_+ = \frac{\dot{X}_b}{\Delta X} + K \tag{C7}$$

and for a negative perturbation

$$\left(\frac{\Delta \dot{X}_c}{\Delta X}\right)_- = -\frac{\dot{X}_b}{\Delta X} + K \tag{C8}$$

Adding (C7) and (C8) gives

$$\left(\frac{\Delta \dot{X}_c}{\Delta X}\right)_+ + \left(\frac{\Delta \dot{X}_c}{\Delta X}\right)_- = \frac{\dot{X}_b}{\Delta X} + K - \frac{\dot{X}_b}{\Delta X} + K$$

But, for a linear system

$$\left(\frac{\Delta \dot{X}_c}{\Delta X}\right)_+ = \left(\frac{\Delta \dot{X}_c}{\Delta X}\right)_- = \left(\frac{\Delta \dot{X}}{\Delta X}\right)$$

Thus,

$$2\left(\frac{\Delta \dot{X}}{\Delta X}\right) = 2K \quad \text{and} \quad \frac{\Delta \dot{X}}{\Delta X} = K$$

Hence, the bias problem is eliminated for explicit calculations by perturbing about an operating point. The actual implementation of this procedure on an explicit simulation is to make a positive perturbation and calculate an $\overline{A}$ matrix $\left(\overline{A}_+\right)$ and then a negative perturbation and calculate another $\overline{A}$ matrix $\left(\overline{A}_-\right)$. Then the matrices $\overline{A}_+$ and $\overline{A}_-$ are averaged.

Implicit Equations

Implicit equations are those that require iteration for solution:

$$\frac{dX}{dt} = f(X)$$

This equation can be written as a difference equation of the form

$$X(n + 1) = X(n) + f\left[X(n + 1)\right]\Delta t \tag{C11}$$

Note that equation (C11) cannot be solved explicitly because of the dependence of f on $X(n + 1)$. In the F100 simulation the steady-state part of the simulation uses a modified Newton-Raphson technique (SMITE) described in reference 11 to achieve an engine balance. This is accomplished by specifying $dX/dt = 0$ in (C1) and iterating to achieve the steady-state balance specified tolerance.

Now this iteration capability is used to derive the $\overline{A}$ and $\overline{C}$ matrix elements. If state 1 is perturbed, a new state vector $\left(\overline{X}'\right)$ is formed, and equation (C1) becomes

$$f\left(\overline{X}'\right) - \dot{\overline{X}}' = 0 \tag{C12}$$

Since $f\left(\overline{X}'\right)$ is known, the error variable can be specified by

$$f\left(\overline{X}'\right) - f\left(\overline{X}'\right)_c = \epsilon \tag{C13}$$

29

The iteration proceeds until equation (C13) is satisfied within some specified tolerance. In equation (C12) the nonzero derivatives result from the perturbation solutions, and they are used to calculate the required partial derivatives.

The problem of bias with this type of solution results when the answer falls within the iteration tolerance, but the error is not zero. Then

$$\dot{X}_c = \dot{X}_b + \dot{X}_n \tag{C14}$$

where $\dot{X}_b$ is the error within the iteration tolerance.

One obvious solution to this problem is to make the iteration tolerance very tight. However, this can have adverse effects, such as the program never achieving a solution because of oscillations about the tolerance or the solution converging but requiring a large amount of computer time.

Another possible solution is to calculate the error. This method is discussed in reference 7.

A final method is to make positive and negative perturbations about the operating point. However, why this works is not clear. The solution of equation (C12) can converge within the specified tolerance. There is no guarantee on which side it will converge. The results in this report and in reference 12 (which discusses the same problem) indicate that the positive-negative perturbation method works. A possible explanation for this (from ref. 12) is that the bias error tends to converge on opposite sides of zero for the different perturbation directions, causing the errors to cancel. Mathematically this is done by

$$\dot{X}_{c_+} = \dot{X}_{b_+} + \dot{X}_n \tag{C15}$$

and

$$\dot{X}_{c_-} = \dot{X}_{b_-} + \dot{X}_n \tag{C16}$$

Adding equations (C15) and (C16) yields

$$\dot{X}_{c_+} + \dot{X}_{c_-} = \dot{X}_{b_+} + \dot{X}_{b_-} + 2\dot{X}_n \tag{C17}$$

From experience we know that

$$\dot{X}_{b_+} + \dot{X}_{b_-} \rightarrow \dot{X}_{b_{sum}} \quad \text{(almost zero)}$$

Thus

$$\dot{X}_c = \dot{X}_n + \frac{\dot{X}_{b_{sum}}}{2} \tag{C18}$$

Note, however, that the iteration errors could possibly add, causing bias to worsen. Once $\dot{X}$ is calculated, divide by ΔX to get the partial derivative.

Perturbation Size

The perturbation size is restricted. It must be in the linear range about the operating point, and it must be larger than the iteration tolerance for implicit solutions. The importance of the latter restriction is evident since no meaningful solution could be achieved otherwise. The former is important to generate the correct linear model. An investigation into the effects of iteration tolerance on perturbation size for implicit solutions was done in reference 11.

APPENDIX D

F100 FULL-STATE LINEAR MODELS

As an example of the linear model generation technique, linear models of the F100 engine were developed at six operating points. The operating-point selection is based on engine operational constraints. The method of selection is described in reference 9. The table of operating points selected is given in reference 1. The points selected for illustration in this report are given in table VI. The $\overline{A}$, $\overline{B}$, $\overline{C}$, and $\overline{D}$ matrices, the eigenvectors, and the matrix of mode shapes are presented for each operating point. Note that operating point 1 is the sea-level-static-idle operating point for which the examples in this report are given.

Operating Point 1 (sea-level-static idle)

THE A MATRIX
```
-2.015        1.110       -1.395        683.9       -1113.       -10.87       -1.151       -.2920
-.4462       -4.081        143.4       -252.5       -124.0        27.70       -.4096       -.8621
 1.006        5.056       -150.9        7.055        279.3       -46.83       0.9030        1.311
 0.1830       0.1994       103.6       -817.0        606.9       -2.683       0.8718D-02-.4589
 0.1027       -.1488       1.797        34.15       -281.2        1.400       -.6243D-01-.4123D-01
 0.3548       -.2446       1.556       -2.510        102.2       -17.60       0.3306        0.5350D-02
 0.2900       -.3917       2.533       -3.095        129.1        3.758       -19.59        0.3250D-02
-.3928        0.2305       57.58        2.665       -109.1        29.60       -.3523       -20.00
-.8145D-02-.1792D-01-.2991       -.1627       -2.352        0.3738       -.1527D-01 6.105
-.1212D-03-.2655D-03-.4431D-02-.2891D-02-.3439D-01 0.5531D-02-.2326D-03 0.9043D-01
-4.146       -20.45        142.4        29.05       -1151.        193.0       -3.712        41.20
 0.6298D-01 0.2537       -210.7        633.1        16.92       -2.923       0.6757D-01 9.411
 0.2795D-02 0.1127D-01-9.361        26.23        0.7524       -.1299       0.2965D-02 0.4183
 0.7068D-01 0.3277D-01-94.00        67.85        295.0        -.4450       -.2620D-02 4.229
-.8396D-02 0.3823D-01-.2791       -.8655D-01 3.459        -.3630        19.93        0.7746D-01
-2.597        3.636       -11.94        578.8       -20.16       -34.36        1.374        -.4735

 0.3121       0.3270       -1.168       2.661        2.660       -.2000D-01-.4785        0.2500D-02
 3.948        3.951        -1.355       0.2200D-02-.5000D-03 0.1760D-01-.9140D-01-.5000D-04
-.8600D-02 0.1650D-01 1.587        0.0000        0.1000D-02-.3930D-01 0.2085        0.3000D-02
-.6971        -.9058       1.740        0.0000       0.0000       0.5286D-01 0.1739       -.2928D-02
 0.4100D-01 0.6467D-01-.1439       0.1669D-02-.5525D-02 0.2044        0.2033        0.3315D-02
-.1350D-02-.2750D-01 0.1260D-01 0.5000D-04-.2850D-01-.1495D-01 0.7310D-01 0.4150D-02
-.2750D-02-.4350D-01 0.1290D-01 0.3000D-04 0.5000D-03-.1625D-01 0.9420D-01 0.1000D-03
 0.3450D-02 0.3000D-02-.1200D-01-.5000D-03-.4500D-02 0.1585D-01-.8180D-01-.1250D-02
-50.00        0.7805D-02 39.70        -.1000D-05 0.0000        -.2202D-02 0.2170D-02-.4392D-02
-.6667        -.6666       0.5881       0.0000       -.5000D-06-.4406D-04 0.2890D-04-.5853D-04
 0.3600D-01-.6000D-01-48.15        0.5000D-03 0.3000D-01 0.1595        -.8595       -.2000D-01
-10.23        -10.27       39.06       -50.01       0.2655D-01-.4395D-02 0.2390D-01-.8765D-02
-.4544        -.4566       1.736       -2.001       -1.999       -.1760D-03 0.1044D-02-.4095D-03
-4.596        -4.614       17.55       -1.420       -1.402       -19.98        0.8607D-01-.4098D-02
 0.3450D-03 0.5000D-04 0.1318D-01 0.0000        0.0000       -.2639D-02-20.01        0.0000
 0.6543       0.5850       -2.463       -.6500D-02 0.0000        24.50        26.55       -50.00
```

THE B MATRIX
```
 0.1656        20.66       -13.92        10.28        0.5637E 05
 0.3390E-01-.5900       -2.556       -21.06        0.6591E 05
-.6665E-01-7.935        5.827        42.42        -.3358E 05
-.4033E-01-9.546        1.538        2.206        -.1925E 05
 0.7451E-02-240.3        1.081       -1.217        0.4340E 05
-.8139E-01-4.590        1.180       -2.162        -.1348E 05
 0.3450E-01 0.2600       2.034       -3.462        -.1078E 05
-.3250E-02 1.230        -2.269       -13.28        34.50
 0.9963E-01-.3673       -.5285E-01-.3465        0.2333E 05
 0.1495E-02-.7397E-02-.7809E-03-.5442E-02 345.1
 30.40        28.65       -23.99       -174.8        0.2863E 06
 0.4394        12.90        0.2822       2.767        0.1807E 05
 0.1916E-01 0.5433        0.1257E-01 0.1209        795.8
 0.1728        0.3210       0.6164       0.3532       3616.
 0.1068E-02 0.7426       -.1113        0.3338       -655.7
-.7700E-02-3.550        -27.19        31.15        -.4155E 05
```

THE C MATRIX
```
 0.1662        -.2432       2.949        56.10        311.4        2.273        -.7570E-01-.5992E-01
 0.1803E-01 0.2394E-02-.1562E-01 0.2525E-01-.9991       -.2300E-01-.3240E-02-.2500E-04
 0.0000        0.0000       0.0000       0.0000       0.0000       0.0000       0.0000       0.0000
-.7525E-05 0.7668E-04-.5000E-03 0.8095E-03-.3200E-01-.7367E-03-.1038E-03-.9300E-06
 0.1020E-03 0.5349E-03-.1439E-01-.7130E-03 0.2831E-01-.4270E-02 0.9140E-04 0.3000E-06
 0.5172E-04 0.6560E-05-.3550E-04 0.6920E-03-.2748E-01-.7065E-04 0.5145E-04-.5000E-06
 0.1950E-04-.1358E-05 0.8900E-05 0.1492E-03-.5836E-02 0.4583E-04 0.3841E-04-.1300E-06

 0.5870E-01 0.1725E-01-.2372       -.2610E-02-.6050E-02 0.3349        0.3208       -.4900E-02
 0.2900E-04 0.1050E-03-.1110E-03 0.1999E-05 0.1000E-04 0.1375E-03-.7425E-03-.4500E-05
 0.0000        0.0000       1.000        0.0000       0.0000       0.0000       0.0000       0.0000
 0.9200E-06 0.3400E-05-.3535E-05-.5000E-07 0.4999E-06 0.4400E-05-.2380E-04-.1000E-06
-.8800E-06-.5499E-06 0.3185E-05 0.0000       -.5000E-06-.3950E-05-.2105E-04-.3500E-06
 0.7650E-06 0.2950E-05-.2825E-05 0.0000       -.9000E-06 0.3650E-05-.2145E-04 0.1000E-06
 0.2200E-06 0.1150E-05-.6750E-06-.4999E-08-.5000E-07 0.8100E-06-.4550E-05-.4999E-08
```

THE D MATRIX
```
0.1069E-010.7800     1.747    -2.087    0.2061E 05
0.3767E-04-.1250E-020.1684     C.2135E-01 126.2
0.00C0     0.0000     0.0000     0.0000    -0.0000
0.3040E-050.5125E-03-.1295E-020.6818E-03 4.023
-.3462E-04-.3842E-020.6017E-030.7159E-02-7.202
0.3485E-050.3460E-030.5783E-040.7515E-04 3.798
0.6955E-060.5350E-040.2018E-03-.7200E-050.8109
```

EIGENVALUES OF THE A MATRIX
REAL PART   IMAGINARY PART

```
  -852.11279      0.00000000
  -268.16113      0.00000000
  -135.01001      0.00000000
  -56.317566      0.00000000
  -49.669357      0.0C000000
  -48.432312      0.00000000
  -40.376266      0.00000000
  -14.119783      0.00000000
  -2.8587856      0.00000000
  -21.319580      0.83925688
  -21.319580     -0.83925688
  -19.747040      0.00000000
  -1.9813099      0.00000000
 -0.74410683      0.20040876
 -0.74410683     -0.20040876
  -20.347610      0.00000000
```

MODIFIED EIGENVECTOR MATRIX
```
-5.0913E-03  1.1117E-02 -1.0607E-02 -1.1186E-02 -3.2395E-03 -1.6743E-02  8.5295E-03  3.9457E-02
 6.9963E-04  4.6972E-03 -5.2165E-03 -3.2217E-03  6.8762E-05  1.7562E-03 -1.5722E-02 -9.2711E-03
 4.2649E-03 -6.1821E-01  1.0000E 00 -4.4879E-02 -2.9384E-04 -4.4450E-03 -8.4954E-03 -1.7911E-01
 1.0000E 00  4.2985E-01  6.6772E-01 -4.7341E-02  5.8370E-04  5.9583E-03 -4.4127E-02 -2.8508E-02
-8.3483E-02  1.0000E 00  2.8190E-01  2.7410E-03  1.0596E-03 -1.6014E-05 -1.0312E-04  6.8297E-02
 4.2838E-04 -1.0986E-02 -8.0417E-03  5.7281E-04 -7.5694E-06  1.5424E-03 -3.8501E-03  1.0230E-01
 5.3573E-04 -1.3706E-02 -1.1038E-02  1.6068E-04  1.1035E-04  1.4338E-03 -5.0783E-03  1.3596E-01
-3.1477E-04  1.9858E-02 -3.4475E-02  5.1967E-03 -3.0293E-05 -1.3367E-03  7.8456E-03  1.3241E-01
 9.9511E-05 -1.5674E-02  1.9785E-02  2.9103E-01 -4.6844E-03 -1.2464E-01  1.0000E 00  3.3394E-01
 1.3289E-05 -2.0565E-03  2.5536E-03  3.5792E-02 -5.7020E-04 -1.5116E-02  1.1882E-01  3.0211E-02
-1.7011E-03  7.3029E-02 -3.3012E-02 -4.0462E-02  2.5072E-05 -4.0994E-03  2.0840E-01  2.4861E-01
-1.6391E-02 -9.0048E-02  9.3643E-02  1.0000E 00  2.0542E-01  1.0000E 00 -1.7101E-01  3.7216E-01
-5.5355E-03 -3.5617E-02  3.6603E-02  3.7805E-01  7.7036E-02  3.7434E-01 -6.3170E-01  1.1213E-01
-1.1670E-03 -4.3952E-02  4.6298E-02  1.0880E-01  8.8351E-03  2.7224E-02  1.3063E-02  9.8219E-01
 9.3368E-07  5.6542E-04  2.0502E-03 -6.8553E-05 -8.3877E-05 -1.0401E-03  4.8912E-03  4.5685E-01
-1.9592E-02 -2.5110E-02 -1.3079E-01 -5.3050E-01  1.0000E 00  6.8761E-01 -7.3419E-02  1.0000E 00
```

```
 1.0000E 00 -1.5230E-02  3.7075E-03 -2.9111E-04  8.9360E-02  1.0000E 00  1.0000E 00  2.8174E-03
-2.4653E-02 -4.7425E-03  4.6298E-03 -1.2327E-04 -3.4627E-03  2.3030E-01  1.7956E-01  1.9916E-03
-1.3541E-01  2.1604E-01  5.9131E-02  1.3307E-02 -1.4976E-02  1.0507E 00  8.2109E-01 -6.4950E-03
 5.3303E-02  1.2950E-01  5.6577E-02  2.2818E-02  3.2737E-03  5.1764E-01  4.3737E-01  1.1779E-02
 1.4933E-01  5.9244E-02  5.6776E-02  3.4132E-02  1.2779E-02  1.4642E-01  1.4726E-01  3.1015E-02
 2.0466E-01 -6.3278E-02 -1.6490E-02 -3.1972E-03  1.7048E-02  1.2594E-01  1.3981E-01  1.9105E-03
 2.0756E-01 -6.4363E-02 -1.5639E-02 -1.1348E-02  1.7666E-02  9.6910E-02  1.1675E-01  1.6741E-02
 6.0822E-02  1.7573E-01 -4.1182E-02  1.6372E-02  3.0538E-03  2.9392E-01  2.5125E-01 -2.8498E-02
 1.1723E-01  1.0560E-01 -1.6137E-01  1.6324E-02  9.8461E-03 -2.9361E-01 -2.1710E-01 -4.9524E-02
-1.5205E-02  1.1320E-02 -1.6896E-02  1.6858E-03 -3.0061E-03  7.8914E-01 -5.5463E-01 -5.1494E-02
 1.1463E-01  4.7965E-02 -9.8700E-02  3.4309E-03  9.9920E-03 -3.3961E-01 -2.5202E-01 -2.9331E-02
 1.7643E-01  5.7803E-02 -1.4001E-01  1.9046E-02  1.5473E-02 -4.5967E-01 -3.0140E-01 -3.5685E-02
-1.7493E-01  1.9831E-02 -4.7190E-02  6.3214E-03  1.0000E 00 -5.6510E-01 -4.6728E-01 -1.1953E-02
 2.3621E-01  3.8796E-01  9.4800E-01  1.0000E 00  1.1776E-02 -5.5405E-01 -3.7592E-01  1.0000E 00
 2.3359E-01  7.7737E-01 -2.6232E-01 -9.7548E-01  1.8956E-02  1.0082E-01  1.2198E-01 -9.6650E-01
-1.1371E-01  1.0000E 00  1.0000E 00  5.7108E-01 -1.7911E-02 -2.7934E-01 -2.3342E-01  5.2575E-01
```

THE MATRIX OF MODE SHAPES, IN MAG. AND ANGLE(DEG.) FORM

	1	2	3	4	5	6	7	8
1	-0.5031D-02	0.1112D-01	-0.1061D-01	-0.1119D-01	-0.3240D-02	-0.1674D-01	0.8529D-02	0.3946D-01
2	0.6996D-03	0.4697D-02	-0.5217D-02	-0.3222D-02	0.6876D-04	0.1756D-02	-0.1572D-01	-0.9271D-02
3	0.4265D-02	-0.6182	1.000	-0.4488D-01	-0.2938D-03	-0.4445D-02	-0.8495D-02	-0.1791
4	1.000	0.4298	0.6677	-0.4734D-01	0.5837D-03	0.5958D-02	-0.4413D-01	-0.2851D-01
5	-0.8348D-01	1.000	0.2819	0.2741D-02	0.1060D-02	-0.1601D-04	-0.1031D-03	0.6830D-01
6	0.4284D-03	-0.1099D-01	-0.8042D-02	0.5728D-03	-0.7569D-05	0.1542D-02	-0.3850D-02	0.1023
7	0.5358D-03	-0.1371D-01	-0.1104D-01	0.1607D-03	0.1103D-03	0.1434D-02	-0.5078D-02	0.1360
8	-0.3148D-03	0.1986D-01	-0.3447D-01	0.5197D-02	-0.3029D-04	-0.1337D-02	0.7846D-02	0.1324
9	0.9951D-04	-0.1567D-01	0.1978D-01	0.2310	-0.4684D-02	-0.1246	1.000	0.3339
10	0.1329D-04	-0.2056D-02	0.2554D-02	0.3579D-01	-0.5702D-03	-0.1512D-01	0.1188	0.3021D-01
11	-0.1701D-02	0.7303D-01	-0.3301D-01	-0.4046D-01	0.2507D-04	-0.4099D-02	0.2084	0.2466
12	-0.1639D-01	-0.9005D-01	0.9364D-01	1.000	0.2054	1.000	-0.1710	0.3722
13	-0.6535D-02	-0.3562D-01	0.3660D-01	0.3781	0.7704D-01	0.3743	-0.6317D-01	0.1121
14	-0.1167D-02	-0.4395D-01	0.4630D-01	0.1088	0.8835D-02	0.2722D-01	0.1306D-01	0.9822
15	0.9337D-06	0.5654D-03	0.2050D-02	-0.6655D-04	-0.8388D-04	-0.1040D-02	0.4891D-02	0.4569
16	-0.1959D-01	-0.2511D-01	-0.1308	-0.5305	1.000	0.6876	-0.7342D-01	1.000

	9	10	11	12	13	14	15	16
1	1.000	0.1108D-01	-121.3	-0.2911D-03	0.8936D-01	1.000	0.0000	0.2817D-02
2	-0.2465D-01	0.4686D-02	-90.69	-0.1233D-03	-0.3463D-02	0.2065	7.058	0.1992D-02
3	-0.1354	0.1584	29.69	0.1331D-01	-0.1498D-01	0.9429	6.993	-0.6495D-02
4	0.5330D-01	0.3993D-01	21.40	0.2282D-01	0.3274D-02	0.4792	4.804	0.1178D-01
5	0.1493	0.5802D-01	1.219	0.3413D-01	0.1276D-01	0.1468	-0.1646	0.3102D-01
6	0.2047	0.4624D-01	-149.6	-0.3197D-02	0.1705D-01	0.1331	-2.988	0.1911D-02
7	0.2076	0.4681D-01	-148.5	-0.1104D-01	0.1767D-01	0.1073	-5.304	0.1674D-01
8	0.6082D-01	0.1276	58.19	0.1637D-01	0.3054D-02	0.2734	4.476	-0.2850D-01
9	0.1172	0.1364	101.8	0.1532D-01	0.9846D-02	0.2582	-171.5	-0.4952D-01
10	-0.1521D-01	0.1438D-01	101.2	0.1686D-02	-0.3006D-02	0.6820	80.10	-0.5149D-02
11	0.1146	0.7760D-01	109.1	0.9431D-02	0.9992D-02	0.2990	-171.6	-0.2933D-01
12	0.1764	0.1071	112.6	0.1905D-01	0.1547D-01	0.3887	-168.3	-0.3569D-01
13	-0.1750	0.3622D-01	112.1	0.6321D-02	1.000	0.5185	-174.6	-0.1195D-01
14	0.2362	0.7247	-22.76	1.000	0.1178D-01	0.4734	-169.2	1.000
15	0.2336	0.5801	53.65	-0.8755	0.1886D-01	0.1119	-5.426	-0.9665
16	-0.1137	1.000	0.0000	0.5711	-0.1791D-01	0.2574	-174.9	0.5258

Operating Point 2

```
THE A MATRIX
 -4.307      0.1764      5.058        405.0      -725.7      -2.044       1.124       -1.059
 -.4275     -5.600       128.4       -232.7      -428.4      27.01        2.242       -2.511
  1.036      6.217      -164.2        -4.970     1054.      -82.41       -5.456        5.084
  0.5753    -.6005D-01   132.7        -573.6      113.7      -8.603      -.5635       -2.118
  0.1228    -.1764       1.191         20.98     -115.9      2.606       0.1715       -.1161
  0.8345    -.1380D-010.4965D-01    -.2644       38.42      -19.83      -.2078        0.1280D-02
  0.6669    -.7323D-020.1071        -.7520       86.64      0.1185      -20.42        0.1295D-02
 -.1022      0.8039      16.21         0.4725    -106.9      29.42       0.5370       -20.01
 -.8544D-02-.1859D-010.1720         -.1205D-01-8.714       0.6922      0.2361D-01    6.626
 -.1266D-03-.2751D-030.2548D-02-.1607D-03-.1289            0.1025D-010.3568D-030.9815D-01
 -1.276     -6.996       23.37         6.140     -1298.     101.5        6.712        36.37
 -.2860D-01-.4633      -52.94         199.2      -28.16     2.224        0.1464        9.757
 -.1268D-02-.2059D-01-2.353           8.855      -1.251     0.9889D-010.6485D-020.4337
 -.1645     -.2527      -24.18         22.28      142.9      1.604       0.1127        4.479
 -.1225D-010.3097D-01-.1032         -.1445D-01 5.759      -.4474       19.82         0.1262
 -1.637      1.887      -2.940         115.6      347.2      -27.11      -1.802       -.4661

  1.035      1.014      -4.126         9.511      9.576     -.6806      -.3843        0.0000
 11.38      11.34       -4.040         0.5000D-04-.1100D-010.5000D-04-.4371         0.5000D-04
 -.2260D-010.7500D-02 5.618         -.1500D-020.1000D-01-.1500D-02 1.059            0.0000
 -2.916     -2.931       5.890       -.2450D-02-.3300D-010.5400D-020.1065           0.1000D-03
  0.1076     0.1008     -.4231         0.5000D-030.1960D-010.5293     0.3272        0.0000
 -.2440D-02-.5000D-040.4185D-02-.1005D-02-.2250D-02-.5000D-050.5185D-01-.5000D-05
 -.3000D-020.5000D-040.1851D-01-.7450D-030.5000D-04-.2600D-030.1724              0.1000D-04
  0.2070D-020.5000D-04-.1110D-010.1000D-040.9050D-020.0000      -.1044            0.0000
-50.00       0.5000D-05 39.47       -.6235D-03-.5605D-020.6710D-03-.3120D-020.0000
 -.6667     -.6667       0.5847     -.8310D-05-.7450D-040.8900D-05-.6245D-040.0000
  0.3010D-010.1750D-01-47.87          0.1500D-020.0000     -.2500D-02-1.303         0.0000
 -9.636     -9.609       38.50       -50.00      -.7295D-010.2675D-02-.3279D-010.5000D-05
 -.4283     -.4272       1.711        -2.000     -2.003      0.1070D-03-.1500D-020.0000
 -4.425     -4.413       17.68        -3.119     -3.168     -19.78      -.2936D-010.5000D-05
 -.1885D-030.0000       0.1980D-010.9970D-03-.5000D-050.1069D-02-20.00          -.5000D-06
  0.5852     0.5910     -2.361         0.5500D-030.4450D-01 30.73       20.16       -50.00

THE B MATRIX
 -.3864E-01-200.5       -111.0        0.2690      -247.0
  0.1987E-01-322.0      -6.044       -65.59       -6326.
  0.1351      818.3      14.75         62.49       0.9318E 05
  0.4313E-01 79.69       2.120         6.348       -3659.
  0.1195E-03-1232.       8.749        -1.966       -57.55
  0.4406E-02-3.520       9.238        -.1921        13.60
  0.8115E-02 155.8       9.147         1.001       -184.0
 -.4561E-02-86.26       -1.478         10.30       -205.9
  0.4537E-01-5.923      -.1244        -.5119        9997.
  0.6811E-03-.6385E-01-.2060E-02-.7579E-02 148.0
  6.326      -1001.     -18.57        -74.85       -.1175E 06
  0.1461     -17.52     -.4516        -1.648       0.1040E 05
  0.6497E-02-.7313      -.2030E-01-.7318E-01 461.6
  0.8676E-01-29.35       0.1166        -1.211       4243.
 -.3538E-03 4.107      -.8741         0.3384       -7.715
  0.2945E-01 248.4      -96.13         21.04        -1698.

THE C MATRIX
  0.4734     -.6987      5.018         94.47       22.43      10.37       0.6890      -.5099
  0.1382E-010.3137E-050.0000           0.5006E-07-.9775E-02-.5345E-040.5315E-040.4999E-08
  0.0000      0.0000     0.0000         0.0000      0.0000     0.0000      0.0000      0.0000
  0.7418E-040.5101E-05-.1454E-040.7130E-04-.1524E-01-.7396E-040.7922E-04-.1950E-06
  0.1655E-040.1287E-03-.2578E-02-.7990E-040.1687E-01-.1075E-02-.8713E-040.2450E-06
  0.1546E-04-.2981E-040.1013E-030.7540E-04-.1599E-010.4324E-030.2128E-03-.3300E-06
  0.9115E-050.4128E-05-.1320E-040.1848E-04-.4145E-020.4306E-040.7697E-04-.9000E-07

  0.4777      0.4840     -1.908       -.7950E-03-.1610E-01 3.370      2.034       0.1001E-04
  0.0000      0.0000     0.0000         0.0000      0.0000     0.4999E-080.4999E-080.4999E-08
  0.0000      0.0000     1.000          0.0000      0.0000     0.0000      0.0000      0.0000
  0.3550E-060.5000E-07-.1530E-050.3500E-070.1000E-060.9997E-08-.1522E-040.0000
 -.3750E-060.3000E-060.1709E-05-.9999E-07-.4000E-06-.4000E-070.1691E-04-.4999E-08
  0.3950E-060.0000     -.1570E-05-.3500E-070.1850E-05 0.0000     -.1577E-040.0000
  0.1220E-060.0000     -.4380E-060.3500E-080.8000E-060.0000      -.4049E-050.0000
```

THE D MATRIX
```
0.4435E-03-235.0       34.51     -7.81€      -628.0
0.6343E-040.1778      C.7403     0.2042E-03C.8590E-02
0.0000      0.0000    0.0000     C.00C0     0.0000
0.3327E-05-.4144E-02-.3104E-020.6226E-04C.1158E-C1
0.1469E-060.1278E-010.2367E-03C.2431E-02-.1526E-C1
-.6490E-07-.1307E-010.1446E-02-.3298E-030.5465E-02
0.2120E-07-.3548E-020.6496E-03C.4837E-C40.2925L-C2
```

EIGENVALUES OF THE A MATRIX

REAL PART	IMAGINARY PART
-562.04395	0.00000000
-248.34012	0.00000000
-60.906693	0.00000000
-50.085373	0.00000000
-49.964691	0.00000000
-43.535172	0.00000000
-30.572876	10.531186
-30.572876	-10.531186
-21.942566	1.5567312
-21.942566	-1.5567312
-18.756088	0.00000000
-12.951914	0.00000000
-7.0543709	0.00000000
-2.8662462	0.00000000
-0.67332858	0.00000000
-1.9776640	0.00000000

MODIFIED EIGENVECTOR MATRIX
```
-7.7125E-03 -2.2732E-02 -2.2661E-C2  6.9213E-04 -2.9085E-04  4.4432E-02  4.3715E-03  4.9862E-C2
 2.6831E-03 -6.6176E-03 -1.6533E-C2  1.8671E-06  2.5127E-06 -5.9830L-02 -1.7604L-02  8.2087E-02
 3.6305E-C2  7.1343E-C1 -1.2322E-C1  1.0472E-04 -4.5909E-05  5.7788E-02  3.6566E-01  2.5335E-C1
 1.0000E CO  1.0000E 00 -2.1333E-C1  1.7506E-04 -6.3305E-05 -2.9768E-02  2.9329E-C1  2.4664E-C1
-1.1296E-01 -4.5479E-01 -3.1290E-02 -4.1612E-04  1.6903E-04  5.9494E-02  3.4206E-C1  2.9895E-01
 6.6690E-04  5.4001E-03  7.7641E-03 -2.2825E-04  9.716E-05 -2.7045E-02 -9.2389E-02 -1.7315E-02
 1.2905E-03  1.0590E-02  8.4919E-03 -1.4121E-04  5.9658E-05 -2.9867E-02 -1.6598E-01 -2.9198E-C3
-1.0174E-03 -1.9113E-02  9.6627E-03  7.5020E-05 -3.3371E-05  3.4121E-02  2.9627E-02 -7.1908E-C2
 3.7914E-04  1.2281E-02  3.7172E-01 -4.374CE-05 -4.0420E-05  1.0000E 00  4.6733E-01 -1.0765E 00
 5.C154E-05  1.6C87E-02  4.5998E-02 -5.9259E-06 -4.9173E-06  1.1986E-01  6.0792E-02 -1.2222E-C1
-4.4924E-03 -5.3133E-02 -8.8973L-02 -6.2227E-06  2.7606E-06  1.3773L-01 -5.0266E-02 -5.5404E-C1
-1.8975E-C2  1.2909E-03  1.0000E CC -1.7981E-02  7.5139E-03 -8.1744L-01  4.3144E-02 -1.C159E 00
-7.5490E-03  5.C731E-C4  3.7953E-C1 -6.74173-03  2.8169E-03 -3.0327E-01  2.9483E-C1 -3.6816E-C1
-1.1223E-03  2.436€E-C2  1.9753E-C1 -1.9983E-03  8.2534E-04 -2.3047E-02  5.2665E-01  7.3020E-02
 2.1851E-05 -7.7308E-C5 -3.7604E-03  9.8247E-05 -4.1581E-05  2.4728E-02  1.4903E-C1 -1.4872E-C1
-1.3936E-02 -2.1583E-C2 -5.9316E-C1  1.0000E 00  1.0000E 0C -1.6733E-01  1.0000E 00  1.0000E 00
```

```
 1.5999E-03 -2.3256E-C2 -1.6816E-C3  6.4933E-02  6.2477E-01  1.0000E 00  8.0668E-02  5.9C16E-C2
-4.8733E-03 -1.6410E-02  2.9654E-C3 -3.9512E-02 -1.0125E-01  6.8818E-01  1.159CE-01  2.7171E-C3
-1.1292E-01  1.2773E-01  1.9583E-C3  8.1499E-02 -9.9954F-02  9.5548E-C1  1.4967E-C1  2.7633E-C3
-1.0536E-C1  1.1802E-01  1.1660E-03  8.3467E-02 -1.9077F-02  8.5072E-C1  1.1053E-C1  7.1283E-C3
-9.3795E-02  7.1161E-02 -1.C938E-C2  3.6652E-01  6.4403E-01  7.4134E-01  4.5231E-C2  3.5441E-C2
 4.2846F-02 -2.4069E-02 -3.C81E-03  2.1590E-01  6.4638E-01  7.3289E-01  5.0088E-02  4.0620E-02
-1.6749E-02 -1.8135E-01  6.3545E-02  3.3573E-01  6.6233E-01  7.1032E-01  4.6786E-02  3.8043E-C2
-5.3182E-02  1.7099E-01 -1.46C8L-02  3.1015E-01  4.8740E-01  9.8767E-01  1.0305E-01  2.7744E-02
 6.3076E-02  1.2978E-01 -2.4715E-02  2.4621E-01  4.3194E-01  1.2814E-01 -1.1502E-C2  1.5498E-C2
 6.4540E-03  1.3928E-C2 -2.5C45E-03  2.1265E-02  1.8576E-02 -1.6517E-02  1.0C00E 00 -4.7589E-C3
 4.6882E-02  6.2859E-02 -1.5532E-C2  1.7214E-01  3.6132E-01  4.8823E-02 -2.C849E-02  1.3817E-02
 5.6170E-02  1.1794E-01 -2.3753E-02  2.5890E-01  4.6797E-01  1.18C0E-01 -5.0782E-02  1.8281E-C2
 1.8568E-02  4.0361E-02 -7.7923E-03  7.52C4E-02  7.9424E-02 -1.1726E-01 -6.6253E-02  1.0000E 00
-4.3936E-01 -1.4275E-01 -3.2384E-C1  7.0616E-01  6.4154E-01  5.6806E-02 -7.2463E-02  3.2352E-C3
 1.0000E CO  1.0000E 00  1.0C0E 0C  9.4764E-01  1.0000E 0C  8.33C5E-01  5.C46CE-02  4.1121E-02
-3.2998E-01  2.4190E-C1 -5.4076E-C2  1.0000E 00  6.9644E-01  2.8523E-01 -1.2090E-02 -7.0826E-03
```

37

THE MATRIX OF MODE SHAPES, IN MAG. AND ANGLE(DEG.) FORM

	1	2	3	4	5	6	7	8
1	-0.7713D-02	-0.2273D-01	-0.2266D-01	0.6921D-03	-0.2909D-03	0.4443D-01	0.3539D-01	-39.99
2	0.2683D-02	-0.6618D-02	-0.1653D-01	0.1867D-05	0.2513D-05	-0.5983D-01	0.5936D-01	-57.10
3	0.3630D-01	0.7135	-0.1232	0.1047D-03	-0.4591D-04	0.5779D-01	0.3146	10.28
4	1.000	1.000	-0.2133	0.1751D-03	-0.6331D-04	-0.2977D-01	0.2711	4.915
5	-0.1130	-0.4548	-0.3129D-01	-0.4161D-03	0.1690D-03	0.5949D-01	0.3212	3.847
6	0.6669D-03	0.5400D-02	0.7764D-02	-0.2282D-03	0.9717D-04	-0.2704D-01	0.6647D-01	-145.6
7	0.1291D-02	0.1059D-01	0.8492D-02	-0.1412D-03	0.5966D-04	-0.2987D-01	0.1174	-136.0
8	-0.1017D-02	-0.1911D-01	0.9663D-02	0.7502D-04	-0.3337D-04	0.3412D-01	0.5499D-01	112.6
9	0.3791D-03	0.1228D-01	0.3717	-0.4874D-04	-0.4042D-04	1.000	0.8298	111.5
10	0.5015D-04	0.1609D-02	0.4600D-01	-0.5926D-05	-0.4917D-05	0.1199	0.9652D-01	108.6
11	-0.4492D-02	-0.5314D-01	-0.8897D-01	-0.6223D-05	0.2761D-05	0.1377	0.3934	140.2
12	-0.1898D-01	0.1291D-02	1.000	-0.1798D-01	0.7514D-02	-0.8174	0.7190	132.6
13	-0.7549D-03	0.5073D-03	0.3795	-0.6742D-02	0.2817D-02	-0.3033	0.2612	130.4
14	-0.1122D-02	0.2437D-01	0.1975	-0.1998D-02	0.8253D-03	-0.2305D-01	0.3760	37.11
15	0.2185D-04	-0.7731D-04	-0.3760D-02	0.9825D-04	-0.4158D-04	0.2473D-01	0.1489	89.94
16	-0.1394D-01	-0.2158D-01	-0.5932	1.000	1.000	-0.1673	1.000	0.0000

	9	10	11	12	13	14	15	16
1	0.1648D-01	131.1	-0.1682D-02	0.6493D-01	0.6248	1.000	0.8067D-01	0.5902D-01
2	0.1210D-01	151.5	0.2965D-02	-0.3951D-01	-0.1012	0.6882	0.1159	0.2717D-02
3	0.1206	-86.48	0.1958D-02	0.8150D-01	-0.9995D-01	0.9555	0.1499	0.2763D-02
4	0.1119	-86.76	0.1186D-02	0.8847D-01	-0.1908D-01	0.8507	0.1105	0.7128D-02
5	0.8495D-01	-98.68	-0.1094D-01	0.3665	0.6440	0.7413	0.4523D-01	0.3544D-01
6	0.3475D-01	74.32	-0.3008D-02	0.2159	0.6464	0.7329	0.5009D-01	0.4062D-01
7	0.1288	140.3	0.6354D-01	0.3357	0.6623	0.7103	0.4679D-01	0.3804D-01
8	0.1266	-62.28	-0.1481D-01	0.3102	0.4874	0.9877	0.1031	0.2774D-01
9	0.1020	-19.08	-0.2471D-01	0.2462	0.4319	0.1281	-0.1150D-01	0.1550D-01
10	0.1085D-01	-20.14	-0.2504D-02	0.2127D-01	0.1858D-01	-0.1652D-01	1.000	-0.4759D-02
11	0.5545D-01	-8.283	-0.1553D-01	0.1721	0.3613	0.4882D-01	-0.2085D-01	0.1382D-01
12	0.9237D-01	-19.53	-0.2375D-01	0.2589	0.4880	0.1180	-0.5078D-01	0.1828D-01
13	0.3143D-01	-20.31	-0.7792D-02	0.7520D-01	0.7942D-01	-0.1173	-0.6625D-01	1.000
14	0.3267	-153.0	-0.3238	0.7062	0.8415	0.5681D-01	-0.7246D-01	0.3235D-02
15	1.000	0.0000	1.000	0.9476	1.000	0.8330	0.5046D-01	0.4112D-01
16	0.2893	-98.75	-0.5409D-01	1.000	0.6964	0.2852	-0.1209D-01	-0.7083D-02

Operating Point 3

```
THE A MATRIX
-7.118      1.866     0.9745     397.1     -563.2    -21.13     -3.848     -1.481
-2.835     -7.777     115.6     -233.6     -70.35     25.26     -3.812     -3.762
 8.490      7.988    -163.7     -.2650     211.8     -83.04     11.38      7.282
 1.400     -.3630     133.3     -572.1     23.25      -7.678    1.041     -2.993
 0.1203    -.2073     1.181      21.80     -105.4     2.468     -.3738     -.1777
 0.6972    -.1376     0.3516     0.0000    6.419     -18.41     0.3450     0.0000
 0.5281    -.3273     0.8162    -.1850D-01 14.28      3.792     -19.25     0.5000D-05
-.7211      0.8281    13.64      0.1230D-01 -17.97    26.03     -.9668     -20.00
-.3884D-01 -.3956D-02 0.9495D-01 -.5394D-01 -.8606    0.3953    -.5494D-01 6.064
-.5766D-03 -.5765D-04 0.1401D-02 -.8220D-03 -.1275D-01 0.5852D-02 -.8241D-03 0.8984D-01
-6.105     -5.132     13.22      0.2385    -152.3     59.70     -8.183     38.14
-.8092D-01 -.3641     -34.88     128.7     -2.238     0.7838    -.9891D-01 9.079
-.3594D-02 -.1619D-01 -1.550     5.719     -.9943D-01 0.3484D-01 -.4340D-02 0.4035
-.1780     -.2163     -15.82     103.2     0.9455     -.1252     4.154
 0.3153D-02 0.1388D-01 -.3637D-01 0.0000   0.4131    -.1592     19.92      0.8839D-01
-.8383      0.9513    -.3655     68.67     30.24     -10.86     1.626     -.4284

 1.550      1.679     -6.161     15.06     15.01      -1.229    -.2620     0.0000
 17.82      17.71     -6.320     0.7500D-02 0.0000    -.1200D-01 -.2540     0.2000D-02
-.4000D-02 -.8000D-01 8.779     -.1500D-02 0.3000D-01 0.4800D-01 0.7735    -.5000D-03
-4.679     -4.890     9.353     0.2000D-02 -.3500D-01 0.1500D-01 0.7100D-01 0.0000
 0.1745     0.1900    -.7062     0.1850D-02 -.5000D-02 1.237     1.087      0.1850D-02
 0.5000D-05 0.6750D-02 0.0000   -.9950D-03 0.0000    0.1885D-02 0.2298D-01 0.0000
 0.0000    -.6750D-02 0.1775D-02 -.2450D-03 0.5000D-04 0.4845D-02 0.4540D-01 0.0000
-.5000D-05  0.6650D-02 -.1295D-02 -.5000D-05 0.0000   -.5380D-02 -.6512D-01 -.1000D-04
-50.00     -.4216D-02 39.76      0.0000    0.0000    -.2017D-02 0.4102D-02 -.5000D-06
-.6667     -.6668     0.5890     0.0000    0.0000    -.3585D-04 0.7293D-04 -.5000D-04
-.5000D-04  0.5450D-01 -48.02    -.3150D-02 -.2650D-01 -.3495D-01 -.5537    -.5000D-04
-9.804     -9.737     38.94      -50.00    -.1120D-01 -.4030D-02 0.4110D-02 -.3530D-02
-.4357     -.4327     1.731      -2.001    -2.001    -.1610D-03 0.2195D-03 -.1410D-03
-4.482     -4.453     17.80      -3.254    -3.243     -19.75    0.1650D-02 -.1055D-02
 0.0000     0.0000    0.1341D-01 0.0000    0.5000D-05 0.0000    -20.00     0.5000D-06
 0.5574     0.5740    -2.230     0.1000D-03 0.5000D-03 26.54     23.94      -50.00

THE B MATRIX
-.9729E-01 -289.8      -232.8     34.54     -263.5
-.2765E-02 -3.460      -94.89    -40.11     -3370.
 0.1787     36.58      283.6      130.2      0.3810E 05
 0.4793E-01 -3.310     26.23      11.58     -1975.
 0.2797E-02 -1683.     13.05      -3.948    -97.15
 0.1244E-01 47.03      4.230      -2.671     18.85
 0.5821E-02 7.420      18.04      -6.084     10.70
-.4372E-02 -4.640      -24.06     -12.02     41.55
 0.2657E-01 0.6600E-01 -1.283     -.6392     2224.
 0.3990E-03 0.1020E-02 -.1919E-01 -.9632E-02 32.88
 4.026      -12.75     -204.1     -94.11    -.2787E 05
 0.8976E-01 -3.403     -2.659     -1.222     2522.
 0.4012E-02 -.1501     -.1189     -.5480E-01 112.0
 0.5541E-01 -2.712     -1.083     -1.499     1059.
-.1342E-04 -.7605      -.1646     0.2648    -3.620
 0.1325E-01 -44.38     -64.71     17.04     -327.5

THE C MATRIX
-.7961      -1.038     5.860      106.9     117.2      12.38     -1.730     -.8501
 0.3337E-01 0.5960E-03 -.1495E-02 0.0000    -.2830E-01 -.6924E-02 -.1510E-02 0.0000
 0.0000     0.0000     0.0000     0.0000    0.0000     0.0000    0.0000     0.0000
 0.5234E-04 0.3697E-04 -.9496E-04 0.1800E-05 -.1737E-C2 -.4301E-03 -.9341E-04 0.3550E-07
 0.8548E-04 0.8850E-04 0.1613E-02 -.2440E-05 0.2132E-02 -.4684E-03 0.1146E-03 -.1050E-07
 0.2008E-04 0.1128E-04 -.2881E-04 0.2900E-05 -.3694E-02 -.1315E-03 0.1039E-03 -.4000E-07
 0.1282E-05 0.1046E-04 -.2706E-04 0.9000E-06 -.9298E-03 -.5421E-04 0.5207E-04 -.7500E-08

 0.8784     0.9275     -3.448     -.1300E-02 0.1650E-01 6.051     5.333     -.2500E-02
-.4999E-08 -.1000E-06  -.4999E-08 -.9997E-08 -.1000E-06 -.5000E-07 -.1094E-03 0.0000
 0.0000     0.0000     1.000      0.0000    0.0000     0.0000    0.0000     0.0000
 0.1150E-07 0.5900E-06 -.1225E-06 0.3000E-07 -.4999E-08 -.3780E-06 -.6354E-05 -.4998E-09
-.3150E-07 -.8150E-06  0.1520E-06 0.4998E-09 0.3350E-06 0.4895E-06 0.7780E-05 -.1650E-07
 0.3150E-07 0.1405E-05 -.2945E-06 0.6000E-07 -.1000E-07 -.1062E-05 -.1379E-04 -.5000E-08
 0.2000E-08 0.4750E-06 -.6700E-07 -.3000E-08 0.0000    -.2990E-06 -.3305E-05 -.4998E-09
```

THE D MATRIX
```
-.5910E-02-222.3     -10.56     -19.33     -313.5
0.2134E-C3 1.006      1.797     C.1C76E-01-2.711
0.0000     0.0000     0.000C     0.0000     0.0000
0.8332E-060.5758E-02-.2924E-C20.6260E-03-.4040E-02
0.3888E-060.2530E-030.2863E-020.2804E-02-.6805E-02
C.3785E-06C.5352E-02-.5275E-030.1622E-030.4470E-02
0.3080E-070.1017E-020.3733I-03C.1966E-03-.1025E-02
```

   EIGENVALUES OF THE A MATRIX
REAL PART   IMAGINARY PART

```
   -570.10107      0.00000000
   -197.71367      0.00000000
    -83.236343     0.00000000
    -61.849380     0.00000000
    -49.990326     0.00000000
    -44.194748     0.00000000
    -33.174606     0.00000000
     -9.0144463    3.8102236
     -9.0144463   -3.8102236
    -23.922791     4.4413338
    -23.922791    -4.4413338
     -5.2559175    0.00000000
    -19.180176     0.00000000
     -0.68158114   0.00000000
    -20.934601     0.00000000
     -2.0057840    0.00000000
```

MODIFIED EIGENVECTOR MATRIX
```
-1.1233E-02 -4.4336E-02  1.8556E-C2 -3.1513E-02 -1.2759E-04 -8.8030E-02 -3.4469E-02  7.5859E-01
 4.7579E-03 -8.9331E-03  3.5777E-03 -2.7854E-02  1.1519E-05  8.9281E-02 -1.1673E-01 -1.2369E-01
 8.7737E-03  7.6875E-01  3.7650E-01 -1.4312E-01 -2.8009E-05 -8.2266E-02 -1.1282E-01  3.3592E-01
 1.0000E 00  1.0000E 00  4.6786E-C1 -2.4209F-01 -1.0459E-05 -2.3555E-03 -1.4015E-01  3.9400E-01
-1.1567E-01 -7.0228E-01  1.0000E 00 -1.5636E-02  7.9372E-04 -1.1499E-01 -2.0753E-01  8.1150E-01
 2.7634E-04  2.6939E-03 -1.0565E-02  5.5912E-03  2.2756E-05  3.7422E-02  1.1551E-02  6.8204E-01
 3.8040E-04  2.9153E-03 -2.0178E-02  3.1365E-03 -1.0307E-06  4.0475E-02 -8.9418E-03  7.4680E-01
-3.8844E-04 -2.5517E-02 -1.5673E-C2  1.6056E-02 -9.5365E-06 -4.8931E-02  6.6439E-02  4.5816E-01
 9.1730E-05  1.0754E-02 -1.2179E-01  3.8384E-01 -1.8046E-04 -9.3122E-01  1.0000E 00  9.9085E-02
 1.2161E-05  1.4027E-03 -1.5390E-02  4.7567E-02 -2.1954E-05 -1.1184E-01  1.1560E-01 -2.9048E-03
-1.0258E-03 -3.3130E-C2  8.9517E-C2 -1.0010E-01  6.4331E-07 -1.1361E-01  3.5930E-01  8.4279E-02
-1.9684E-02  6.5456E-04 -2.2830E-C1  1.0000E 00  2.8674E-03  1.0000E 00  5.3165E-01  1.5179E-01
-7.8305E-03  2.5991E-04 -8.7971E-02  3.8009E-01  1.0737E-03  3.7178E-01  1.9228E-01  9.8809E-03
-1.6600E-03  3.5665E-02 -1.0184E-01  2.0469E-01  2.3148E-04  4.7414E-02 -1.7231E-01  9.8003E-02
-7.8547E-06 -4.8264E-05  5.9332E-02 -1.3264E-03  1.0189E-07 -3.2952E-02  1.3720E-02  1.0000E 00
-1.4926E-02 -5.6702E-02 -2.9100E-02 -5.0715E-01  1.0000E 00  2.9625E-01 -5.2436E-01  2.0657E-01
```

```
-1.4427E-01  3.3814E-02  9.1899E-02  9.4850E-01 -4.1088E-03  9.1783E-02 -4.2327E-03  5.1845E-02
-1.3081E-01  1.0881E-04  1.2146E-01  2.9088E-01  4.0614E-03  9.1188E-02 -7.0472E-03 -9.2160E-03
-2.1557E-01  2.0574E-01  1.9392E-C1  1.0000E 00  1.3254E-02  1.6488E-01 -9.8844E-05  2.3134E-02
-1.8068E-01  1.8696E-01  1.8163E-01  9.5269E-01  1.1499E-02  1.2846E-01  5.3270E-04  2.6319E-02
 3.7642E-01  4.4511E-01  4.5244E-01  9.5824E-01  1.3388E-02  6.2465E-02  2.0661E-02  3.5111E-02
 2.0787E-01 -1.2290E-01 -3.7883E-02  6.1444E-01 -3.6761E-03  3.6351E-02  2.2611E-03  2.9050E-02
 3.6143E-01 -7.9929E-02 -1.0378E-01  6.0248E-01  4.1344E-03  2.2648E-02 -4.7282E-03  3.0759E-02
 2.6523E-01  6.2967E-02 -2.0304E-01  6.9842E-01 -4.1262E-03  7.6402E-02  2.0185E-02  1.0316E-02
 4.0012E-01  1.1312E-01 -7.8444E-01 -2.4293E-02 -2.2087E-02 -2.5811E-02  3.7801E-02 -5.5420E-03
 3.3049E-C2  1.5965E-02 -8.5307E-C2 -1.8163E-04 -2.2596E-03  1.0000E 00  3.9618E-03  1.6512E-03
 3.2490E-01 -1.6224E-02 -4.3730E-C1 -7.9636E-02 -1.4455E-02 -3.3727E-02  2.2091E-02 -6.5210E-02
 4.3131E-C1  2.6721E-02 -6.8659E-01 -2.2416E-02 -2.0752E-02 -6.5657E-02  3.4782E-02 -4.4273E-03
 1.2560E-01  1.6563E-02 -2.3642E-C1 -6.9221E-04 -6.8635E-03 -8.5635E-02  1.1714E-02  1.0000E 00
 8.8670E-01  7.0688E-01  5.7621E-C1 -8.3191E-02 -4.1389E-01 -8.8379E-02 -3.8300E-01 -2.7052E-02
 1.0000E 00  2.0002E-01 -1.7152E-C1  5.1775E-01  1.0000E 00  2.4545E-02  1.0000E 00  3.3741E-02
 1.0646E 00  1.0000E 00  1.0000F C0  2.5317E-01  4.2861E-02 -2.8312E-02  6.7497E-02 -1.5317E-02
```

THE MATRIX OF MODE SHAPES, IN MAG. AND ANGLE(DEG.) FORM

	1	2	3	4	5	6	7	8
1	-0.1123D-01	-0.4434D-01	0.1856D-01	-0.3151D-01	-0.1276D-03	-0.8803D-01	-0.3447D-01	0.5460
2	0.4758D-02	-0.8933D-02	0.3578D-02	-0.2785D-01	0.1152D-04	0.8928D-01	-0.1167	0.1273
3	0.8774D-02	0.7687	0.3765	-0.1431	-0.2801D-04	-0.8227D-01	-0.1128	0.2822
4	1.000	1.000	0.4679	-0.2421	-0.1046D-04	-0.2356D-02	-0.1401	0.3065
5	-0.1157	-0.7023	1.000	-0.1564D-01	0.7937D-03	-0.1150	-0.2075	0.6325
6	0.2763D-03	0.2694D-02	-0.1057D-01	0.5591D-02	0.2276D-04	0.3742D-01	0.1155D-01	0.5042
7	0.3804D-03	0.2915D-02	-0.2018D-01	0.3136D-02	-0.1031D-05	0.4048D-01	-0.8942D-02	0.5867
8	-0.3884D-03	-0.2552D-01	-0.1567D-01	0.1606D-01	-0.9536D-05	-0.4893D-01	0.6644D-01	0.3743
9	0.9173D-04	0.1075D-01	-0.1218	0.3838	-0.1805D-03	-0.9312	1.000	0.2915
10	0.1216D-04	0.1403D-02	-0.1539D-01	0.4757D-01	-0.2195D-04	-0.1118	0.1156	0.2346D-01
11	-0.1026D-02	-0.3313D-01	0.8952D-01	-0.1001	0.6433D-06	-0.1136	0.3593	0.2373
12	-0.1968D-01	0.6546D-03	-0.2283	1.000	0.2867D-02	1.000	0.5317	0.3233
13	-0.7830D-02	0.2599D-03	-0.8797D-01	0.3801	0.1074D-02	0.3718	0.1923	0.8979D-01
14	-0.1660D-02	0.3566D-01	-0.1018	0.2047	0.2315D-03	0.4741D-01	-0.1723	0.6308
15	-0.7855D-05	-0.4826D-04	0.5933D-02	-0.1326D-02	0.1019D-06	-0.3295D-01	0.1372D-01	1.000
16	-0.1493D-01	-0.5670D-01	-0.2910D-01	-0.5071	1.000	0.2963	-0.5244	0.7668

	9	10	11	12	13	14	15	16
1	55.77	0.6924D-01	-24.80	0.9485	-0.4109D-02	0.9178D-01	-0.4233D-02	0.5185D-01
2	178.4	0.8588D-01	-44.95	0.2909	0.4061D-02	0.9119D-01	-0.7047D-02	-0.9216D-02
3	77.69	0.1999	1.693	1.000	0.1325D-01	0.1649	-0.9864D-04	0.2313D-01
4	69.64	0.1843	0.8250	0.9327	0.1150D-01	0.1285	0.5327D-03	0.2632D-01
5	20.12	0.4486	-0.4679	0.9582	0.1339D-01	0.6246D-01	0.2066D-01	0.3511D-01
6	28.05	0.9094D-01	-152.1	0.6144	-0.3676D-02	0.3635D-01	0.2261D-02	0.2905D-01
7	19.17	0.5699D-01	-142.4	0.6025	0.4134D-01	0.2265D-01	-0.4728D-01	0.3076D-01
8	14.93	0.1503	117.8	0.6984	-0.4126D-02	0.7640D-01	0.2018D-01	0.1032D-01
9	-31.09	0.5604	126.8	-0.2429D-01	-0.2209D-01	-0.2581D-01	0.3780D-01	-0.5542D-02
10	-50.02	0.6137D-01	124.4	-0.1816D-03	-0.2260D-02	1.000	0.3962D-02	0.1651D-02
11	-30.46	0.3094	137.1	-0.7964D-01	-0.1445D-01	-0.3373D-01	0.2209D-01	-0.6521D-02
12	-25.61	0.4859	132.8	-0.2242D-01	-0.2075D-01	-0.6566D-01	0.3478D-01	-0.4427D-02
13	-40.54	0.1690	131.0	-0.6922D-03	-0.6863D-02	-0.8564D-01	0.1171D-01	1.000
14	-38.69	0.6449	5.815	-0.8319D-01	-0.4139	-0.8833D-01	-0.3830	-0.2705D-01
15	0.0000	0.1863	85.61	0.8178	1.000	0.2455D-01	1.000	0.3374D-01
16	-34.02	1.000	0.0000	0.2532	0.4286D-01	-0.2831D-01	0.6750D-01	-0.1532D-01

THE A MATRIX
```
-1.171      0.5732D-01 5.183      416.7      -813.2     -.7133     0.4008     -.3028
-.1259      -1.502     130.4      -238.2     -424.5     7.532      0.6992     -.7102
0.2984      1.642      -159.5     -5.241     1034.      -23.32     -1.652     1.445
0.1538      -.3350D-02 129.6      -559.6     118.0      -2.592     -.1830     -.5880
0.3205D-01-.4310D-01 1.120       21.34      -110.4     0.6823     0.4963D-01-.3341D-01
0.8100      -.1984D-010.2541      -1.292     160.5      -19.72     -.2917     0.1410D-02
0.6266      -.6680D-020.7950D-01-2.265      412.0      0.7880D-01-20.49     -.4240D-02
-.1078      0.7927     57.93      1.965      -391.9     30.44      0.5966     -20.01
-.9830D-02-.1767D-010.5607      -.4675D-01-31.96      0.7294     0.4744D-01 6.992
-.1460D-03-.2618D-030.8471D-02-.6230D-03-.4739      0.1082D-010.7028D-030.1036
-1.446      -7.291     85.01      25.60      -5015.     113.0      7.993      35.69
-.3360D-01-.5103      -195.7     734.9      -113.3     2.543      0.1687     10.23
-.1493D-02-.2268D-01-8.698      32.66      -5.033     0.1130     0.7518D-020.4545
-.1764      -.2732     -89.49     70.34      551.8      1.776      0.1139     4.698
-.1324D-010.3146D-01-.3588     -.7485D-01 21.57      -.4884     19.81      0.1307
-1.826      1.995      -10.37     438.1      1342.      -30.62     -2.177     -.4800
```
```
0.2768      0.2600     -1.128     2.679      2.579      -.2007     -.8355D-010.5000D-04
3.081       3.063      -1.105     0.1330D-020.1195D-010.5000D-05-.1115      0.0000
-.7950D-02-.9000D-02 1.484       -.1350D-02-.2400D-010.2800D-020.2718      -.5000D-04
-.7597      -.7625     1.559      0.1300D-02-.5000D-030.1350D-020.2800D-01-.5000D-04
0.2914D-010.2897D-01-.1170      0.1400D-030.1600D-020.1978      0.1224      0.5000D-05
-.2590D-02-.1000D-030.8675D-020.0000      -.7150D-020.8400D-030.7112D-01-.1000D-04
0.1900D-030.2500D-010.8160D-02-.5000D-050.2850D-01-.2835D-020.1136      0.0000
0.3195D-020.1000D-03-.1174D-010.5000D-050.1910D-01-.2255D-02-.9690D-010.1000D-04
-50.00      0.5000D-05 39.27      -.6600D-03-.5935D-020.2121D-02-.1743D-010.1000D-05
-.6666      -.6667     0.5818     -.8795D-05-.7915D-040.2826D-04-.2556D-030.0000
0.3890D-010.3250D-01-47.72      0.7350D-020.9550D-01-.2040D-01-1.325      0.0000
-9.405      -9.419     38.26      -50.00     -.5900D-020.7100D-03-.4356D-010.0000
-.4180      -.4187     1.700      -2.000     -2.000     0.2850D-04-.1952D-020.0000
-4.323      -4.336     17.59      -3.192     -3.090     -19.76     -.4459D-010.5000D-05
-.3985D-03-.5000D-050.2042D-01-.5000D-06-.5000D-050.5650D-03-20.00     -.1000D-05
0.5985      0.6006     -2.424     0.5000D-04-.4150D-01 30.85      20.40      -50.00
```

THE B MATRIX
```
-.4110E-01-61.57      -30.09     0.1855     -186.0
0.1934E-01 66.33      -1.522     -17.26     -3519.
0.1314      -145.4     3.577      16.34      0.5214E 05
0.4105E-01-15.21      0.3764     1.761      -1807.
0.4120E-03-299.5      1.778      -.5378     -161.4
-.6090E-02 18.11      11.88      -.7660E-01 310.0
0.2773E-01 29.35      10.44      0.3425     301.6
-.2121E-01 46.18      -1.270     9.650      -1060.
0.1767      3.432      -.1280     -.5200     0.2296E 05
0.2580E-020.2711E-01-.1759E-02-.7722E-02 340.4
24.47       664.1      -17.71     -81.35     -.2642E 06
0.5307      5.621      -.4019     -1.904     0.2397E 05
0.2382E-010.3991      -.1873E-01-.8444E-01 1063.
0.3357      29.72      0.3654     -1.290     9662.
-.1354E-02-4.450      -.7336     0.3485     17.73
0.7771E-01-239.0      -83.75     21.10      162.5
```

THE C MATRIX
```
0.5118E-01-.2216      5.798      111.8      -69.26     3.520      0.2494     -.1784
0.4174E-020.1718E-05-.6230E-040.2339E-03-.1401E-01-.3105E-040.3074E-04-.4427E-05
0.0000      0.0000     0.0000     0.0000     0.0000     0.0000     0.0000     0.0000
0.1565E-030.6509E-05-.6405E-040.3292E-03-.6320E-01-.1005E-030.1021E-03-.4650E-06
0.2064E-040.1447E-03-.1057E-01-.3652E-030.7187E-01-.1354E-02-.1143E-030.3800E-06
0.1645E-04-.3027E-040.3587E-030.3111E-03-.5873E-010.4691E-030.2237E-03-.3050E-06
0.9703E-050.4620E-05-.5000E-040.7630E-04-.1504E-010.3944E-040.8110E-04-.1250E-06
```
```
0.1523      0.1516     -.6119     -.2000E-030.3500E-02 1.074      0.6558     0.0000
0.2490E-050.2241E-04-.212E-050.0000      0.2971E-04-.3533E-05-.8715E-050.0000
0.0000      0.0000     1.000      0.0000     0.0000     0.0000     0.0000     0.0000
0.5625E-060.8900E-06-.1787E-050.5000E-080.2000E-05-.3150E-06-.1692E-040.4999E-08
-.5140E-06-.5200E-060.1958E-05-.2000E-07-.1550E-050.2450E-060.1851E-040.0000
0.2460E-060.1000E-07-.1582E-050.0000      0.1485E-05-.2650E-06-.1523E-040.0000
0.2950E-070.4999E-08-.4360E-060.0000      0.7300E-06-.9250E-07-.3963E-050.4998E-09
```

THE D MATRIX
```
0.0000      66.03      4.466     -2.460    -628.6
0.9570E-040.1070      0.1739     0.1800E-03-3.110
0.0000      0.0000     0.0000     0.0000     0.0000
0.1328E-040.2139E-01-.4313E-020.6746E-04-.7927
0.8977E-06-.9988E-020.2439E-030.1963E-020.1017E-01
0.1250E-060.9305E-020.1191E-02-.3588E-03-.6599E-01
0.2500E-060.2435E-020.5341E-030.3421E-04-.1645E-01
```

    EIGENVALUES OF THE A MATRIX
    REAL PART   IMAGINARY PART

```
    -547.34229        0.00000000
    -242.02245        0.00000000
    -63.958786        0.00000000
    -33.659134        16.220993
    -33.659134       -16.220993
    -50.000046        0.00000000
    -43.145950        0.00000000
    -38.926193        0.00000000
    -21.324432        0.00000000
    -20.143570        1.0338373
    -20.143570       -1.0338373
    -13.043441        0.00000000
    -2.0527363        0.00000000
    -1.5882740        0.00000000
    -0.84857059       0.00000000
    -0.68102890       0.00000000
```

MODIFIED EIGENVECTOR MATRIX
```
-2.2230E-03 -6.6168E-03 -4.9358E-03  3.1688E-03  1.8144E-02 -1.1993E-07  9.5710E-03  4.1238E-05
 7.5756E-04 -1.8480E-03 -4.4930E-03 -7.5024E-03  1.8652E-02  7.0025E-08 -1.5317E-02 -1.6142E-02
 3.9353E-02  7.2256E-01 -2.1814E-01  5.7012E-01  1.7232E-01 -7.0356E-06  2.3303E-02 -3.4759E-02
 1.0000E 00  1.0000E 00 -3.3354E-01  4.5838E-01  1.5090E-01 -1.1374E-05 -6.8452E-02 -1.0047E-01
-1.1814E-01 -4.6664E-01 -1.1486E-01  5.6896E-01  3.4104E-01 -7.0541E-08 -1.2389E-02 -7.8540E-02
 7.0958E-04  5.8061E-03  7.9861E-03 -8.3142E-02  2.3245E-02  6.8296E-07 -3.6595E-03  1.0412E-02
 1.6463E-03  1.4218E-02  1.7504E-02 -1.9626E-01  6.6595E-02  1.7676E-08 -7.6025E-04  2.6492E-02
-1.1070E-03 -2.0471E-02  1.0254E-02  1.7391E-02 -3.2996E-02  2.8418E-07  1.7098E-03 -7.6388E-03
 4.5213E-04  1.3700E-02  4.1954E-01  6.7089E-01 -1.0028E 00 -3.5207E-06  1.0000E 00  1.0000E 00
 5.9798E-05  1.7940E-03  5.2113E-02  8.6958E-02 -1.1490E-01 -4.2675E-07  1.1974E-01  1.1823E-01
-5.1750E-03 -5.7308E-02 -1.2658E-01 -1.1496E-01 -5.8957E-01 -3.5740E-08  1.4890E-01  2.4128E-01
-1.9547E-02  2.7481F-03  1.0000E 00  1.8891E-01 -1.2252E 00  2.3493E-05 -6.8257E-01  9.6690E-02
-7.7731E-03  1.0854E-02  3.8051E-01  8.8657E-02 -4.5035E-01  8.8073E-06 -2.5303E-01  3.5564E-02
-6.9161E-04  2.7272E-02  2.1527E-01  4.8815E-01 -1.1413E-01  1.1205E-06 -1.4918E-02 -1.5579E-02
 2.3238E-05 -3.2092E-04 -6.9057E-03  6.2566E-02 -1.7339E-01  4.6238E-08  7.4150E-04 -2.6372E-02
-1.4625E-02 -2.2198E-02 -3.9661E-01  1.0000E 00  1.0000E 00  1.0000E 00 -1.9590E-01 -2.9190E-01
```

```
-4.6184E-03  2.4202E-04 -3.0669E-03  1.1864E-02 -1.5433E-01  1.0000E 00  1.0000E 00  5.4442E-01
-2.3999E-03  7.2430E-04 -1.6469E-03 -5.1074E-03 -1.5730E-03  2.1310E-02  6.8185E-01  4.6742E-01
 6.3475E-02 -2.7162E-02  1.4038E-02  1.5441E-01 -1.4170E-02  7.1875E-02  9.4588E-01  6.3415E-01
 5.7825E-02 -2.5127E-02  1.2364E-02  1.4369E-01 -2.5484E-02  1.4598E-01  8.3242E-01  5.3156E-01
-1.7936E-02 -2.5885E-02 -2.4534E-02  3.6761E-01 -1.2887E-01  7.4616E-01  7.3387E-01  3.8498E-01
-2.0655E-02  7.5549E-03 -1.8442E-03  1.5645E-01 -1.1810E-01  7.3254E-01  6.8965E-01  3.6848E-01
-6.9071E-02  4.6350E-02 -6.0195E-02  3.4825E-01 -1.1990E-01  7.3025E-01  6.9093E-01  3.6771E-01
 9.7194E-02 -3.4953E-02  4.6534E-02  2.7099E-01 -7.6491E-02  4.7154E-01  8.5674E-01  5.2030E-01
 7.2964E-02 -2.1813E-02  5.4464E-02  1.2955E-01 -3.7265E-02  2.3448E-01  7.1807E-03 -2.4968E-02
 7.6854E-03 -2.3489E-03  5.6144E-03  1.1217E-02  1.0588E-02 -1.1602E-01 -2.2515E-02  1.0000E 00
 3.7397E-02 -9.9504E-03  3.1947E-02  8.1351E-02 -3.2300E-02  2.0643E-01 -6.4756E-02 -7.0711E-02
 6.8086E-02 -2.0290E-02  5.1141E-02  1.3743E-01 -4.5209E-02  2.8581E-01 -1.7694E-02 -8.0364E-02
 2.3021E-02 -6.9710E-03  1.7621E-02  4.0107E-02  1.0000E 00  9.4335E-01 -2.6224E-02 -1.0557E-01
-3.0036E-01 -3.0055E-01 -3.1042E-01  4.2595E-01 -8.7823E-02  3.8514E-01 -9.7337E-02 -1.4303E-01
 1.0000E 00  1.0000E 00  1.0000E 00  1.0000E 00 -1.3022E-01  7.7193E-01  7.2346E-01  3.8480E-01
-2.0736E-02 -6.0929E-02 -6.5086E-02  7.9306E-01 -4.8297E-02  1.3458E-01  1.1804E-01  3.6657E-02
```

THE MATRIX OF MODE SHAPES, IN MAG. AND ANGLE(DEG.) FORM

	1	2	3	4	5	6	7	8
1	-0.2197D-02	-0.1153D-01	-0.4396D-02	0.7824D-02	-164.3	-0.4072D-05	-0.9809D-02	0.5459D-03
2	0.6751D-03	-0.2812D-02	-0.3052D-02	0.3223D-02	118.5	-0.3900D-09	0.5419D-02	0.1856D-02
3	0.5541D-02	1.000	-0.2642	0.3173D-01	-31.38	0.9352D-06	-0.1298D-01	0.2297
4	1.000	0.8272	-0.3965	0.3507D-01	36.84	0.8960D-05	0.6525D-03	0.2474
5	-0.9121D-01	-0.7889	-0.3104	0.9526D-01	-51.18	0.1602D-04	0.6525D-03	0.3625
6	0.1431D-03	0.4772D-02	0.5277D-02	0.2216D-02	115.5	0.1116D-06	0.1789D-02	-0.6282D-01
7	0.3565D-03	0.1121D-01	0.1225D-01	0.5706D-02	132.0	-0.3389D-06	0.2144D-02	-0.1352
8	-0.2747D-03	-0.4910D-01	0.2056D-01	0.2794D-02	-134.7	-0.1442D-06	-0.7412D-03	0.8884D-01
9	0.7902D-04	0.2243D-01	0.3832	0.3229	-65.13	0.6268D-05	-0.5015	-0.7742D-01
10	0.1031D-04	0.2896D-02	0.4760D-01	0.3928D-01	-65.76	0.7621D-06	-0.6032D-01	-0.8281D-02
11	-0.8355D-03	-0.3920D-01	-0.1222	0.4027D-01	22.10	0.1879D-07	-0.5261D-01	-0.5331D-01
12	-0.2523D-01	0.7107D-01	1.000	1.000	0.0000	0.5109D-03	1.000	-0.5024D-01
13	-0.1004D-01	0.2783D-01	0.3809	0.3754	-0.4534	0.1916D-03	0.3723	-0.1718D-01
14	-0.2626D-02	0.7735D-01	0.2047	0.1120	-32.35	0.4552D-04	0.2530D-01	0.5201D-01
15	-0.2633D-04	-0.1725D-02	-0.5016D-02	0.3714D-02	-36.69	0.2553D-06	-0.1567D-02	1.000
16	-0.1674D-01	-0.9920D-01	-0.2274	0.6603	-120.1	1.000	0.1936	0.9312

	9	10	11	12	13	14	15	16
1	0.2372D-01	0.5491D-02	147.0	1.000	0.7954	1.000	-0.1131D-02	-0.1104
2	-0.5486D-02	0.2263D-02	157.3	0.2221	0.2161	-0.2517D-01	0.3081D-03	0.1150D-02
3	0.7662D-02	0.1272	-78.59	0.9807	0.8949	0.2459	-0.1903D-01	-0.3157D-01
4	0.8914D-01	0.1251	-87.25	0.8595	0.7537	0.3479	-0.3742D-01	-0.4292D-01
5	0.3857	0.1410	-115.5	0.9436	0.7465	0.9362	-0.8514D-01	-0.1084
6	0.1096	0.3690D-01	97.55	0.2400	0.1842	0.2836	0.4496D-02	-0.3208D-01
7	0.2583	0.4728D-01	112.6	0.2551	0.1860	0.3644	0.4158D-01	-0.4132D-01
8	0.1628	0.1098	-57.37	0.3216	0.2904	0.9558D-01	-0.2826D-01	-0.1285D-01
9	0.2086	0.1098	-33.99	-0.1854	-0.1700	-0.4129D-01	-0.3490D-01	0.4972D-02
10	0.1830D-01	0.1141D-01	-34.69	0.4457	1.000	-0.1945D-01	-0.3561D-02	-0.1497D-02
11	0.1519	0.6241D-01	-28.79	-0.2246	-0.2061	-0.5112D-01	-0.2096D-01	0.6235D-01
12	0.2364	0.9573D-01	-37.29	-0.2406	-0.2483	-0.1418D-01	-0.3975D-01	0.1541D-02
13	0.6974D-01	0.3209D-01	-37.83	-0.3580	-0.3406	-0.5141D-01	-0.1315D-01	1.000
14	0.7036	0.8957	-162.7	-0.2767	-0.2965	0.8171D-01	-0.9180	-0.2540D-01
15	0.7780	1.000	0.0000	0.2679	0.1952	0.3911	1.000	-0.4576D-01
16	1.000	0.3385	-116.1	-0.6832D-01	-0.7976D-01	0.2124D-01	-0.1988	-0.1479D-01

THE A MATRIX
```
-2.289      0.1099      5.133      410.9     -782.2      -1.354      0.8252     -.5953
-.2272     -2.935       128.6     -236.1     -421.0      14.51       1.235      -1.384
0.56C1      3.222      -160.4     -5.380      1040.     -45.28      -3.187      2.786
0.3048     -.2448D-01   130.4     -563.9      115.5      -4.880     -.3420     -1.141
0.6028D-01-.8437D-01    1.121      21.42     -111.5       1.331     0.9735D-01-.6560D-01
0.8305     -.1631D-01   0.1253    -.5565      77.11     -19.77      -.2409     0.1700D-02
0.6223     -.1403D-010.6350D-01-1.181        202.0       0.1880    -20.56     0.4400D-02
-.1182      0.7847      30.02      0.9900     -203.5      30.24       0.6468    -20.01
-.9372D-02-.1714D-010.2702       -.2310D-01-16.18        0.7073     0.5198D-01 6.793
-.1380D-03-.2527D-030.4012D-02-.3100D-03-.2403          0.1049D-010.7829D-030.1007
-1.376     -6.987       41.26      12.55     -2469.       107.5       7.575      36.11
-.3141D-01-.4745       -99.19      372.8     -52.34       2.283       0.1996     9.985
-.1397D-02-.2109D-01-4.409        16.57     -2.325        0.1014     0.8855D-020.4439
-.1725     -.2573      -45.32      39.61      273.6       1.654       0.1053     4.589
-.1266D-010.3075D-01-.1818       -.8345D-01 10.88       -.4758      19.81       0.1286
-1.698      1.907      -4.850      216.3      670.2      -29.04      -2.058     -.4760
```

```
0.5626      0.5527     -2.238      5.096      5.094      -.3931     -.1265     -.5000D-05
6.153       6.151      -2.134      0.5000D-040.1200D-01-.1350D-02-.2130       0.5000D-04
-.1500D-01-.1900D-01   2.975       0.1500D-02-.1500D-010.0000       0.5320     0.0000
-1.548     -1.543       3.123      0.1000D-03-.1100D-010.4250D-020.5350D-010.0000
0.5892D-010.5550D-01-.2324       -.6500D-030.0000       0.3920      0.2389     -.5000D-04
-.2350D-02-.8900D-020.6670D-020.5000D-030.0000           0.1100D-020.6455D-010.0000
-.2350D-02-.2500D-010.1050D-010.0000       0.0000        0.5500D-030.1011      -.5000D-04
0.3150D-020.7500D-02-.1085D-010.0000        0.5000D-030.5000D-04-.1069        0.5000D-04
-50.00     -.4350D-02  39.37     -.6500D-030.0000        0.5000D-05-.8315D-020.5000D-05
-.6667     -.6667       0.5833    -.8600D-050.5000D-060.5000D-07-.1333D-030.5000D-07
0.3050D-010.7500D-01-47.80       -.1500D-020.2500D-01-.3000D-02-1.254        0.5000D-03
-9.603     -9.618       38.40     -50.00       0.5000D-040.7645D-02-.1995D-010.0000
-.4269     -.4277       1.707     -2.001      -2.000       0.3335D-03-.8645D-030.5000D-06
-4.415     -4.422       17.65     -3.098      -3.089      -19.76      -.4061D-010.0000
0.3900D-030.0000        0.2036D-010.5150D-030.0000      -.5000D-05-20.00      0.0000
0.5910      0.5950     -2.379      0.0000     -.5000D-02  30.88       20.15     -50.00
```

THE B MATRIX
```
-.1302E-01-159.5      -56.50       1.322       739.0
-.1494E-01-3.975      -2.387      -32.03      -4620.
0.1657     -31.41       6.132       29.28       0.6164E 05
0.5108E-01-.3000       0.6525      3.208      -2079.
-.1826E-02-609.9        3.489      -.7817      -231.9
-.5300E-02-6.050        10.76      -.2800      -93.82
-.6750E-03 151.3        10.66      -.4230      -1062.
-.6045E-02-.7888       -1.230       9.790      -828.0
0.6726E-01 1.911       -.1095      -.4761       0.1252E 05
0.1283E-020.1210E-01-.1491E-02-.7055D-02 185.4
12.04       50.88      -14.64      -68.37      -.1518E 06
0.2753      36.44      -.3745      -1.521       0.1296E 05
0.1233E-01 1.747      -.1753E-01-.6730E-01 575.0
0.1657      25.49       0.2595     -1.058       5255.
0.4276E-03-1.842      -.7276       0.3429       40.99
0.6152E-01-57.27      -79.75       18.96       -699.0
```

THE C MATRIX
```
0.9222E-01-.4346       5.794       111.7      -70.96       6.841       0.4809     -.3399
0.7769E-020.3471E-05-.5365E-040.2030E-03-.1675E-01-.6134E-040.6082E-040.4999E-08
0.0000      0.0000      0.0000      0.0000      0.0000      0.0000      0.0000      0.0000
0.1915E-030.5921E-05-.3150E-040.1570E-03-.3076E-01-.9057E-040.9339E-04-.3750E-06
0.1912E-040.1340E-03-.5030E-02-.1750E-030.3420E-01-.1245E-02-.1051E-030.5000E-06
0.1549E-04-.2962E-040.1772E-030.1530E-03-.2969E-010.4555E-030.2180E-03-.4350E-06
0.9242E-050.6605E-05-.2606E-040.3760E-04-.7652E-020.3824E-040.7877E-04-.9500E-07
```

```
0.3063      0.3101     -1.216       0.6150E-030.5550E-02 2.124       1.281       0.0000
0.0000      0.0000     -.3650E-050.4999E-080.4994E-070.0000      -.1456E-040.5006E-08
0.0000      0.0000       1.000       0.0000      0.0000      0.0000      0.0000      0.0000
0.3600E-060.7000E-06-.1810E-05-.5000E-070.5006E-07-.3500E-07-.1580E-040.5006E-08
-.4550E-06-.7499E-060.1960E-050.3000E-07-.4000E-060.3500E-070.1745E-04-.4999E-08
0.3550E-060.1150E-05-.1675E-05-.4000E-070.4994E-070.8500E-07-.1495E-040.5006E-08
0.1250E-060.3350E-06-.4350E-06-.6500E-070.0000      -.5000E-08-.3810E-050.5006E-08
```

45

THE D MATRIX
```
-.6056E-02 125.9      8.720      -4.424     -796.5
0.8989E-04 0.1341     0.3291     0.2350E-04 -.1482
0.0000     0.0000     0.0000     0.0000     0.0000
-.8716E-05 -.2044E-01 -.5000E-03 0.9415E-04 -.1255E-01
0.1905E-05 -.3901E-03 0.2003E-03 0.2253E-02 0.5005E-01
-.5250E-06 0.2104E-02 0.1177E-02 -.2756E-03 -.4265E-01
0.7550E-07 0.6260E-03 0.5243E-03 0.5582E-04 -.7575E-02
```

EIGENVALUES OF THE A MATRIX

REAL PART	IMAGINARY PART
-551.70679	0.00000000
-243.72264	0.00000000
-63.676819	0.00000000
-32.630035	15.138564
-32.630035	-15.138564
-49.993179	0.00000000
-43.530563	0.00000000
-41.179535	0.00000000
-21.002594	1.1867085
-21.002594	-1.1867085
-20.030380	0.00000000
-12.805978	0.00000000
-3.4393711	0.00000000
-0.67419291	0.00000000
-1.9637203	0.00000000
-1.6019726	0.00000000

MODIFIED EIGENVECTOR MATRIX
```
-4.2737E-03 -1.2709E-02 -9.4923E-03  5.2164E-03  3.2912E-02 -2.8542E-05  2.2520E-02  9.2817E-03
 1.4729E-03 -3.5627E-03 -8.9745E-03 -1.4072E-02  3.8955E-02 -7.8262E-08 -3.0951E-02 -3.1924E-02
 3.8654E-02  7.1884E-01 -2.0549E-01  5.3382E-01  2.1683E-01  8.9465E-06  3.6179E-02  1.1729E-02
 1.0000E 00  1.0000E 00 -3.1876E-01  4.2987E-01  1.9816E-01  7.8303E-06 -5.7556E-02 -6.8026E-02
-1.1764E-01 -4.6543E-01 -9.9753E-02  5.3424E-01  3.5593E-01  2.9611E-05  1.2733E-02 -1.2300E-02
 6.8731E-04  5.6185E-03  7.8418E-03 -8.9374E-02  1.4335E-02  8.5802E-06 -1.2631E-02 -4.0752E-03
 1.5789E-03  1.3525E-02  1.5553E-02 -2.0162E-01  5.4487E-02  5.3447E-06 -1.2204E-02 -8.6401E-04
-1.1055E-01 -2.0331E-02  1.0999E-02  1.9318E-02 -4.6820E-02 -4.9457E-06  1.3583E-02  9.7482E-03
 4.2739E-04  1.3125E-02  4.1163E-01  6.4546E-01 -1.0154E 00 -3.0531E-06  1.0000E 00  1.0000E 00
 5.6505E-05  1.7183E-03  5.1097E-02  8.3615E-02 -1.1585E-01 -3.6898E-07  1.1983E-01  1.1904E-01
-4.9419E-03 -5.5351E-02 -1.2357E-01 -9.0202E-02 -5.9081E-01  3.9783E-07  1.3951E-01  1.9082E-01
-1.9486E-02  2.1663E-03  1.0000E 00  1.6281E-01 -1.1816E 00  1.4101E-03 -8.3629E-01 -2.4986E-01
-7.7504E-03  8.5748E-04  3.8061E-01  7.8319E-02 -4.3304E-01  5.2685E-04 -3.1043E-01 -9.2315E-02
-9.4880E-04  2.6150E-02  2.1197E-01  5.0956E-01 -7.6402E-02  1.5768E-04 -2.0409E-02  4.1406E-05
 2.7583E-05 -2.7249E-04 -6.2514E-03  7.9372E-02 -1.6387E-01 -3.8589E-06  1.0061E-02  8.9559E-04
-1.4162E-02 -2.1476E-02 -4.1420E-01  1.0000E 00  1.0000E 00  1.0000E 00 -2.0327E-01 -1.3570E-01
```

```
-1.5797E-04 -9.3075E-03 -3.1619E-03  2.8587E-02  1.0000E 00  1.2778E-01  8.0445E-02  1.0000E 00
 2.4563E-04 -5.8954E-03 -1.0014E-03 -1.2351E-02 -3.7058E-02  1.5826E-01 -5.7909E-03  6.9205E-01
-4.1909E-02  5.7564E-02  7.5030E-03  1.5012E-01 -6.6914E-03  2.0351E-01 -9.5454E-03  9.4362E-01
-3.9113E-02  5.2452E-02  6.5271E-03  1.4329E-01  8.5612E-02  1.5621E-01 -9.2148E-04  8.3362E-01
-4.0135E-02  2.8804E-02 -1.2357E-02  3.9659E-02  8.3158E-01  7.7813E-02  5.0398E-02  7.4002E-01
 1.6537E-02 -1.1206E-02 -6.9541E-04  1.7881E-01  8.1919E-01  8.3560E-02  5.8383E-02  7.1359E-01
 1.0675E-02 -1.1297E-01 -1.5745E-03  3.6058E-01  8.1244E-01  7.7666E-02  5.4647E-02  6.8973E-01
-3.1079E-02  1.0133E-01  1.5565E-02  2.8664E-01  5.4075E-01  1.4993E-01  3.3150E-02  9.0579E-01
 8.8536E-04  9.1882E-02  1.5152E-02  1.5466E-01  3.4746E-01 -1.3202E-02  2.4859E-02  5.9410E-02
-5.7229E-05  9.6481E-03  1.5688E-03  1.3251E-02 -2.6146E-02  1.0000E 00 -7.7684E-03 -2.9134E-02
 5.4319E-03  4.9415E-02  8.5631E-03  1.0107E-01  3.0534E-01 -2.6681E-02  2.3090E-02 -1.3570E-02
 1.2066E-03  8.5069E-02  1.4132E-02  1.6423E-01  4.1024E-01 -5.4770E-02  3.0019E-02  4.1565E-02
 6.9758E-05  2.8693E-02  4.7111E-03  4.7530E-02 -1.7626E-01 -7.1373E-02  1.0000E 00  1.4153E-01
-3.1495E-01 -2.7991E-01 -2.9374E-01  4.8449E-01  6.2309E-01 -8.3030E-02  2.1156E-02 -3.5185E-02
 1.0000E 00  1.0000E 00  1.0000E 00  1.0000E 00  9.5562E-01  8.2782E-02  5.8603E-02  7.5207E-01
-9.3137E-02  4.0871E-03 -3.1310E-02  8.3969E-01  3.5954E-01 -7.7338E-03 -3.2028E-03  1.8230E-01
```

THE MATRIX OF MODE SHAPES, IN MAG. AND ANGLE(DEG.) FORM

	1	2	3	4	5	6	7	8
1	-0.4274D-02	-0.1271D-01	-0.9492D-02	0.2356D-01	-35.99	-0.2854D-04	0.2252D-01	0.9282D-02
2	0.1473D-02	-0.3563D-02	-0.8974D-02	0.2929D-01	-64.86	-0.7826D-07	-0.3095D-01	-0.3192D-01
3	0.3865D-01	0.7188	-0.2055	0.4074	22.89	0.8946D-05	0.3618D-01	0.1173D-01
4	1.000	1.000	-0.3188	0.3347	20.25	0.7830D-05	-0.5756D-01	-0.6803D-01
5	-0.1176	-0.4654	-0.9975D-01	0.4539	11.33	0.2961D-04	0.1273D-01	-0.1230D-01
6	0.6873D-03	0.5619D-02	0.7842D-02	0.6400D-01	-125.9	0.8580D-05	-0.1263D-01	-0.4075D-02
7	0.1579D-02	0.1352D-01	0.1555D-01	0.1477	-119.9	0.5345D-05	-0.1220D-01	-0.8640D-03
8	-0.1105D-02	-0.2033D-01	0.1100D-01	0.3581D-01	112.6	-0.4946D-05	0.1358D-01	0.9748D-02
9	0.4274D-03	0.1312D-01	0.4116	0.8508	102.6	-0.3053D-05	1.000	1.000
10	0.5650D-04	0.1718D-02	0.5110D-01	0.1010	99.18	-0.3600D-06	0.1198	0.1190
11	-0.4942D-02	-0.5535D-01	-0.1236	0.4225	143.7	0.3978D-06	0.1395	0.1908
12	-0.1949D-01	0.2166D-02	1.000	0.8434	127.2	0.1410D-02	-0.8363	-0.2499
13	-0.7750D-02	0.3575D-03	0.3906	0.3112	124.7	0.5288D-03	-0.3104	-0.9231D-01
14	-0.9488D-03	0.2615D-01	0.2120	0.3643	53.53	0.1577D-03	-0.2041D-01	0.4141D-04
15	0.2758D-04	-0.2725D-03	-0.6251D-02	0.1416	111.7	-0.3859D-05	0.1006D-01	0.8956D-03
16	-0.1416D-01	-0.2148D-01	-0.4142	1.000	0.0000	1.000	-0.2033	-0.1357

	9	10	11	12	13	14	15	16
1	0.6582D-02	136.0	-0.3162D-02	0.2359D-01	1.000	0.1278	0.8045D-01	1.000
2	0.4172D-02	132.6	-0.1001D-02	-0.1235D-01	-0.3706D-01	0.1583	-0.5791D-02	0.6920
3	0.5035D-01	-81.06	0.7503D-02	0.1501	-0.6691D-02	0.2035	-0.9545D-02	0.9436
4	0.4627D-01	-81.71	0.6527D-02	0.1433	0.8561D-01	0.1562	-0.9215D-03	0.8336
5	0.2845D-01	-130.9	-0.1236D-01	0.3966	0.8316	0.7781D-01	0.5040D-01	0.7400
6	0.1413D-01	79.12	-0.6954D-03	0.1788	0.8192	0.8356D-01	0.5838D-01	0.7136
7	0.9024D-01	129.6	-0.1574D-02	0.3606	0.8124	0.7767D-01	0.5465D-01	0.6897
8	0.7495D-01	-62.05	0.1557D-01	0.2866	0.5408	0.1499	0.3315D-01	0.9058
9	0.6497D-01	-44.45	0.1515D-01	0.1547	0.3475	-0.1320D-01	0.2486D-01	0.5941D-01
10	0.6822D-02	-45.34	0.1569D-02	0.1325D-01	-0.2615D-01	1.000	-0.7768D-02	-0.2913D-01
11	0.3515D-01	-36.73	0.3503D-02	0.1011	0.3053	-0.2668D-01	0.2309D-01	-0.1357D-01
12	0.6016D-01	-44.19	0.1413D-01	0.1642	0.4102	-0.5477D-01	0.3002D-01	0.4156D-01
13	0.2029D-01	-44.06	0.4711D-02	0.4753D-01	-0.1763	-0.7137D-01	1.000	0.1415
14	0.2979	-173.6	-0.2937	0.4845	0.6231	-0.8303D-01	0.2116D-01	-0.3518D-01
15	1.000	0.0000	1.000	1.000	0.9556	0.8278D-01	0.5860D-01	0.7521
16	0.6592D-01	-132.5	-0.3131D-01	0.8337	0.3595	-0.7734D-02	-0.3203D-02	0.1823

THE A MATRIX
```
-1.015      0.4626      5.427       430.7      -660.5      -5.168      -1.552      -.2493
-.2271     -1.852       102.8      -227.3      -70.96      11.79       -.7220      -.6399
0.5935      1.917      -115.9       0.3312     185.9      -20.86       1.888       0.9431
0.4220D-010.2219D-01 97.88       -500.4       175.0      -1.445       0.1167      -.2981
0.6233D-01-.4657D-010.7580        19.70      -89.76       0.5613      -.1039      -.2568D-01
0.3507     -.1233       0.2842      0.2649     53.81      -18.60       0.5443      -.5000D-05
0.277d     -.3571       0.7406      0.9950D-01 130.8       4.069      -18.67       0.0000
-.4214      0.5473      83.36      -.1325     -132.1       28.20      -1.336      -20.00
-.5023D-020.6630D-02-.7106        0.2485     -1.766       0.1806      -.1794D-01 5.732
-.7502D-040.9861D-04-.1062D-010.4418D-02-.2569D-010.2673D-02-.2690D-030.8491D-01
-2.925     -9.041       27.14      -.7450     -917.3       102.8      -9.271       42.16
0.5807D-01-.1009      -227.6       800.7       17.66      -2.066       0.1794       8.816
0.2580D-02-.4483D-02-10.12        35.59       0.7834     -.9180D-010.7982D-020.3918
-.5120D-01-.1301      -103.2       106.6       479.4       0.2203D-01-.5740D-01 4.001
-.4983D-020.1561D-010.7750D-010.2982        2.119      -.1824       19.97       0.5859D-01
-1.360      1.090       8.851       390.9      85.89      -12.19       2.318      -.3778

0.3027      0.3026     -1.126       2.317       2.302      -.1776      -.1923      -.1000D-04
3.039       3.043      -1.103      -.1000D-050.2171D-01-.5005D-02-.6707D-010.0000
0.0000     -.1000D-04 1.184        0.0000      0.2170D-010.9999D-020.1789      -.5000D-05
-.7345     -.7165       1.490       0.2450D-02-.2150D-010.5755D-010.2240D-010.5000D-04
0.2885D-010.2905D-01-.1062        0.1600D-030.5500D-020.1557       0.1909      -.5000D-05
0.0000      0.0000      -.5000D-05-.5000D-050.0000       0.5000D-020.5276D-010.0000
0.0000     -.5000D-040.0000       -.5000D-05-.5000D-040.2495D-020.1270      -.5000D-05
0.5000D-050.5000D-040.3100D-030.5000D-050.5000D-04-.6995D-02-.1261      0.5000D-05
-50.00      0.1593D-01 39.89       0.0000      0.0000      0.1250D-02-.1500D-05-.5000D-06
-.6666     -.6663       0.5910      0.1000D-07-.5000D-070.1666D-040.0000      -.1000D-07
-.3550D-020.5000D-03-48.21        0.1250D-020.0000      -.4370D-01-.8810      0.5000D-04
-10.71     -10.72       39.63      -50.00      -.1629       0.3749D-020.1788D-010.5000D-05
-.4761     -.4766       1.761      -2.000      -2.008       0.1500D-030.8047D-030.5000D-06
-4.864     -4.872       18.01      -2.534      -2.589      -19.84       0.3934D-010.0000
0.0000      0.2867D-010.1043D-010.0000      -.3910D-01-.1500D-02-19.99       0.0000
0.5726      0.5175      -2.118     -.4850D-020.0000       22.31       28.64      -50.00
```

THE B MATRIX
```
0.2038E-01-9.805      -9.222       5.907      -1085.
0.3746E-01-3.854      -2.686      -10.50      -2153.
0.9210E-01 23.46       6.906       23.73       0.4057E 05
0.1774E-01 1.547       0.7326      1.627      -1690.
-.7865E-03-189.9       0.7584     -.6619      -126.4
0.1730E-02 5.843      -.3999      -1.594       806.2
-.2683E-01 12.04       3.075      -4.668      -75.32
-.8026E-01-24.82      -4.828      -14.57      -2564.
0.1188     -.3885E-01-.5609E-01-.1985        0.1783E 05
0.1694E-020.2137E-02-.7912E-03-.2749E-02 264.7
38.53      -117.2      -34.03      -117.6      -.2212E 06
0.3485      2.811       0.6698      2.336       0.2261E 05
0.1594E-010.1293       0.2956E-010.1034       1005.
0.1864     -5.033       0.7565     -.2186E-01 9765.
-.8530E-02-.7192      -.7061E-010.1482      -117.2
0.4443E-01 20.90      -16.89       13.77       497.9
```

THE C MATRIX
```
-.6229E-01-.2344       3.138       79.39       185.9       2.701      -.2590      -.1055
0.1132E-010.1358E-02-.2907E-02-.6250E-03-.6156      -.1554E-01-.6317E-020.4850E-05
0.0000      0.0000      0.0000      0.0000      0.0000      0.0000      0.0000      0.0000
0.1569E-030.9251E-04-.1935E-03-.4485E-04-.4132E-01-.1056E-02-.4199E-030.1550E-06
0.7778E-040.2000E-03-.1460E-010.2305E-04-.2438E-01-.1707E-020.2466E-03-.1075E-06
0.9565E-040.9280E-05-.1650E-04-.7800E-04-.6786E-01-.1047E-03-.1200E-030.1999E-07
0.3232E-040.4083E-05-.7250E-05-.1370E-04-.1588E-010.1370E-040.1798E-040.1300E-07

0.1170      0.1089     -.4287      -.1070E-02-.1720E-010.6226       0.7798      -.4999E-05
-.3350E-050.0000       0.0000      0.3050E-05-.1350E-04-.3280E-04-.6007E-030.0000
0.0000      0.0000      1.000       0.0000      0.0000      0.0000      0.0000      0.0000
-.1030E-06-.3450E-060.2650E-070.0000       0.1000E-07-.1969E-05-.3999E-040.0000
0.4300E-070.3850E-06-.1150E-07-.4800E-07-.5006E-080.1129E-050.2353E-04-.5002E-09
-.3050E-060.5000E-070.0000       0.4999E-080.0000      -.3350E-05-.6539E-040.0000
-.1120E-06-.3500E-070.4998E-090.5002E-090.4999E-08-.8175E-06-.1542E-040.1000E-08
```

48

THE D MATRIX
```
-.6015E-03-48.41     -.7564      -3.077     -301.0
0.2099E-03-.5145E-010.1373      0.1794E-01 2.264
0.0000     0.0000     0.0000     0.0000     0.0000
0.4335E-C5-.6375E-02-.4092E-02C.1249E-020.5119
0.4501E-C50.3269E-020.9029E-030.4112E-02-.1485
0.1935E-05-.6512E-020.9289E-040.1269E-03-.9626E-01
0.7040E-06-.1519E-020.3071E-030.5360E-04-.1293E-01
```

```
    EIGENVALUES OF THE A MATRIX
    REAL PART       IMAGINARY PART

    -506.73145      0.00000000
    -139.98358      0.00000000
    -64.450974      0.00000000
    -49.715607      5.7025499
    -49.715607     -5.7025499
    -49.998520      0.00000000
    -45.165405      0.00000000
    -22.648819      0.00000000
    -13.368243      0.00000000
    -20.343048      0.84707332
    -20.343048     -0.84707332
    -0.89456981     0.00000000
    -0.76271462     0.00000000
    -1.6238403      0.00000000
    -19.166748      0.00000000
    -1.9968775      0.00000000
```

MODIFIED EIGENVECTOR MATRIX
```
-2.1974E-03 -1.1535E-02 -4.3955E-03 -9.6448E-03 -5.4222E-03 -4.0715E-06 -9.8094E-03  5.4593E-04
 6.7507E-04 -2.8117E-03 -3.0520E-C3  1.2947E-03 -4.3703E-03 -3.8995E-10  5.4193E-03  1.8559E-03
 5.5408E-03  1.0000E 00 -2.6421E-01  1.0571E-02  4.3616E-02  9.3516E-07 -1.2983E-02  2.2971E-01
 1.0000E CO  8.2721E-01 -3.9848E-01  4.9098E-02  7.0406E-03  8.9599E-C6  4.7567E-02  2.4739E-01
-9.1210E-02 -7.8886E-01 -3.1038E-01 -1.4501E-02  1.3393E-01  1.6017E-05  6.5245E-C4  3.6252E-01
 1.4310E-04  4.7721E-03  5.2767E-C3  1.0437E-03 -2.9543E-03  1.1162E-07  1.7890E-C3 -6.2816E-02
 3.5647E-04  1.1211E-02  1.2250E-C2  4.2017E-04 -8.0587E-03 -3.3887E-07  2.1438E-03 -1.3524E-01
-2.7467E-04 -4.9101E-02  2.0559E-02 -3.9506E-03  2.0596E-05 -1.4419E-07 -7.4125E-04  8.8843E-02
 7.9024E-05  2.2425E-02  3.8325E-C1 -1.5715E-01  4.2881E-01  6.2679E-06 -5.0153E-01 -7.7417E-02
 1.0306E-05  2.8955E-03  4.7602E-02 -1.9696E-02  5.1947E-02  7.6208E-07 -6.0321E-02 -8.2808E-03
-8.3550E-04 -3.9198E-02 -1.2225E-01  5.2462E-02  2.2163E-02  1.8786E-08 -5.2610E-02 -5.3315E-C2
-2.5229E-02  7.1069E-02  1.0000E 00  1.0000E 00  1.0000E 00  5.1092E-04  1.0000E 00 -5.0237E-02
-1.0036E-02  2.7833E-02  3.8093E-01  3.7240E-01  3.7634E-01  1.9164E-04  3.7233E-01 -1.7179E-02
-2.6257E-03  7.7346E-02  2.0468E-01  3.4682E-02  1.5458E-01  4.5517E-05  2.5302E-02  5.2013E-C2
-2.6327E-03 -1.7253E-03 -5.0157E-03  7.5954E-04  5.1970E-03  2.5534E-07 -1.5672E-03  1.0000E 00
-1.6740E-02 -9.9198E-02 -2.2742E-01 -9.0241E-01  2.4031E-01  1.0000E 00  1.9361E-01  9.3119E-01
```

```
 2.3719E-02 -1.6139E-03 -7.5963E-C3  1.0000E CO  7.9540E-01  1.0000E 00 -1.1306E-03 -1.1038E-C1
-5.4857E-03 -1.2153E-03 -2.9599E-03  2.2207E-01  2.1612E-01 -2.5169E-02  3.0815E-04  1.1496E-03
 7.6615E-03 -9.9503E-02  1.4983E-01  9.8070E-01  8.9492E-01  2.4587E-01 -1.9025E-02 -3.1574E-02
 8.9144E-02 -1.1895E-01  1.3096E-01  8.5946E-01  7.5366E-01  3.4794E-01 -3.7422E-02 -4.2919E-02
 3.8574E-01 -1.8798E-01  6.6671F-C2  9.4356E-01  7.4654E-01  9.3615E-01 -8.5138E-02 -1.0841E-01
 1.0957E-01  3.1734E-02 -4.1431E-C2  2.4002E-01  1.8424E-01  2.8356E-01  4.4956E-03 -3.2085E-02
 2.5833E-C1  2.5467E-02 -6.1825E-02  2.5506E-01  1.8595E-01  3.6444E-01  4.1578E-02 -4.1316E-02
 1.6276E-01 -3.3268E-02  1.5171E-01  3.2162E-01  2.9036E-01  9.5577E-02 -2.8259E-02 -1.2849E-02
 2.0860E-01  2.9655E-02  1.5240E-01 -1.8541E-01 -1.7002E-01 -4.1290E-02 -3.4904E-02  4.9725E-03
 1.8301E-02  2.8891E-02  1.587CE-02  4.4566E-01  1.0000E 00  1.9452E-02 -3.5608E-03 -1.4966E-03
 1.5193E-01  2.4634E-02  8.4757E-02 -2.2461E-01 -2.0613E-01 -5.1124E-02 -2.0958E-02  6.2350E-03
 2.3643E-01  1.8153E-02  1.3416E-01 -2.4062E-01 -2.4827E-01 -1.4180E-02 -3.9752E-02  1.5410E-03
 6.9742E-02  5.6624E-03  4.5023E-02 -3.5800E-01 -3.4064E-01 -5.1411E-02 -1.3149E-02  1.0000E 00
 7.0364E-01 -1.1214E 00 -5.8915E-01 -2.7674E-01 -2.9649E-01  8.1712E-02 -9.1803E-01 -2.5397E-02
 7.7798E-01  1.0000E 00  1.0000E 00  2.6789E-01  1.9523E-01  3.9108E-01  1.0000E 00 -4.5756E-02
 1.0000E 00 -4.5298E-01  1.5437E-01 -6.8323E-02 -7.9764E-02  2.1239E-02 -1.9882E-01 -1.4766E-02
```

THE MATRIX OF MODE SHAPES, IN MAG. AND ANGLE(DEG.) FORM

	1	2	3	4	5	6	7	8
1	-0.2223D-02	-0.6617D-02	-0.4936D-02	0.1302D-01	-35.09	-0.1199D-06	0.9571D-02	0.4124D-04
2	0.7576D-03	-C.1848D-02	-0.4493D-02	0.1422D-01	-66.91	0.7002D-07	-0.1532D-01	-0.1614D-01
3	0.3935D-01	0.7226	-C.2181	0.4211	28.18	-0.7036D-05	0.2330D-01	-0.3476D-01
4	1.000	1.000	-0.3335	0.3412	26.78	-0.1137D-04	-0.6845D-01	-0.1005
5	-0.1181	-0.4666	-0.1149	0.4691	14.06	-0.7054D-07	-0.1239D-01	-0.7854D-01
6	0.7096D-03	C.5806D-02	0.7986D-02	0.6104D-01	-113.4	0.6830D-06	-0.3659D-02	0.1041D-01
7	0.1646D-02	0.1422D-01	C.1750D-01	C.1466	-116.3	0.1768D-07	-0.7603D-03	0.2649D-01
8	-0.1107D-02	-0.2047D-01	0.1025D-01	0.2637D-01	107.2	0.2842D-06	0.1710D-02	-0.7839D-02
9	0.4521D-03	0.1370D-01	0.4195	0.8531	101.2	-0.3521D-05	1.000	1.000
10	0.5980D-04	0.1794D-02	C.5211D-01	0.1019	97.88	-0.4267D-06	0.1197	0.1182
11	-0.5175D-02	-C.5731D-01	-0.1266	0.4247	146.0	-0.3574D-07	0.1489	0.2413
12	-0.1955D-01	0.2748D-02	1.000	0.8766	126.2	0.2349D-04	-0.6826	0.9669D-01
13	-0.7773D-02	0.1085D-02	C.3805	0.3246	123.9	0.8807D-05	-0.2530	0.3556D-01
14	-0.6916D-03	0.2727D-01	0.2153	0.3545	58.16	0.1120D-05	-0.1492D-01	-0.1558D-01
15	0.2324D-04	-0.3209D-03	-0.6906D-02	0.1303	115.2	0.4624D-07	0.7415D-03	-0.2637D-01
16	-0.1462D-01	-0.2220D-01	-0.3966	1.000	0.0000	1.000	-0.1959	-0.2919

	9	10	11	12	13	14	15	16
1	-0.4818D-02	0.2175D-02	130.5	0.1186D-01	-C.1543	1.000	1.000	0.5444
2	-0.2400D-02	0.1272D-02	111.3	-0.5107D-02	-0.1573D-02	0.2131D-01	0.6818	0.4674
3	0.6348D-01	0.2162D-01	-107.7	0.1544	-0.1417D-01	0.7188D-01	0.9459	0.6342
4	0.5782D-01	0.1980D-01	-108.8	0.1437	-0.2548D-01	0.1460	0.8324	0.5316
5	-0.1794D-02	0.2522D-01	-178.5	0.3676	-0.1289	0.7462	0.7339	0.3850
6	-0.2065D-01	0.5499D-02	58.72	0.1565	-0.1181	0.7325	0.6897	0.3685
7	-0.6907D-01	0.5372D-01	97.40	0.3482	-0.1199	0.7302	0.6909	0.3677
8	0.9719D-01	0.4115D-01	-31.91	0.2710	-0.7649D-01	0.4715	0.8567	0.5203
9	0.7296D-01	0.4149D-01	-66.83	0.1295	-0.3726D-01	0.2345	0.7181D-02	-0.2497D-01
10	0.7685D-02	0.4303D-02	-67.70	0.1122D-01	0.1059D-01	-0.1160	-0.2252D-01	1.000
11	0.3740D-01	0.2366D-01	-62.30	0.8135D-01	-0.3230D-01	0.2064	-0.6476D-01	-0.7071D-01
12	0.6809D-01	0.3690D-01	-66.64	0.1374	-0.4521D-01	0.2858	-0.1769D-01	-0.8036D-01
13	0.2302D-01	0.1301D-01	-67.27	0.4011D-01	1.000	0.9434	-0.2622D-01	-0.1056
14	-0.3004	0.3055	179.1	0.4260	-0.8782D-01	0.3851	-0.9734D-01	-0.1490
15	1.000	1.000	0.0000	1.000	-0.1302	0.7719	0.7235	0.3848
16	-0.2074D-01	0.6304D-01	178.1	0.7931	-0.4830D-01	0.1346	0.1180	0.3666D-01

APPENDIX E

COMPARISON OF NONLINEAR AND FULL-STATE LINEAR

MODEL TRANSIENT RESPONSES

Presented in this appendix is a comparison of transients run on the nonlinear and full-state linear models. Responses of states and outputs are shown in figures 9 and 10 for a +3-percent change in fuel flow and nozzle area. The operating point is sea-level-static idle. (The plots already shown in the main text are omitted.) The responses are for P_{T7}, $P_{T4.5}$, P_{T7M}, $T_{T2.5H}$, $T_{T2.5C}$, T_{T3}, T_{T5}, T_{T6C}, T_{T7M}, WFAN, T_{T4}, SMAF, SMHC, $DP_{2.5QP}$, and $DP_{2.55C}$. The offset at zero time for the nonlinear transient is due to the small startup transient in the simulation. Sometimes these startup-transient offsets seem quite large. For example, for the SMAF comparisons for a +3-percent change in fuel flow (fig. 9(ℓ)), the startup transient caused an offset of -0.00075 at zero time. The actual surge margin is 0.10418, thus the drift is 0.7 percent of the actual. This is a very small error, and the startup transient is essentially negligible. The scale used makes the difference look worse than it actually is. The immediate response at zero time for the output responses (e.g., fig. 9(ℓ)) are inherent in the linear model (ref. 8). Output variables can change instantaneously with time. In the linear model this is accomplished through the $\overline{D}$ matrix. The steady-state errors in the comparisons are due to the averaging method used to generate the $\overline{B}$ and $\overline{D}$ matrices. If these matrices had been calculated by forcing the steady-state match only in the positive direction, the steady-state error would be almost zero, and only off by the startup transient. Note from the comparisons that the linear model at sea-level-static idle does approximate the dynamics of the nonlinear simulation quite well. The same comparisons were made at the other operating points, and the results were as good or better than those presented. Thus, the linear models can be used to represent the engine over its full operating envelope.

Some states of the original 16, specifically, $T_{T4.5HI}$, $T_{T4.5LO}$, T_{T4HI}, and T_{T4LO}, are not shown because they were not output in the nonlinear simulation.

APPENDIX F

THE PROBLEM OF STARTUP TRANSIENTS

Startup transients occur when the calculations made at zero time in a simulation, in which no input is provided, have a small error. For an engine simulation this means that a balance point is not reached (i.e., there is an error between the compressor and turbine match). In steady-state calculations this is not a problem because a balance is forced. However, in transient calculations a different calculation path is generally made through the simulation, and, depending on how tables are read and how quantities are calculated, small errors may result.

In general, most digital transient simulations do have small startup transients. Usually, however, when gross transients (e.g., acceleration from idle to full power) are being studied, startup transients are negligible.

In model validation small transients are of interest, such as a +3-percent change in nozzle area. Because a small nozzle-area change has a small effect on an engine, a question arose as to how a startup transient would effect this validation. In the F100 simulation the startup transient was essentially zero so no problems resulted. To investigate this problem, a small error was introduced at zero time. This was accomplished by changing the pressure ratio across the compressor slightly from the steady-state calculation. This caused a difference between the power extracted by the compressor and that supplied by the turbine. The results are shown in figure 11 for a 5-percent change in nozzle area input to the simulation at 0.1 second. From zero time to time equal 0.1 second, nothing was done to the simulation. Without the small error in compressor pressure ratio, the response to the step (figs. 11(a) and (b)) is well behaved and approaches the steady-state value calculated by the simulation (steady-state part). Also, the transients show no change from 0 to 0.1 second.

When the small error in the compressor-pressure ratio is introduced the startup transient becomes much larger than the input. Figure 11(a) shows that at 0.1 second there is a loss of 5 rpm from the operating point. The error built up is large when the step is applied.

However, the speed never recovers to the predicted steady-state value. If this transient is used to compare with the linear model, the comparison will be very poor. The linear model is derived from the steady-state part of the simulation. Thus, a positive step in nozzle area would match the curve without the startup transient. In effect, the comparison would be what is shown in figure 11(a).

Figure 11(b) shows the same transients but for fan speed. At 0.1 second there is little difference in the two transients (the error input was into the compressor). But at 0.1 second the curves diverge since there is a large error buildup in the compressor-

turbine match. The fan speed must change to reflect this error, and thus when there is a starting transient, the fan speed does not recover to the predicted steady-state value. Again, when the error is eliminated, the speed behaves well.

The results of this analysis show that great care must be used to make sure that startup transients have been eliminated when validating linear models that require small inputs.

APPENDIX G

FOURTH-ORDER MODELS

Presented in this appendix are the $\overline{ABR}$, $\overline{BBR}$, $\overline{CBR}$, and $\overline{DBR}$ for the reduced-order models. The models are

$$\dot{\overline{X}} = \overline{ABR}\,\overline{X} + \overline{BBR}\,\overline{U} \tag{G1}$$

$$\overline{Y} = \overline{CBR}\,\overline{X} + \overline{DBR}\,\overline{U} \tag{G2}$$

Also presented are the eigenvalues for the $\overline{ABR}$ matrices

$$\left|\overline{ABR} - \lambda \overline{I}\right| = 0 \tag{G3}$$

The six operating points are the same as listed in appendix D and are shown again in table VII for reference.

54

Operating Point 1 (sea-level-static idle)

MATRIX A3P =

	1	2	3	4
1	-2.149	0.6785	85.74	-662.7
2	0.7537D-01	-5.437	123.8	-145.8
3	0.8682D-01	4.924	-140.1	25.70
4	0.1399	-0.1935	5.714	-243.6

MATRIX BBR =

	1	2	3	4	5
1	1.275	15.31	-14.06	6.183	0.5555D 05
2	1.038	-6.352	-1.571	-34.67	0.5512D 05
3	1.099	2.528	2.329	39.43	4298.
4	0.4224D-01	-241.1	1.240	-1.610	0.4163D 05

MATRIX CBR =

	1	2	3	4
1	0.2275	-0.3059	9.286	372.8
2	0.1749D-01	0.2800D-02	-0.1506D-01	-1.143
3	0.3165D-02	-0.4891	5.903	1.989
4	-0.2484D-04	0.3969D-04	-0.4823D-03	-0.3662D-01
5	0.1650D-04	0.5936D-03	-0.1478D-01	0.3623D-02
6	0.5097D-04	0.6505D-05	0.4075D-04	-0.2710D-01
7	0.2111D-04	-0.2884D-05	0.3373D-04	-0.5188D-02

MATRIX DBR =

	1	2	3	4	5
1	0.5337D-01	-0.4695	2.018	-2.628	0.1767D 05
2	0.1679D-03	0.4511D-02	0.1664	0.2495D-01	148.0
3	0.6082	-0.7252	-0.2431	-4.857	1841.
4	0.7186D-05	0.6971D-03	-0.1359D-02	0.7972D-03	4.720
5	-0.1484D-04	-0.2731D-02	0.3182D-03	0.7678D-02	-3.855
6	0.4533D-05	0.3542D-03	0.5760D-04	0.7493D-04	3.817
7	0.6720D-06	0.3846D-04	0.2092D-03	-0.2071D-04	0.7410

Eigenvalues

REAL PART	IMAGINARY PART
-0.87832969	0.00000000
-2.6616826	0.00000000
-142.80557	0.00000000
-245.00836	0.00000000

Operating Point 2

MATRIX ABR =

	1	2	3	4
1	-3.684	-0.6320	103.0	-789.0
2	1.200	-6.137	79.95	-522.8
3	-1.659	5.819	-154.8	729.0
4	0.2584	-0.2028	5.581	-103.7

MATRIX BBR =

	1	2	3	4	5
1	0.7260	-257.7	-107.9	-1.972	-0.1500D 05
2	0.6320	-458.4	13.40	-73.93	-0.1327D 05
3	0.8555	647.3	-16.04	59.29	0.7941D 05
4	0.1891D-01	-1229.	10.16	-1.938	-399.6

MATRIX CBR =

	1	2	3	4
1	1.109	-0.8876	24.65	70.15
2	0.1382D-01	0.3152D-05	-0.7751D-07	-0.9650D-02
3	0.1093	-0.1181	1.136	-24.47
4	0.7315D-04	0.5169D-05	0.5422D-06	-0.1508D-01
5	-0.3066D-04	0.1294D-03	-0.2594D-02	0.1449D-01
6	0.4003D-04	-0.3016D-04	0.1166D-03	-0.1430D-01
7	0.1332D-04	0.4075D-05	-0.9470D-05	-0.3745D-02

MATRIX DBR =

	1	2	3	4	5
1	0.1647	-232.1	41.22	-8.291	-3459.
2	0.6344D-04	0.1782	0.7403	0.2073D-03	0.7989D-02
3	0.1329	-23.97	1.113	-1.199	-2464.
4	0.3239D-05	-0.3606D-02	-0.3110D-02	0.6736D-04	0.1239D-01
5	-0.8887D-08	0.1247D-01	-0.2915D-03	0.2437D-02	-0.1710D-01
6	0.3111D-07	-0.1163D-01	0.1737D-02	-0.3235D-03	0.5144D-02
7	0.4271D-07	-0.2992D-02	0.7025D-03	0.5175D-04	0.2557D-02

Eigenvalues

REAL PART	IMAGINARY PART
-3.1516863	0.00000000
-5.5467604	0.00000000
-60.662508	0.00000000
-198.91636	0.00000000

56

Operating Point 3

MATRIX ABR =

	1	2	3	4
1	-7.879	0.9396	98.10	-592.0
2	-3.031	-8.405	67.88	-97.23
3	5.137	7.877	-152.2	159.8
4	0.2454	-0.3006	5.846	-97.76

MATRIX BBR =

	1	2	3	4	5
1	0.6766	-325.5	-263.6	26.37	-6251.
2	0.6269	105.6	-139.0	-67.69	-5763.
3	0.8802	-98.04	225.4	109.1	0.3298D 05
4	0.4199D-01	-1675.	13.53	-5.122	-349.4

MATRIX CBR =

	1	2	3	4
1	-0.1689	-1.501	28.78	154.6
2	0.3305D-01	0.6804D-03	-0.1709D-02	-0.3215D-01
3	-0.7572D-01	-0.8768D-01	0.8535	-3.239
4	0.3228D-04	0.4222D-04	-0.1078D-03	-0.1977D-02
5	0.7168D-04	0.8988D-04	-0.1622D-02	0.2062D-02
6	0.1824D-04	0.1069D-04	-0.2667D-04	-0.3672D-02
7	0.9230D-06	0.9995D-05	-0.2572D-04	-0.9107D-03

MATRIX DBR =

	1	2	3	4	5
1	0.1879	-183.5	-8.129	-25.23	-1559.
2	0.2079D-03	0.9867	1.794	0.1238D-01	-2.719
3	0.8509D-01	5.206	-4.855	-2.705	-576.3
4	0.4685D-06	0.4561D-02	-0.3128D-02	0.7268D-03	-0.4405D-02
5	0.1519D-06	-0.8408D-03	0.2865D-02	0.2832D-02	-0.7376D-02
6	0.2653D-06	0.5091D-02	-0.4673D-03	0.1529D-03	0.4778D-02
7	-0.3444D-08	0.9200D-03	0.4092D-03	0.1885D-03	-0.9336D-03

Eigenvalues

REAL PART	IMAGINARY PART
-5.9363691	1.8557230
-5.9363691	-1.8557230
-81.667400	0.00000000
-172.74548	0.00000000

MATRIX ABR =

	1	2	3	4
1	-0.9975	-0.1766	106.5	-877.5
2	0.3233	-1.662	80.38	-503.0
3	-0.4455	1.536	-150.4	680.9
4	0.7116D-01	-0.5453D-01	5.526	-97.28

MATRIX BBR =

	1	2	3	4	5
1	0.7961	-48.54	-28.97	-0.6660	-9199.
2	0.6307	105.0	6.019	-19.68	-7538.
3	0.8835	-135.1	-7.237	15.11	0.4364D 05
4	0.3587D-01	-298.0	2.321	-0.5710	-491.7

MATRIX CBR =

	1	2	3	4
1	0.2564	-0.2845	28.84	-1.747
2	0.4173D-02	0.1307D-05	-0.7787D-06	-0.1404D-01
3	0.1136	-0.1270	4.087	-88.94
4	0.1550D-03	0.6621D-05	0.5959D-05	-0.6216D-01
5	-0.3741D-04	0.1461D-03	-0.1065D-01	0.5913D-01
6	0.4192D-04	-0.3076D-04	0.4211D-03	-0.5070D-01
7	0.1366D-04	0.4574D-05	-0.3548D-04	-0.1314D-01

MATRIX DBR =

	1	2	3	4	5
1	0.1977	74.49	7.321	-2.664	-2472.
2	0.9685D-04	0.1070	0.173c	0.1764D-03	-3.120
3	0.5122	19.07	1.758	-1.358	-5532.
4	0.1305D-04	0.2140D-01	-0.4331D-02	0.7069D-04	-0.7896
5	0.1503D-05	-0.1133D-01	-0.6118D-03	0.1966D-02	-0.1487D-01
6	-0.1225D-06	0.1001D-01	0.1576D-02	-0.3559D-03	-0.5224D-01
7	0.2130D-06	0.2575D-02	0.5967D-03	0.3574D-04	-0.1348D-01

Eigenvalues

REAL PART	IMAGINARY PART
-0.86640031	0.00000000
-1.5322735	0.00000000
-56.991700	0.00000000
-190.93434	0.00000000

Operating Point 5

MATRIX ABR =

	1	2	3	4
1	-1.961	-0.3216	104.1	-839.4
2	0.6604	-3.232	79.31	-508.2
3	-0.8983	3.016	-151.3	696.9
4	0.1382	-0.1064	5.552	-98.96

MATRIX BBR =

	1	2	3	4	5
1	0.7680	-147.4	-54.62	0.3312	-9176.
2	0.5902	0.7827	10.89	-36.39	-9957.
3	0.9134	-32.71	-13.01	27.99	0.5235D 05
4	0.3266D-01	-607.4	4.467	-0.8482	-652.6

MATRIX CBR =

	1	2	3	4
1	0.5007	-0.5556	29.88	-6.866
2	0.7768D-02	0.3799D-05	-0.1414D-04	-0.1636D-01
3	0.1132	-0.1197	2.067	-44.95
4	0.1900D-03	0.6005D-05	0.8149D-06	-0.3027D-01
5	-0.3545D-04	0.1350D-03	-0.5067D-02	0.2853D-01
6	0.4068D-04	-0.3010D-04	0.2080D-03	-0.2589D-01
7	0.1312D-04	0.4535D-05	-0.1877D-04	-0.6749D-02

MATRIX DBR =

	1	2	3	4	5
1	0.1863	139.2	13.86	-4.817	-3131.
2	0.8916D-04	0.1345	0.3291	0.2741D-04	-0.1415
3	0.2512	0.9063	1.563	-1.113	-3236.
4	-0.8940D-05	-0.1983D-01	-0.5101D-03	0.9520D-04	-0.1344D-01
5	0.2426D-05	-0.5765D-03	-0.5172D-03	0.2271D-02	0.5789D-01
6	-0.8103D-06	0.3437D-02	0.1529D-02	-0.2852D-03	-0.5343D-01
7	0.1269D-07	0.1166D-02	0.5840D-03	0.5401D-04	-0.1107D-01

Eigenvalues

REAL PART	IMAGINARY PART
-1.6673768	0.00000000
-3.0882016	0.00000000
-57.643485	0.00000000
-193.06924	0.00000000

MATRIX ABR =

	1	2	3	4
1	-1.159	0.2999	91.41	-553.4
2	-0.4326D-01	-2.154	63.36	-138.0
3	0.2093	1.827	-107.2	114.5
4	0.7411D-01	-0.6340D-01	4.156	-77.34

MATRIX BBR =

	1	2	3	4	5
1	1.176	-15.01	-10.02	4.136	-8622.
2	0.9912	-3.966	-4.557	-16.10	-4955.
3	1.031	14.07	6.113	20.40	0.3420D 05
4	0.4048D-01	-189.8	0.7533	-0.8214	-344.0

MATRIX CBR =

	1	2	3	4
1	-0.2873D-02	-0.2996	16.83	238.6
2	0.1089D-01	0.1620D-02	-0.3626D-02	-0.7189
3	-0.1884D-01	-0.1824	4.257	-16.35
4	0.1275D-03	0.1101D-03	-0.2430D-03	-0.4826D-01
5	0.4972D-04	0.2068D-03	-0.1462D-01	0.2112D-01
6	0.9012D-04	0.1431D-04	-0.4249D-04	-0.6970D-01
7	0.3266D-04	0.4030D-05	-0.9717D-05	-0.1583D-01

MATRIX DBR =

	1	2	3	4	5
1	0.1594	-47.58	-0.7485	-3.780	-1127.
2	0.1975D-03	-0.6159D-01	0.1365	0.2138D-01	1.668
3	0.7961	-2.578	-1.016	-3.319	-4555.
4	0.3630D-05	-0.7057D-02	-0.4148D-02	0.1479D-02	0.4707
5	0.4405D-05	0.2886D-02	0.9740D-03	0.4198D-02	-0.2233
6	0.2118D-06	-0.6671D-02	0.6720D-04	0.1953D-03	-0.9091D-01
7	0.2087D-06	-0.1510D-02	0.3080D-03	0.5381D-04	-0.9650D-02

Eigenvalues

REAL PART	IMAGINARY PART
-1.0627800	0.00000000
-1.5121531	0.00000000
-65.526587	0.00000000
-119.70158	0.00000000

APPENDIX H

COMPARISON OF FULL-STATE AND REDUCED-ORDER (4th ORDER)

MODEL TRANSIENT RESPONSES

Transients run with the full-state and reduced-order linear models are compared herein. The responses of reconstructed states and outputs are shown in figures 12 and 13 for a +3-percent change in fuel flow and nozzle area. The operating point is sea-level-static idle. (Plots shown in the main text are omitted.) The responses shown are for $T_{T2.5H}$, $T_{T2.5C}$, T_{T3}, T_{T4}, T_{T5}, T_{T6C}, T_{T7M}, WFAN, T_{T4}, SMAF, SMHC, $DP_{2.5QP}$, and $DP_{2.5SC}$. In the comparisons for the reconstructed states, there are immediate responses at zero time. This is due to the loss of frequency information when generating a reduced-order model. The discarded states are approximated by $\dot{X} = 0$, and then reconstructed from linear relations with the retained states an inputs. The loss of high-frequency information is observed by the faster rise time for the reconstructed states. In general, after 0.1 second the reconstructed states from the reduced-order model agree well with the full-state model. Immediate responses for the outputs (figs. 12 and 13(h) to (m)) are inherent in the models (ref. 8). The output variables can change instantaneously with time through the $\overline{D}$ matrix. In the comparisons of output responses, the offset remained the same for the reduced-order model. The difference in rise time between the output responses can be attributed to loss of high-frequency information. Again, after 0.1 second, the fourth-order responses approximate the full-state responses quite well.

The same procedure was used at the other five operating points, and the agreement between transient responses was as good or better than that shown for the sea-level-static-idle operating point. From this analysis the fourth-order models can be used for control studies since they adequately represent the engine over its whole operating range.

REFERENCES

1. De Hoff, Ronald L.; et al.: F100 Multivariable Control Synthesis Program, Design of a Multivariable Controller Utilizing Linear Quadratic Regulator Methods, Vols. I and II. Systems Control, Inc. (Vt.), Jan. 1977. (Also AFAPL-TR-77-35, June 1977.)

2. Szuch, John R.; et al.: F100 Multivariable Control Synthesis Program - Evaluation of a Multivariable Control Using a Real-Time Engine Simulation. NASA TP-1056, 1977.

3. Merrill, Walter C.: Design of Turbofan Engine Controls Using Output Feedback Regulator Theory. NASA TM X-73622, 1977.

4. Teren, Fred: Minimum Time Acceleration of Aircraft Turbofan Engines by Using an Algorithm Based on Nonlinear Programming. NASA TM-73741, 1977.

5. Miller, Ronald J.; and Hackney, Ronald D.: F100 Multivariable Control System Engine Models/Design Criteria. PWA-FR-7809, Pratt & Whitney Aircraft, 1976. (Also AFAPL-TR-76-74, AD-AO33.)

6. F100-PW-100(3) Transient Engine Simulation Deck User's Manual For Deck CCD 1103-1.0. FR-6867, Pratt & Whitney Aircraft, 1975.

7. Weinberg, Marc S.; and Adams, Gary R.: Low Order Linearized Models of Turbine Engines. ASD-TR-75-24, Aeronautical Systems Division, 1975.

8. Seldner, Kurt; and Cwynar, David S.: Procedures for Generation and Reduction of Linear Models of a Turbofan Engine. NASA TP 1261, 1978.

9. Adams, R. J.; De Hoff, R. L.; and Hall, W. E., Jr.: Modeling and Instrumentation Requirements for Multivariable Control of an Advanced Turbofan Engine. AIAA Paper 77-834, July 1977.

10. Kwakernaak, Huibert; and Sivan, Raphael: Linear Optimal Control Systems. Wiley-Interscience, 1972.

11. Sellers, James F.; and Daniele, Carl J.: DYNGEN - A Program For Calculating Steady-State and Transient Performance of Turbojet and Turbofan Engines. NASA TN D-7901, 1975.

12. Schuerman, J. A.; Fischer, K. E.; and McLaughlin, P. W.: High Frequency Dynamic Engine Simulation. NASA CR-135313, 1977.

TABLE I. - TYPICAL ENGINE FLIGHT CONDITIONS

Operating point	Flight condition	Significance
1	Sea-level takeoff (SLTO)	Maximum nonaugmented (intermediate) thrust and maximum augmented thrust rating points (T_{T4}, stability, thrust primary importance).
2	Sea-level ram	Burner case pressure limit as well as extremely high fan and compressor blade and vane loading along this boundary. High structural and vibratory stress. High fan and compressor speeds may be reached here.
3	Supersonic dash	High steady-state inlet distortion and subsequent reduced stability margin. Possible inlet disturbance due to popping or swallowing the inlet shock waves during maneuvers.
4	Extreme envelope definition	Control must satisfy performance, stability, and safety limits. Also distortion and augmentor light problems. In addition, may reach or exceed fan and compressor speed limits.
5	Low-pressure limited-flight condition	Ignition limits for both main burner and augmentor occur along this boundary. Flame out and ignition instability possible.
6	Subsonic-cruise and combat maneuvering condition	Thrust specific fuel consumption (TSFC = thrust per unit mass of fuel) and therefore fuel flow and F/A ratio important. Transient engine response characteristics during combat mission. Also severe transient inlet distortion due to aircraft attitude changes.

TABLE II. - EIGENVALUES FOR TWO DIFFERENT PERTURBATION SIZES AT THE SEA-LEVEL-STATIC-IDLE OPERATING POINT

(a) Positive perturbations only

Change in state, ΔX, percent			
+0.5		+1.0	
Eigenvalues of A matrix			
Real	Imaginary	Real	Imaginary
-860.24312	0	-849.45871	0
-267.76119	0	-264.38152	0
-106.45859	0	-118.70167	0
-52.072414	24.775151	-50.905953	15.076307
-52.072414	-24.775151	-50.905953	-15.076307
-51.736044	0	-51.779746	0
-43.674746	0	-43.546884	↓
-28.475954	0	-26.871969	
-4.8312091	2.4935793	-8.1525361	
-4.8312091	-2.4935793	-3.9743200	↓
-20.034792	.38079509	-20.057634	.23031854
-20.034792	-.38079500	-20.057634	-.23031854
-2.0269044	0	-2.0128254	0
-.68641882	.22144251	-.69555555	.20482900
-.68641882	-.22144251	-.69555555	-.20482900
-21.033073	0	-20.914347	0

(b) Positive and negative perturbations

Change in state, ΔX, percent			
+0.5		+1.0	
Eigenvalues of A matrix			
Real	Imaginary	Real	Imaginary
-852.11287	0	-869.70083	0
-268.16126	↓	-422.82995	0
-135.01001		-133.54989	0
-56.317567		-50.563185	7.5119157
-49.669363		-50.563185	-7.5119157
-48.432318		-52.253414	0
-40.376271		-42.606607	↓
-14.119784		-23.852079	
-2.8587858	↓	-12.163400	↓
-21.319590	.83925693	-19.973461	.52786244
-21.319590	-.83925693	-19.973461	-.52786244
-19.747053	0	-.74937136	.24305228
-1.9813104	0	-.74937136	-.24305228
-.74410687	.20040877	-2.4917681	0
-.74410687	-.20040877	-1.9956926	0
-20.347614	0	-21.620234	0

TABLE III. - EIGENVALUES FOR

SEA-LEVEL-STATIC-IDLE

OPERATING POINT

Vector	Eigenvalues of A matrix	
	Real	Imaginary
1	-852.11287	0
2	-268.16126	↓
3	-135.01001	
4	-56.317567	
5	-49.669363	
6	-48.432318	
7	-40.376271	
8	-14.119704	
9	-2.8587858	↓
10	-21.319598	.83925693
11	-21.319590	-.83925693
12	-19.747853	0
13	-1.9813104	0
14	-.74410687	.20040877
15	-.74410687	-.20040877
16	-20.347614	0

TABLE IV. – MATRIX OF MODE SHAPES, IN MAGNITUDE AND ANGLE (DEG) FORM FOR SEA-LEVEL-STATIC-IDLE

OPERATING POINT

STATE OR VECTOR	1	2	3	4	5	6	7	8
1	-0.5091D-02	0.1112D-01	-0.1061D-01	-0.1119D-01	-0.3240D-02	-0.1674D-01	0.8529D-02	0.3946D-01
2	0.6996D-03	0.4697D-02	-0.5217D-02	-0.3222D-02	0.6876D-04	0.1756D-02	-0.1572D-01	-0.9271D-02
3	0.4265D-02	-0.6182	1.000	-0.4488D-01	-0.2938D-03	-0.4445D-02	-0.8495D-02	-0.1791
4	1.000	0.4298	0.6677	-0.4734D-01	0.5837D-03	0.5958D-02	-0.4413D-01	-0.2851D-01
5	-0.8348D-01	1.000	0.2819	0.2741D-02	0.1060D-02	-0.1601D-04	-0.1031D-03	0.6830D-01
6	0.4284D-03	-0.1099D-01	-0.8042D-02	0.5728D-03	-0.7569D-05	0.1542D-02	-0.3850D-02	0.1023
7	0.5358D-03	-0.1371D-01	-0.1104D-01	0.1607D-03	0.1103D-03	0.1434D-02	-0.5078D-02	0.1360
8	-0.3148D-03	0.1986D-01	-0.3447D-01	0.5197D-02	-0.3029D-04	-0.1337D-02	0.7846D-02	0.1324
9	0.9951D-04	-0.1567D-01	0.1978D-01	0.2910	-0.4684D-02	-0.1246	1.000	0.3339
10	0.1329D-04	-0.2056D-02	0.2554D-02	0.3579D-01	-0.5702D-03	-0.1512D-01	0.1188	0.3021D-01
11	-0.1701D-02	0.7303D-01	-0.3301D-01	-0.4046D-01	0.2507D-04	-0.4099D-02	0.2084	0.2486
12	-0.1639D-01	-0.9005D-01	0.9364D-01	1.000	0.2054	1.000	-0.1710	0.3722
13	-0.6535D-02	-0.3562D-01	0.3660D-01	0.3781	0.7704D-01	0.3743	-0.6317D-01	0.1121
14	-0.1167D-02	-0.4395D-01	0.4630D-01	0.1088	0.8835D-02	0.2722D-01	0.1306D-01	0.9822
15	0.9337D-06	0.5654D-03	0.2050D-02	-0.6855D-04	-0.8388D-04	-0.1040D-02	0.4891D-02	0.4569
16	-0.1959D-01	-0.2511D-01	-0.1308	-0.5305	1.000	0.6876	-0.7342D-01	1.000

	9	10	11	12	13	14	15	16
1	1.000	0.1108D-01	0.0000	0.0000	0.0000	0.0000	0.0000	0.0000
2	-0.2465D-01	0.4686D-02	0.1100D 08	0.1200D 08	0.1300D 08	0.1400D 08	0.1500D 08	0.1600D 08
3	-0.1354	0.1584	-121.3	-0.2911D-03	0.8936D-01	1.000	0.0000	0.2817D-02
4	0.5330D-01	0.9993D-01	-90.69	-0.1233D-03	-0.3463D-02	0.2065	7.058	0.1992D-02
5	0.1493	0.5802D-01	29.69	0.1331D-01	-0.1498D-01	0.9429	6.993	-0.6495D-02
6	0.2047	0.4624D-01	21.40	0.2282D-01	0.3274D-02	0.4792	4.804	0.1178D-01
7	0.2076	0.4681D-01	1.219	0.3413D-01	0.1278D-01	0.1468	-0.1646	0.3102D-01
8	0.6082D-01	0.1276	-149.6	-0.3197D-02	0.1705D-01	0.1331	-2.988	0.1911D-02
9	0.1172	0.1364	-148.5	-0.1164D-01	0.1767D-01	0.1073	-5.304	0.1674D-01
10	-0.1521D-01	0.1438D-01	58.19	0.1637D-01	0.3054D-01	0.2734	4.476	-0.2850D-01
11	0.1146	0.7760D-01	101.8	0.1632D-01	0.9846D-02	0.2582	-171.5	-0.4952D-01
12	0.1764	0.1071	101.2	0.1686D-02	-0.3006D-02	0.6820	80.10	-0.5149D-02
13	-0.1750	0.3622D-01	109.1	0.9431D-02	0.9992D-02	0.2990	-171.6	-0.2933D-01
14	0.2362	0.7247	112.6	0.1905D-01	0.1547D-01	0.3887	-168.3	-0.3569D-01
15	0.2336	0.5801	112.1	0.6321D-02	1.000	0.5185	-174.6	-0.1195D-01
16	-0.1137	1.000	-22.76	1.000	0.1178D-01	0.4734	-169.2	1.000

TABLE V. - MODAL REDUCTION AT SEA-LEVEL-STATIC-IDLE

OPERATING POINT

(a) States and corresponding
eigenvalues

States	Eigenvalues, rad/sec
1	-2.86, -0.744±0.20
2	-0.744±0.20
3	-135.01, -0.744±0.20
5	-268.16

(b) Possible models
(states 1, 2, 3, and 5)

Model	Eigenvalues, rad/sec
1	-2.86, -0.744±0.20, -268.16
2	-0.744±0.20, -135.01, -268.16

TABLE VI. - OPERATING-POINT DEFINITION

FOR 16TH-ORDER LINEAR MODELS

Operating point	Power lever angle, deg	Altitude, km	Mach number	Data (pages)
1	20	0	0	33 - 35
2	83	0	0	36 - 38
3		0	1.2	39 - 41
4		13.7	.9	42 - 44
5		9.14	.9	45 - 47
6	20	9.14	.9	48 - 50

TABLE VII. - OPERATING-POINT DEFINTION

FOR FOURTH-ORDER LINEAR MODELS

Operating point	Power lever angle, deg	Altitude, km	Mach number	Data (pages)
1	20	0	0	55
2	83	0	0	56
3		0	1.2	57
4		13.7	.9	58
5		9.14	.9	59
6	20	9.14	.9	60
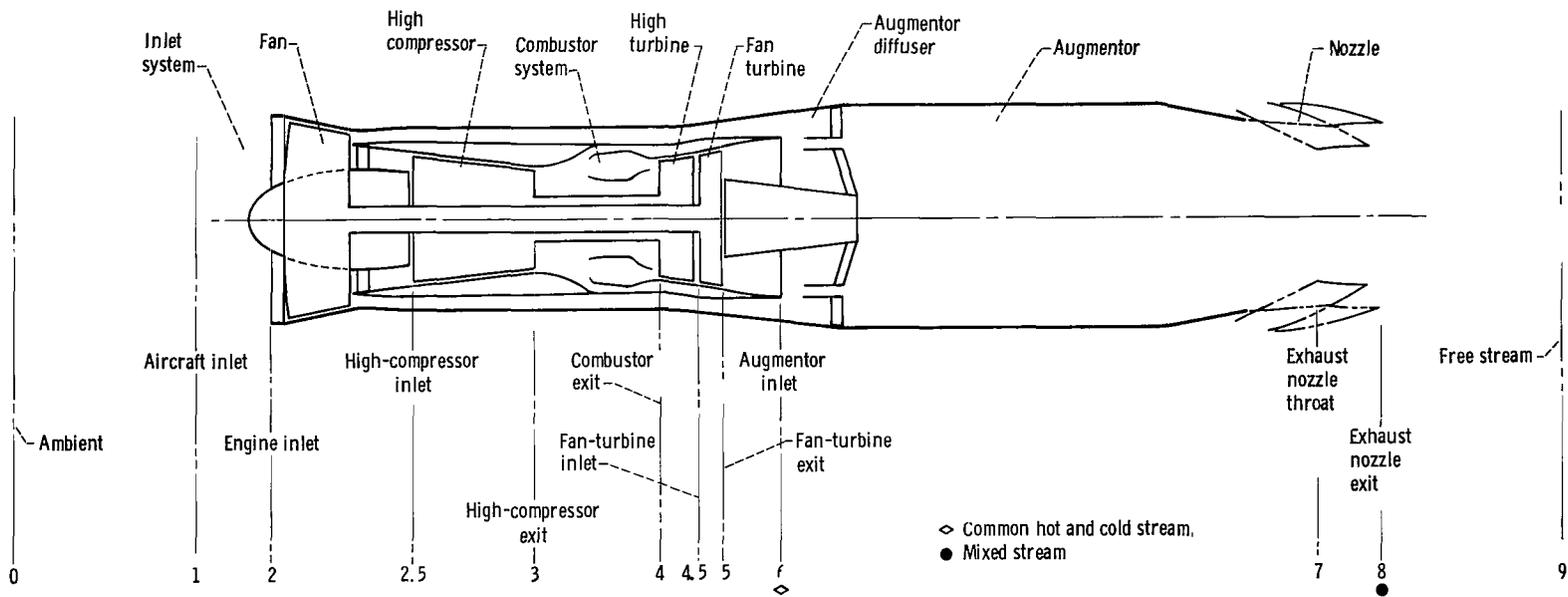
Figure 1. - F100 component and station identification.

CD-12309-07
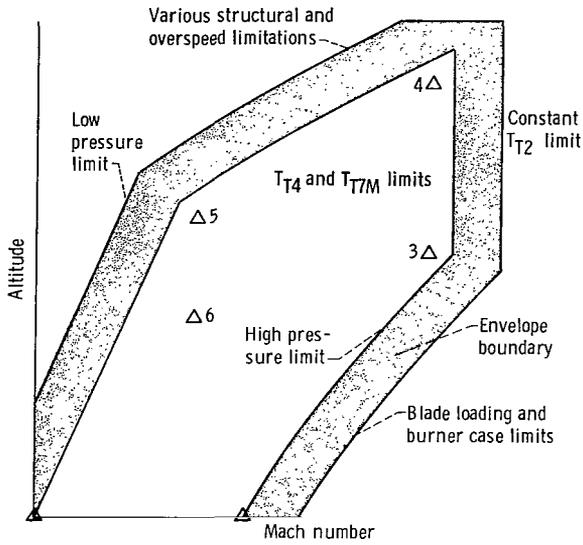
Figure 2. – Typical engine operating envelope with constraints.
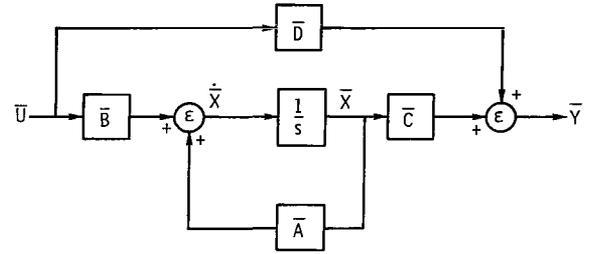
Figure 3. – Linear engine model.

Perturbation,
percent

○ +0.5
□ +1.0
▲ Eigenvalues coincide

(a) Positive perturbation.   (b) Positive and negative perturbations averaged.
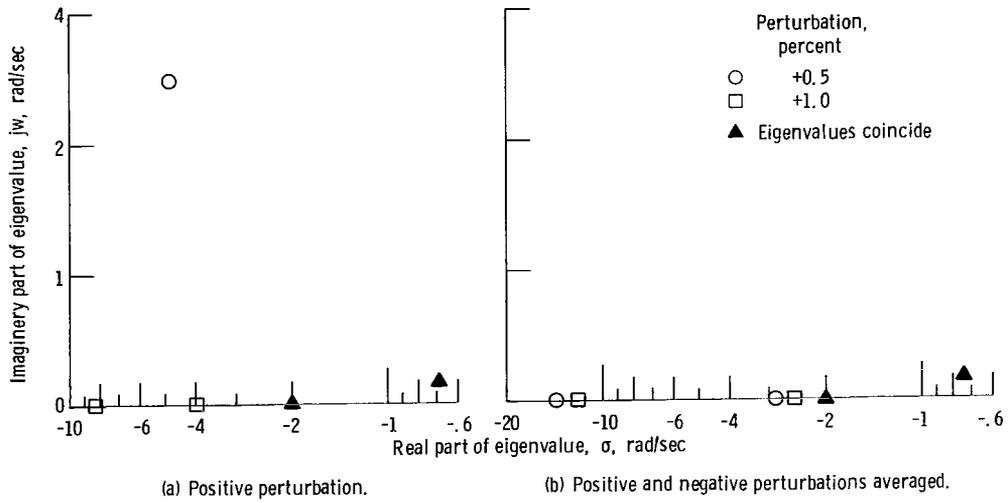
Figure 4. – Eigenvalue shift (upper left-half plane).

(a) Fan speed.

(b) Compressor speed.

(c) Burner-exit temperature.

(d) Engine net thrust.
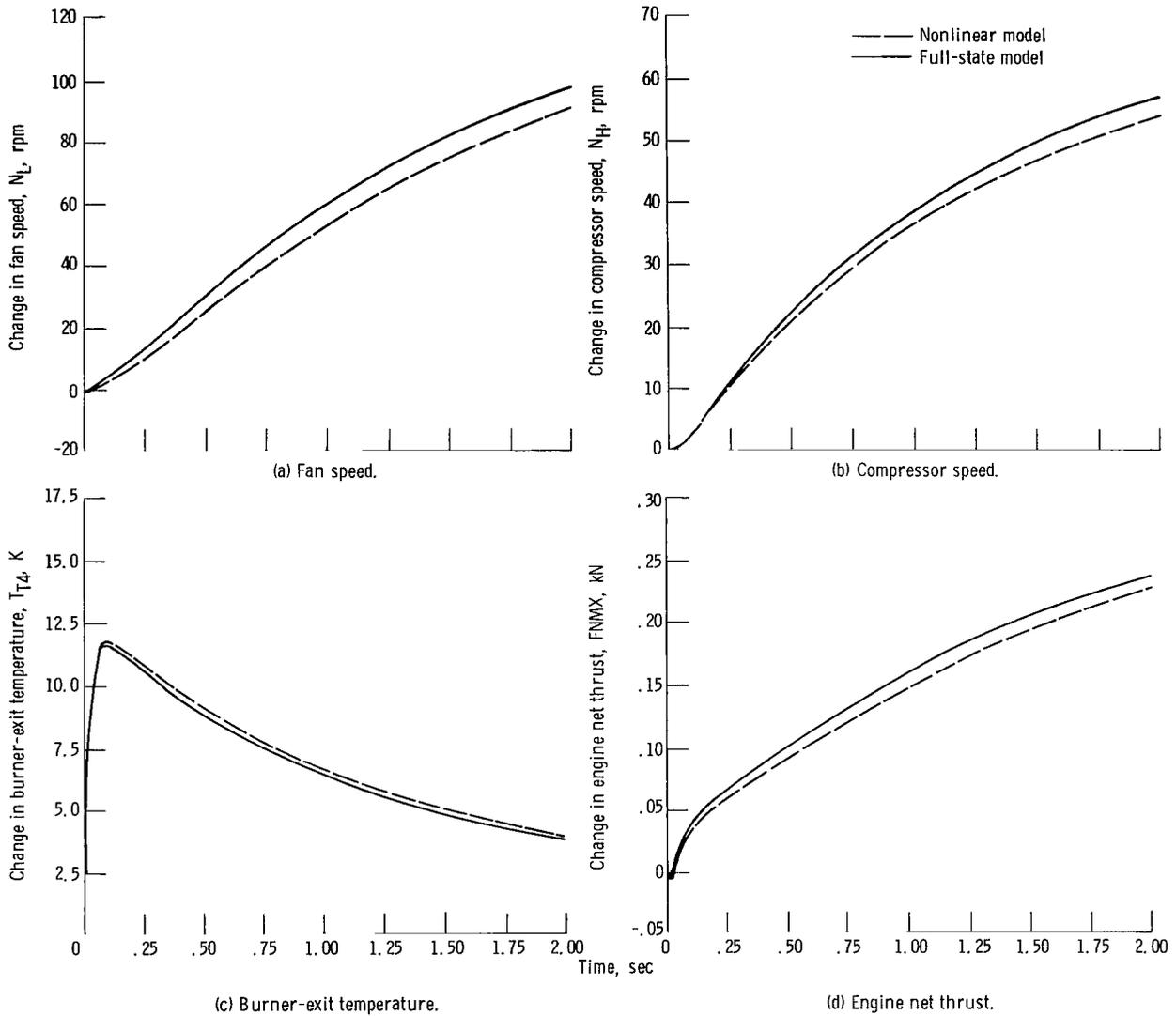
Figure 5. – Comparison of nonlinear and full-state linear-model responses to a +3 percent step in fuel flow; sea-level-static-idle operating point.
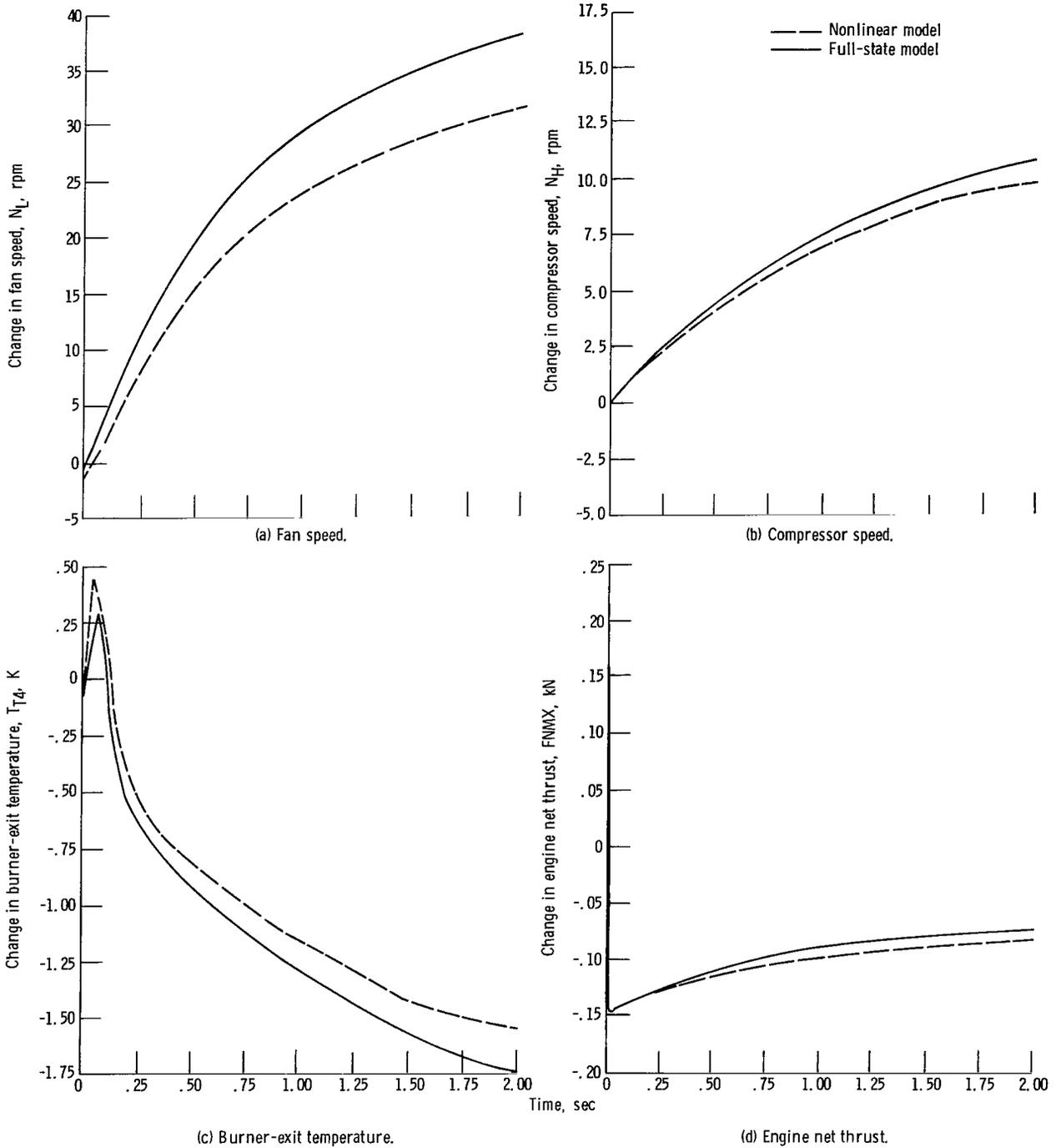
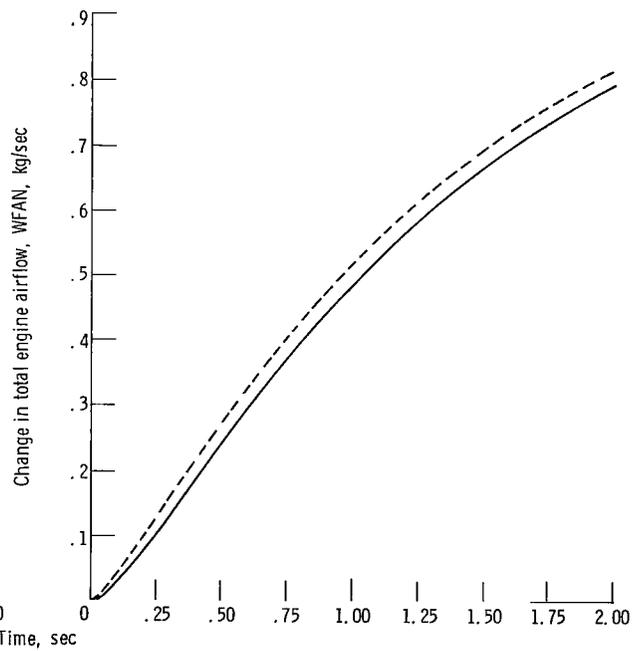Figure 6. – Comparison of nonlinear and full-state linear model responses to a +3 percent step in nozzle area; sea-level-static-idle operating point.

70
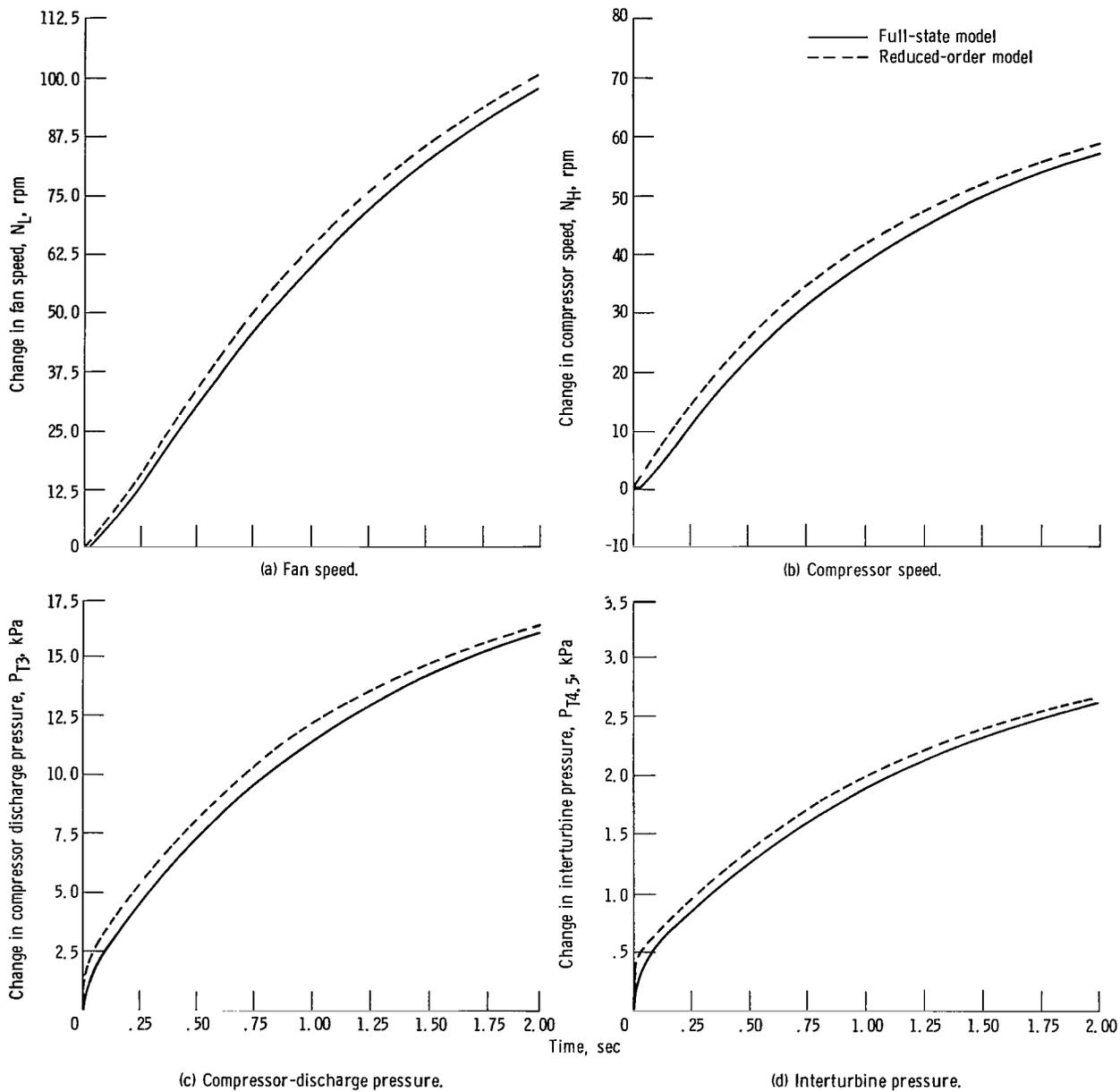
Figure 7. – Comparison of full-state and reduced-order linear-model responses to a +3 percent step in fuel flow; sea-level-static-idle operating point.

71

(e) Augmentor pressure.
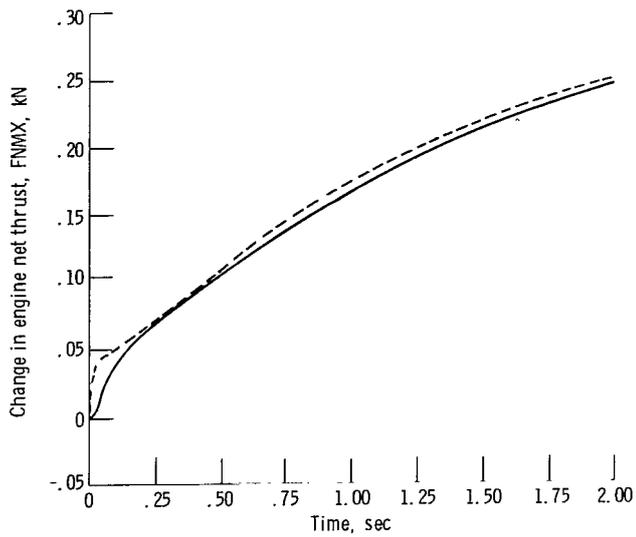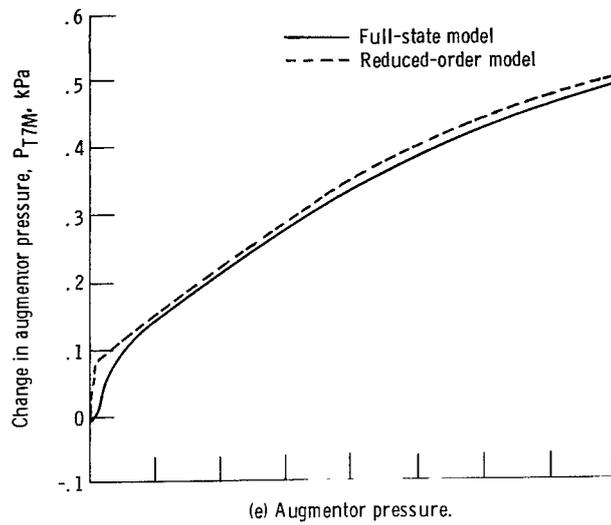
(f) Engine net thrust.

Figure 7. – Concluded.
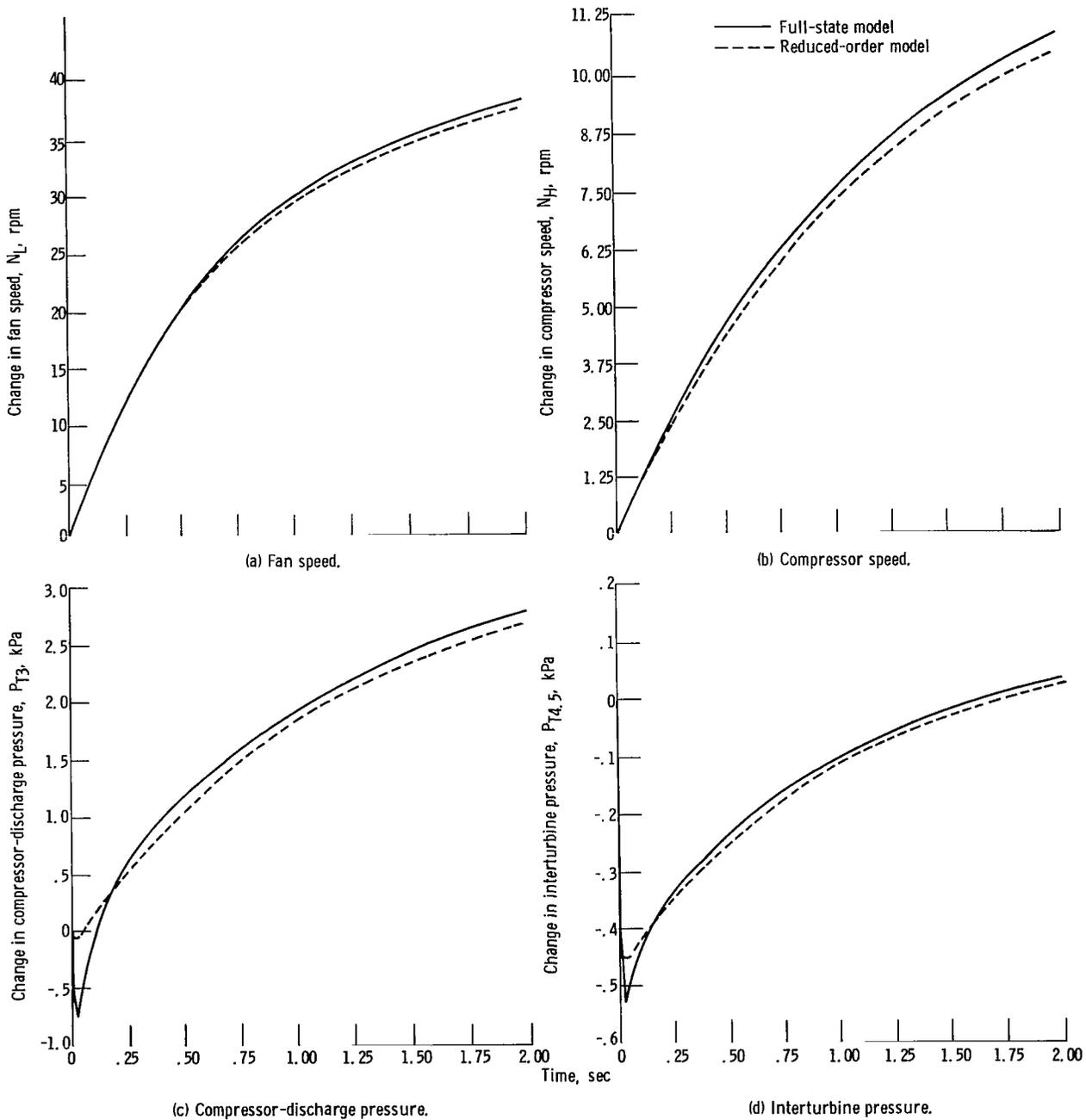
Figure 8. - Comparison of full-state and reduced-order linear-model responses to a +3 percent step in nozzle area; sea-level-static-idle operation.

73

(e) Augmentor pressure.

(f) Engine net thrust.
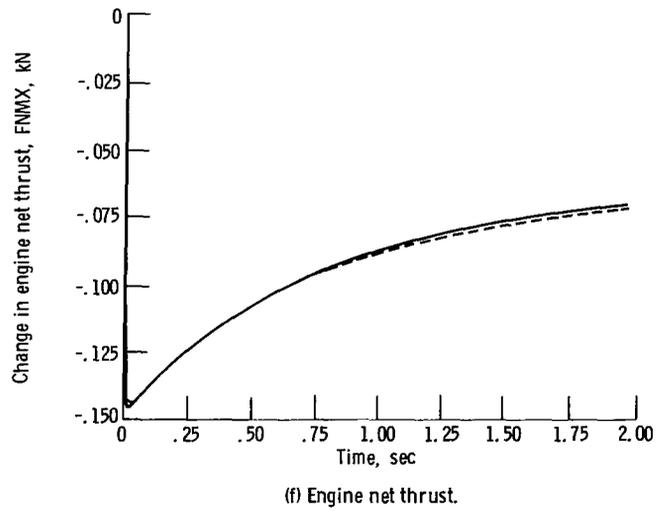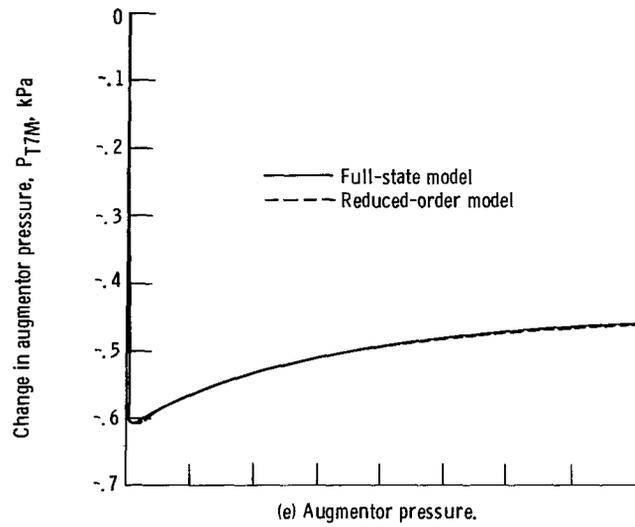
Figure 8. – Concluded.
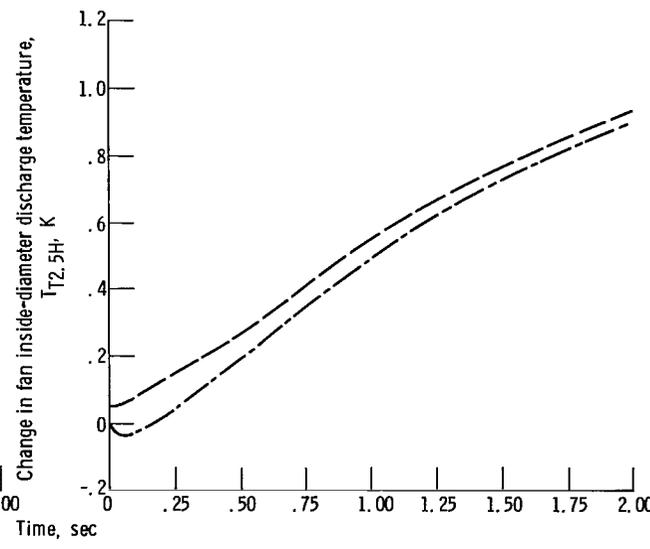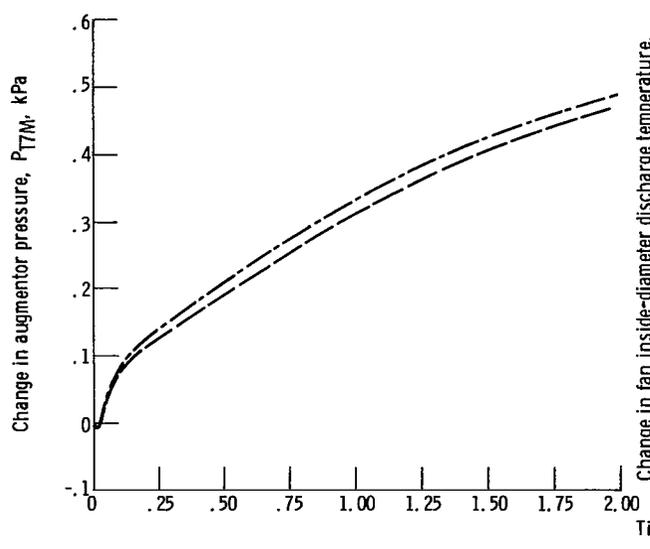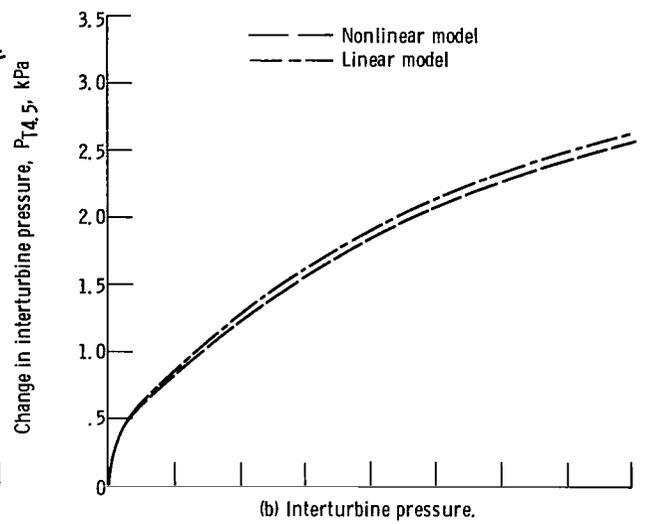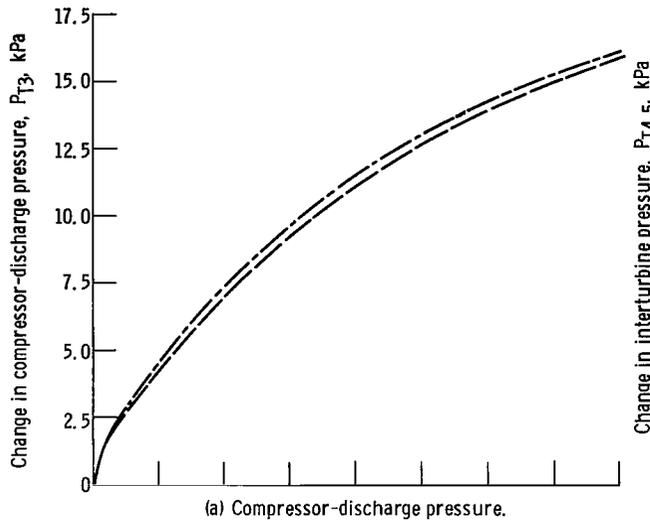
Figure 9. – Comparison of nonlinear- and linear-model responses to a +3 percent step in fuel flow; sea-level-static-idle operating point.
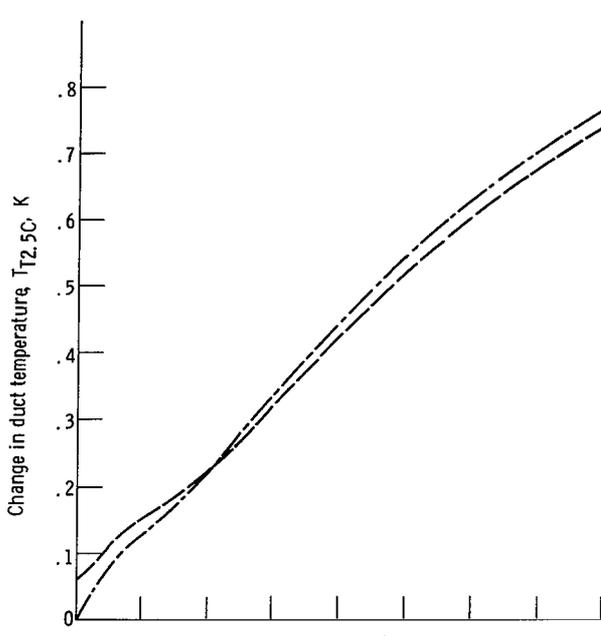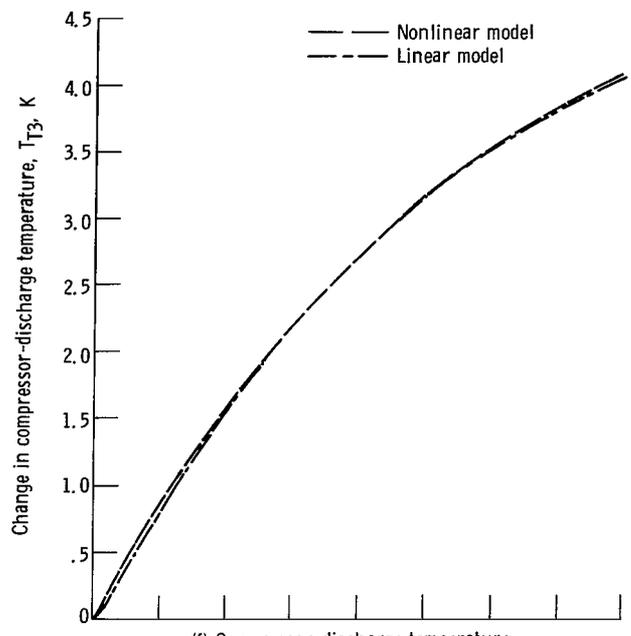
(e) Duct temperature.

(f) Compressor-discharge temperature.
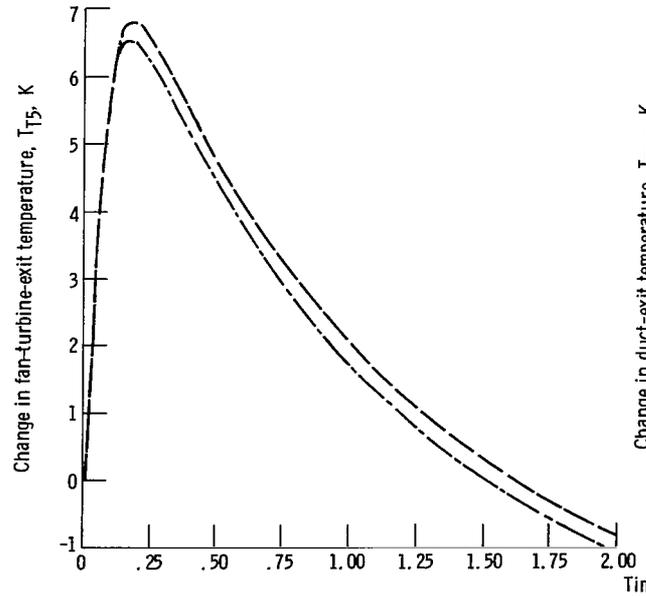
(g) Fan-turbine-exit temperature.
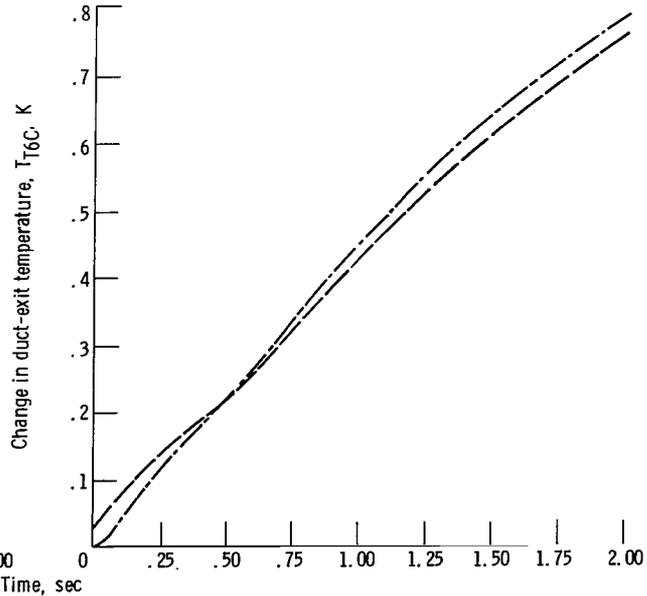
(h) Duct-exit temperature.

Figure 9. - Continued.
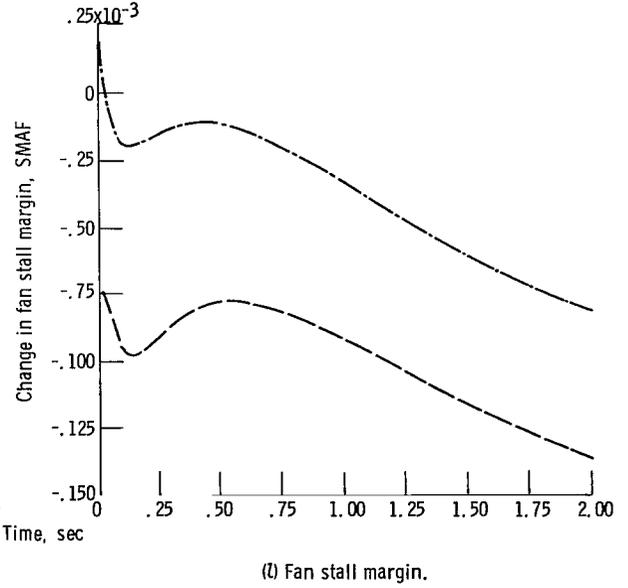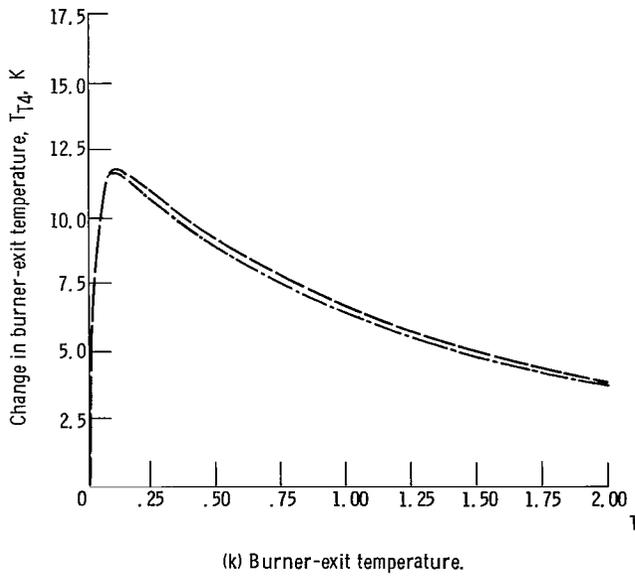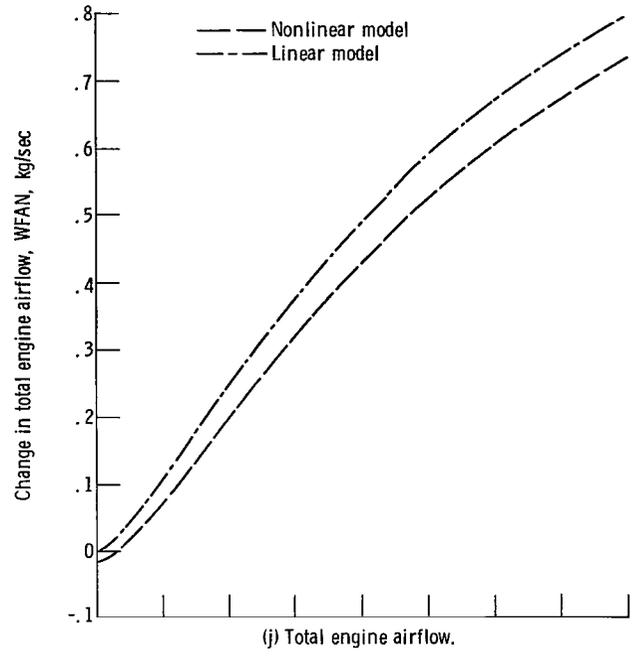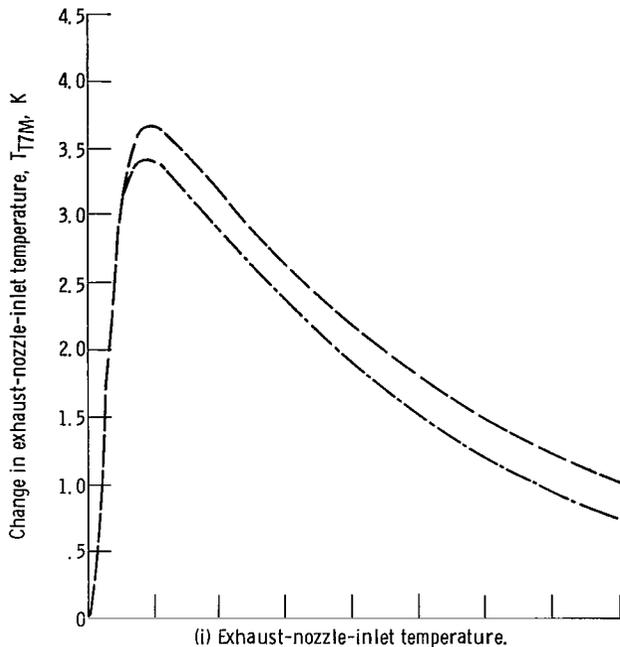
(i) Exhaust-nozzle-inlet temperature.

(j) Total engine airflow.

(k) Burner-exit temperature.

(l) Fan stall margin.

Figure 9. – Continued.

Figure 9. – Concluded.
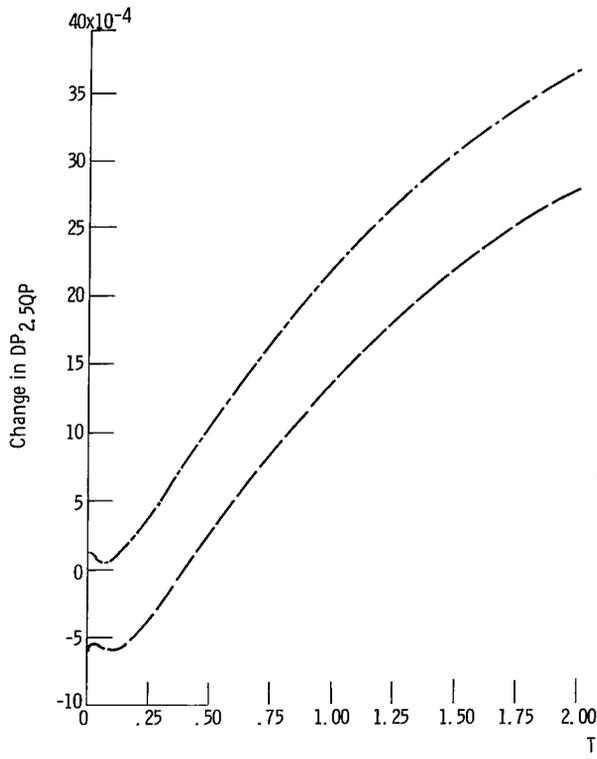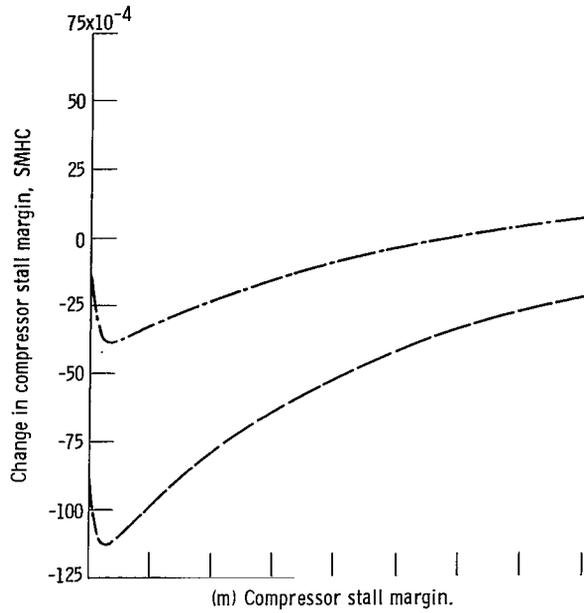
(m) Compressor stall margin.

(n) Empirical fan-exit ΔP/P parameter.

(o) Theoretical fan-exit ΔP/P parameter.

(a) Compressor-discharge pressure.

(b) Interturbine pressure.

(c) Augmentor pressure.

(d) Fan inside-diameter discharge temperature.
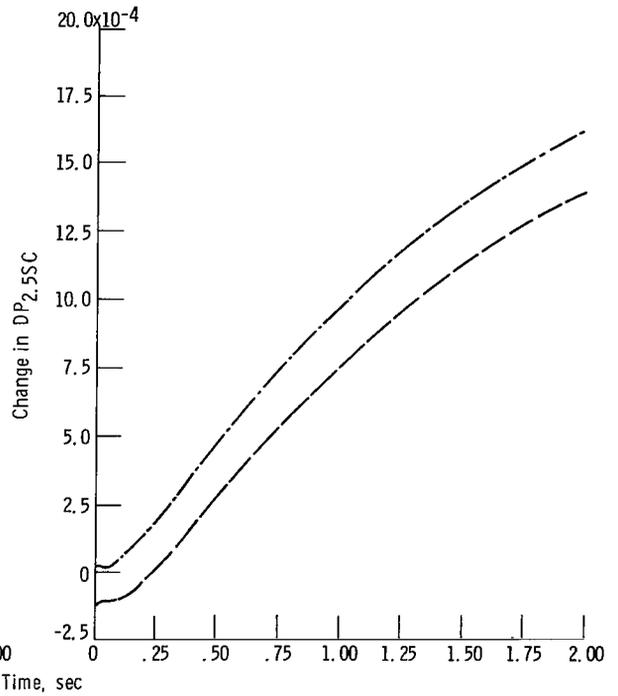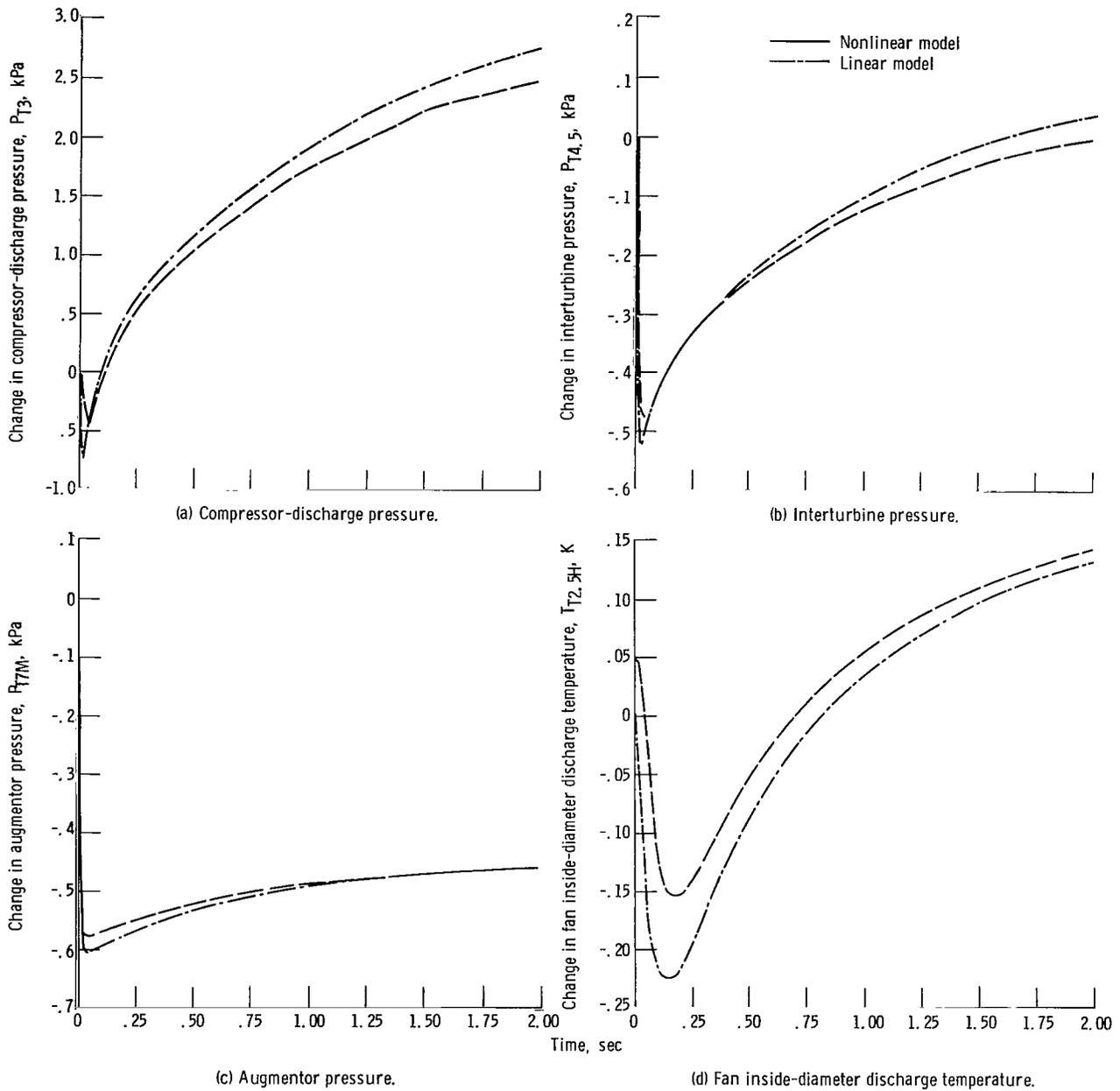
Figure 10. - Comparison of nonlinear- and linear-model responses to a +3 percent step in nozzle area; sea-level-static-idle operating point.

(e) Duct temperature.

(f) Compressor-discharge temperature.

(g) Fan-turbine-exit temperature.

(h) Duct-exit temperature.

Figure 10. – Continued.

80

(i) Exhaust-nozzle-inlet temperature.

(j) Total engine airflow.

(k) Burner-exit temperature.

(l) Fan stall margin.

Figure 10. – Continued.

81

(m) Compressor stall margin.
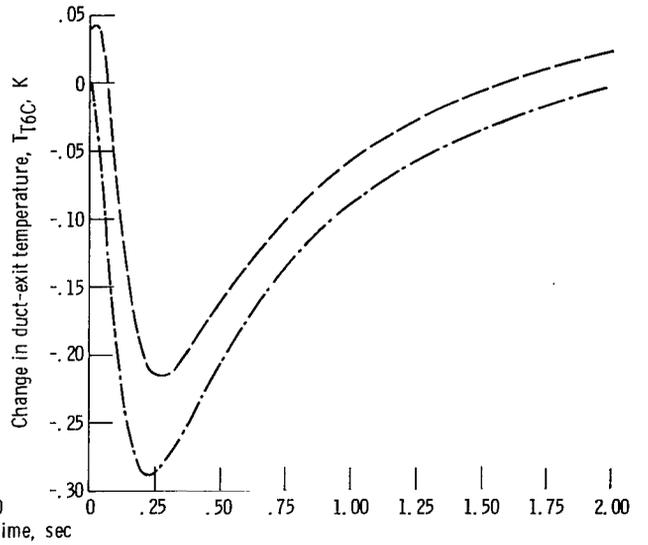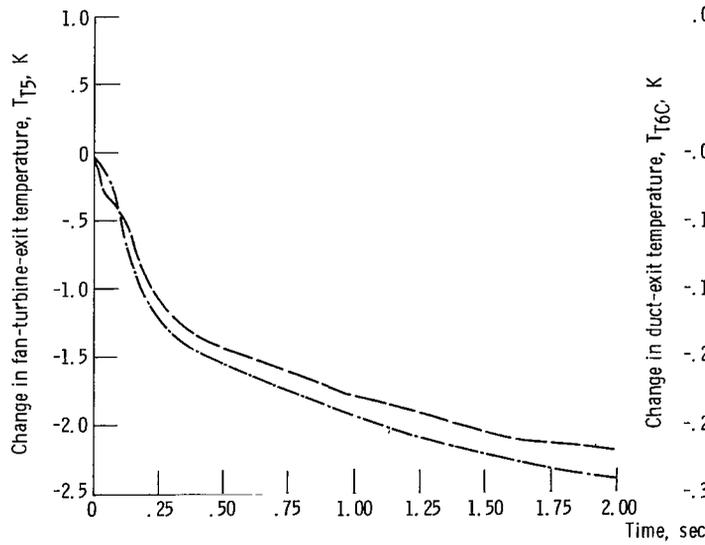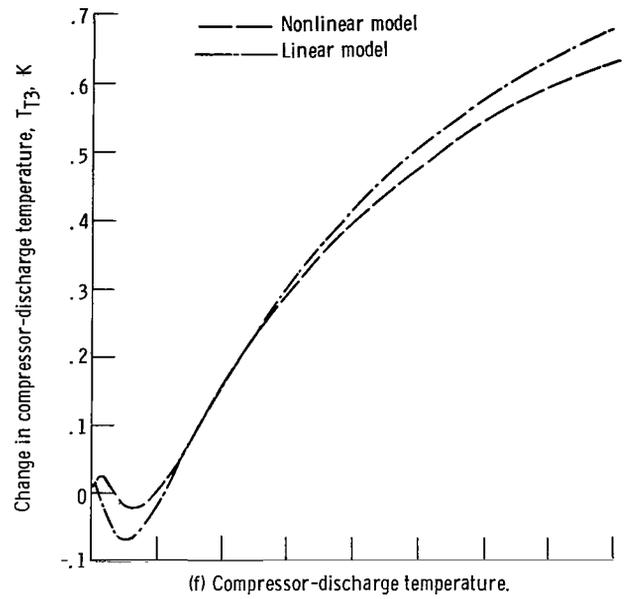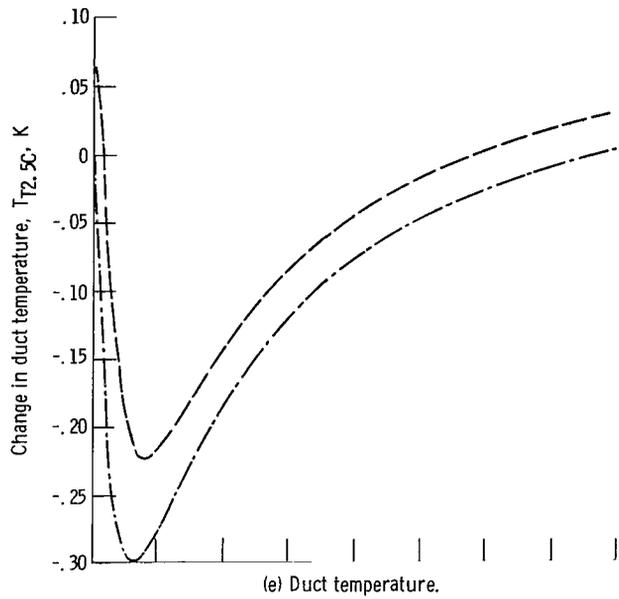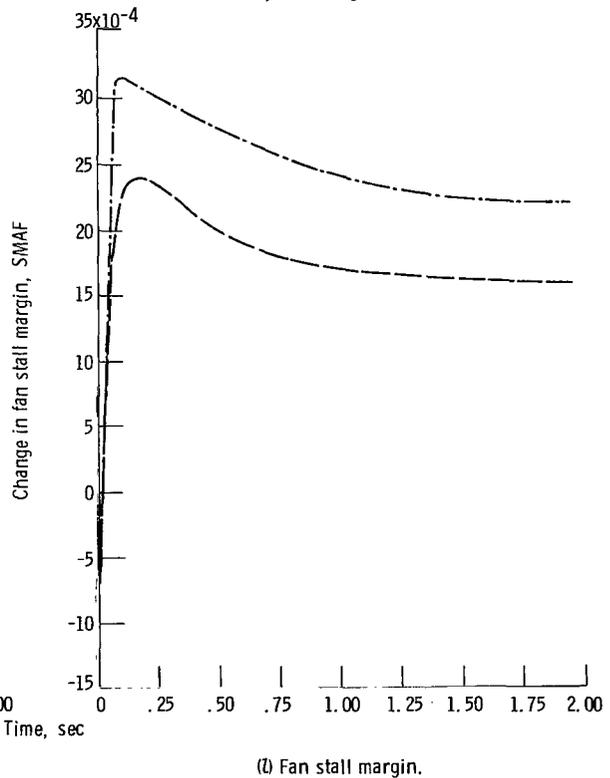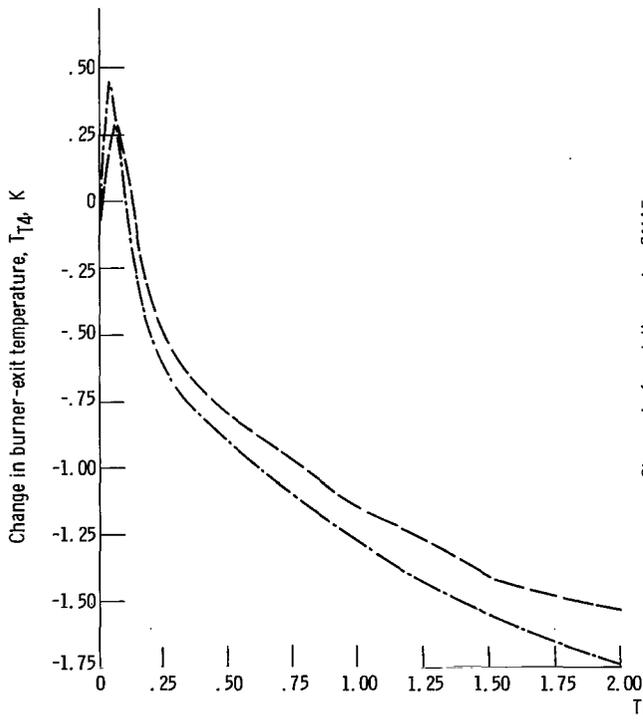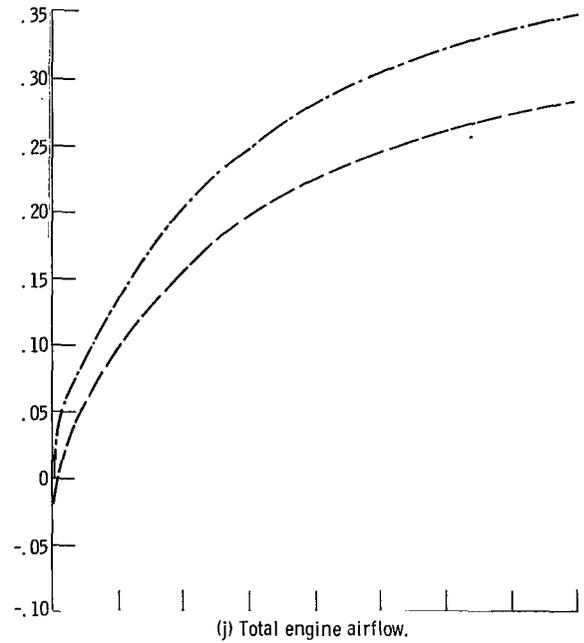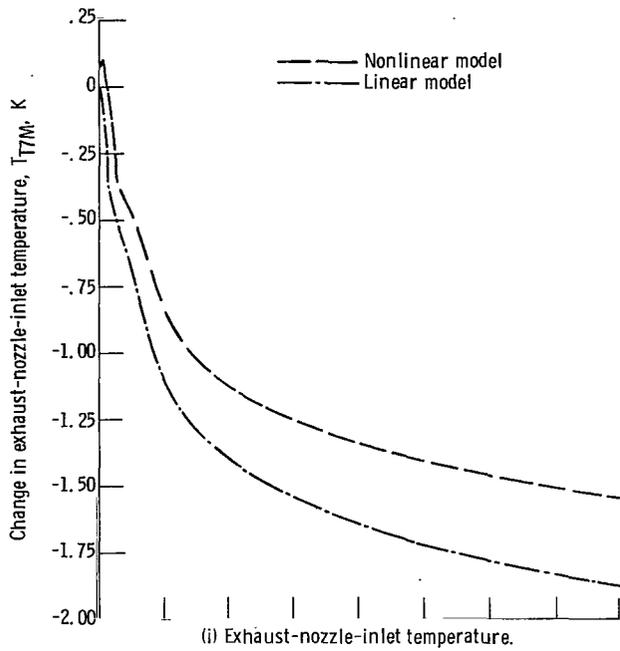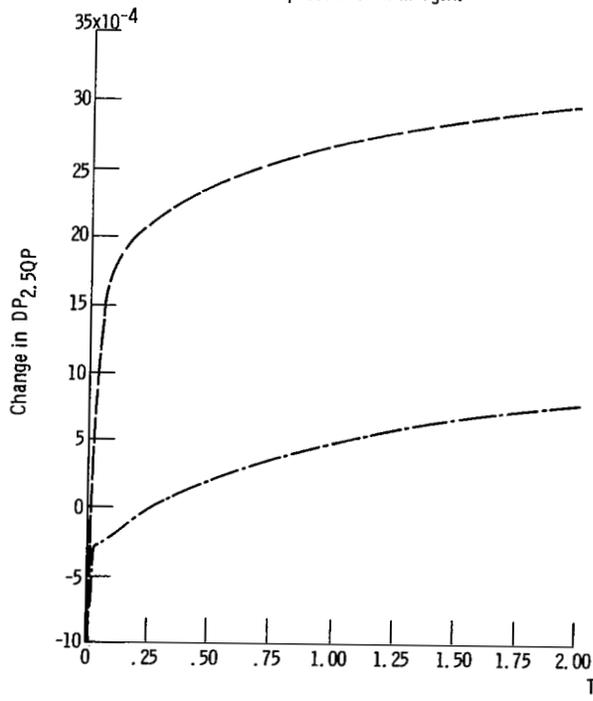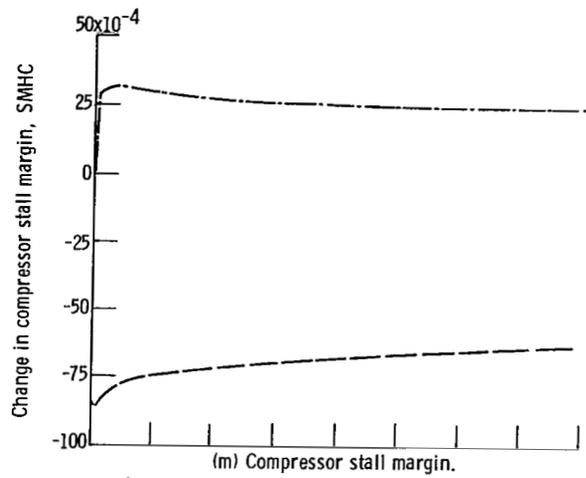
(n) Empirical fan-exit $\Delta P/P$ parameter.
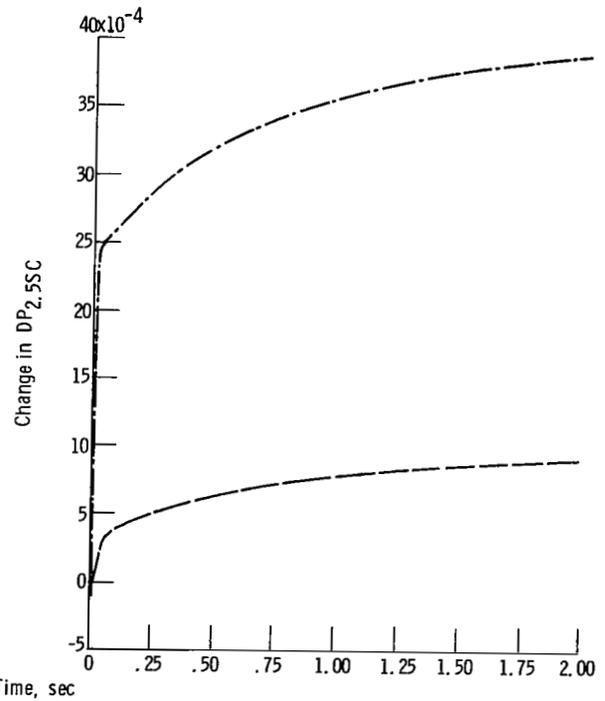
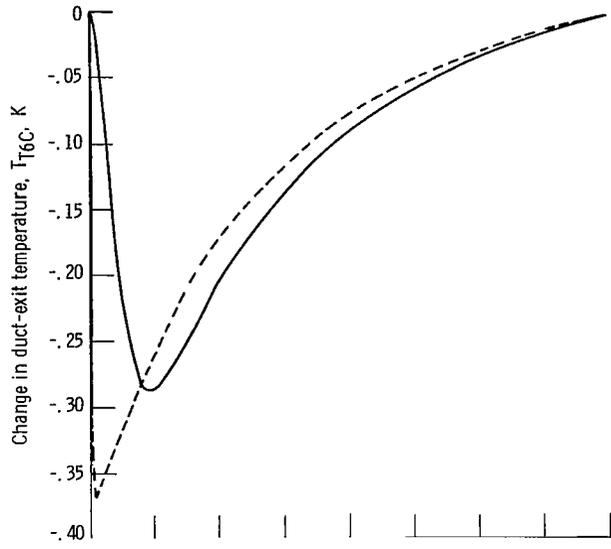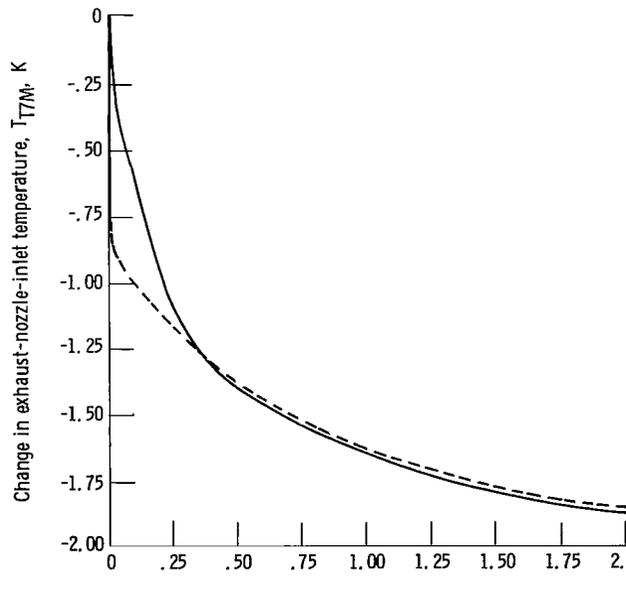(o) Theoretical fan-exit $\Delta P/P$ parameter.

Figure 10. - Concluded.

(a) Compressor speed.

(b) Fan speed.
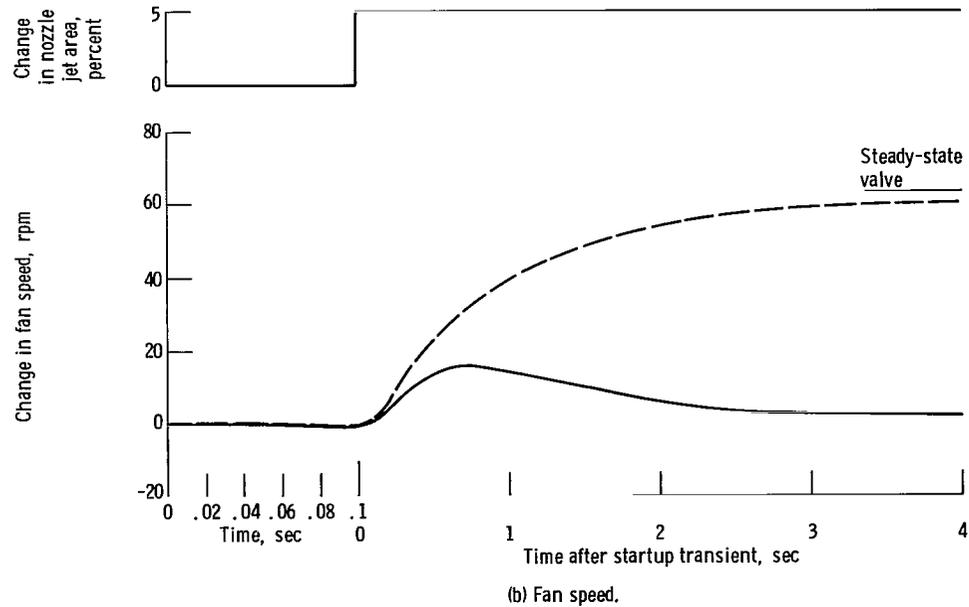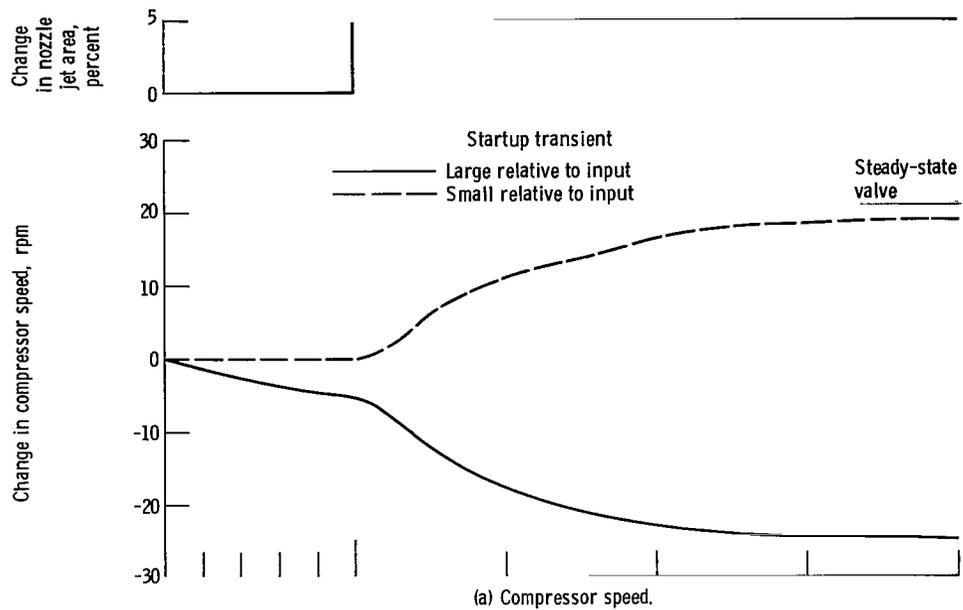
Figure 11. - Effect of startup transient.

83
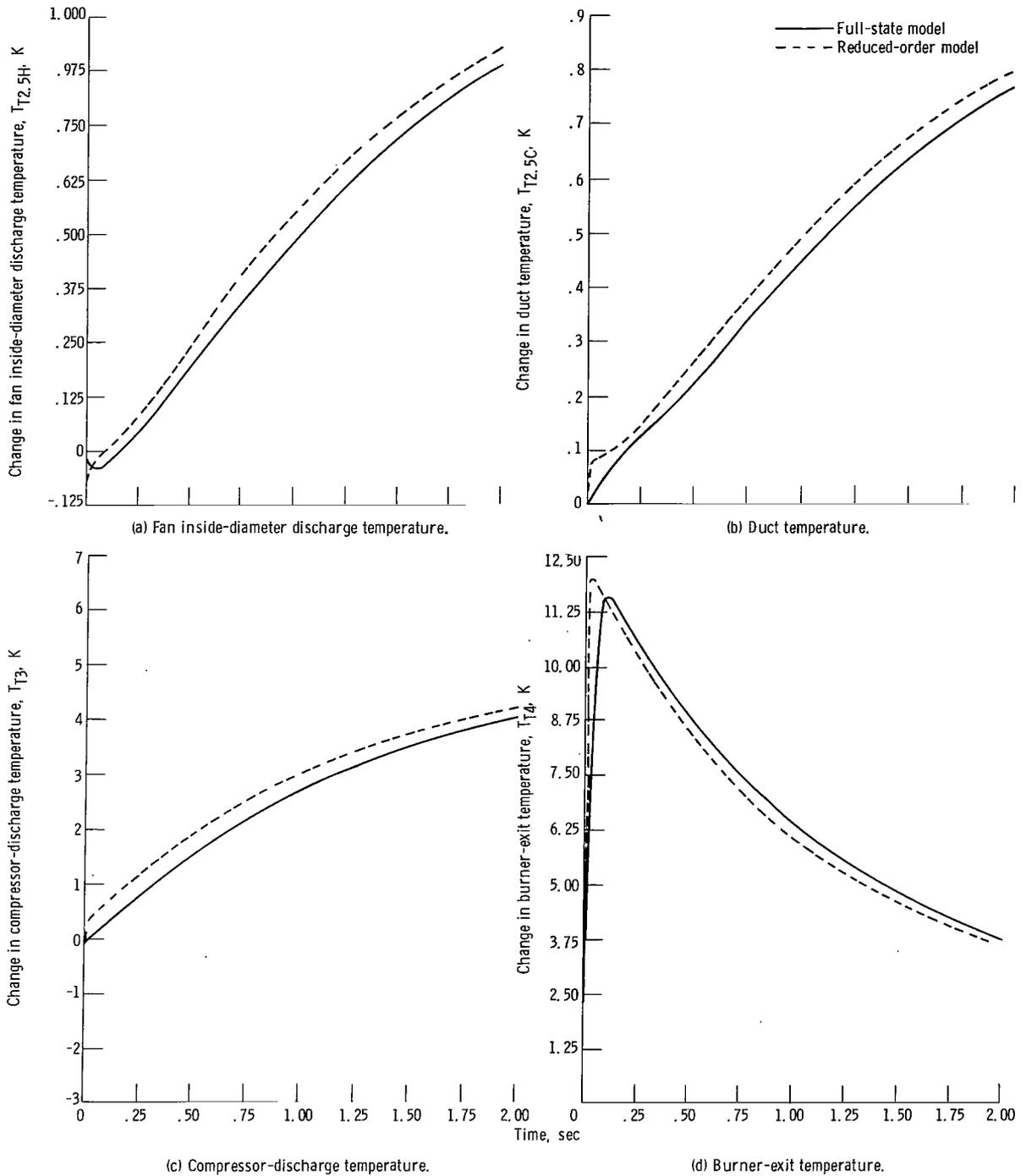
Figure 12. – Comparison of full-state and reduced-order (4th) linear-model responses to a +3 percent step in fuel flow; sea-level-static-idle operating point.
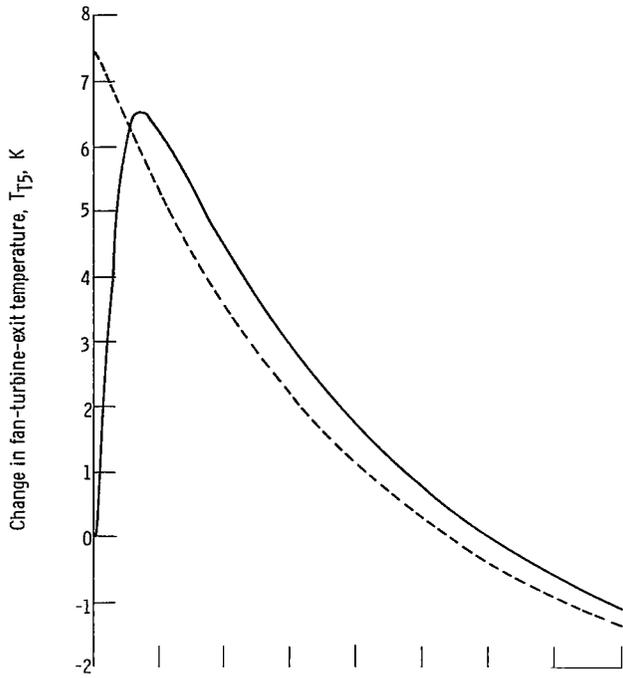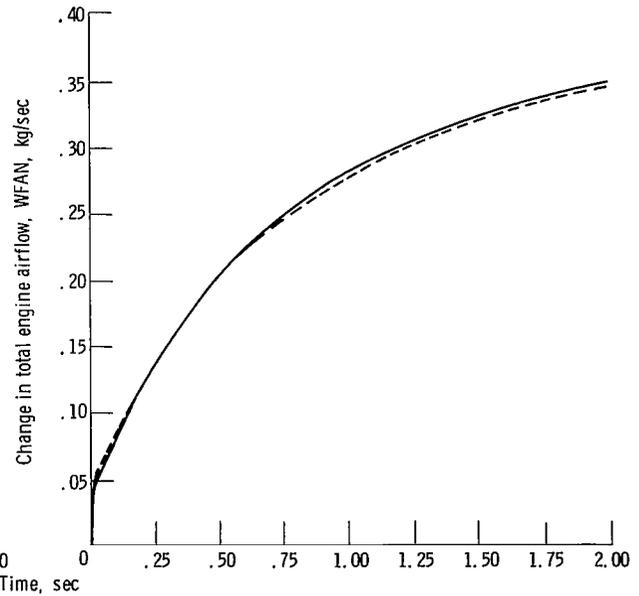
(e) Fan-turbine-exit temperature.
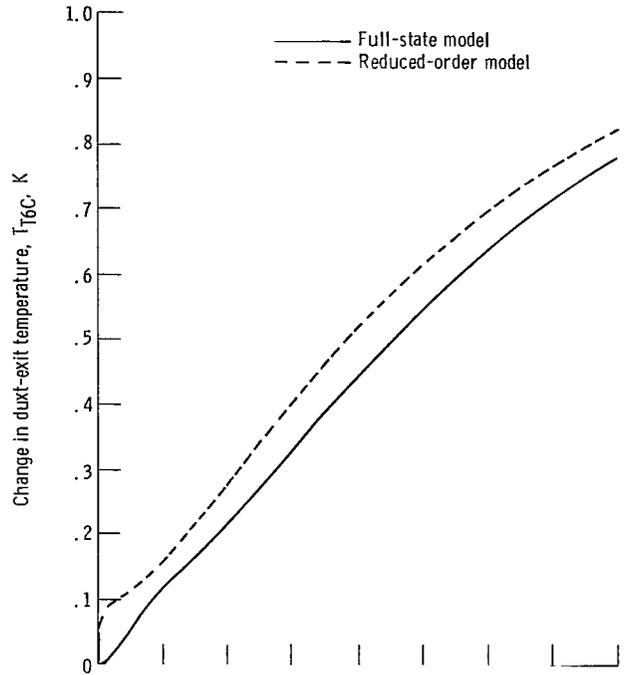
(f) Duct-exit temperature.
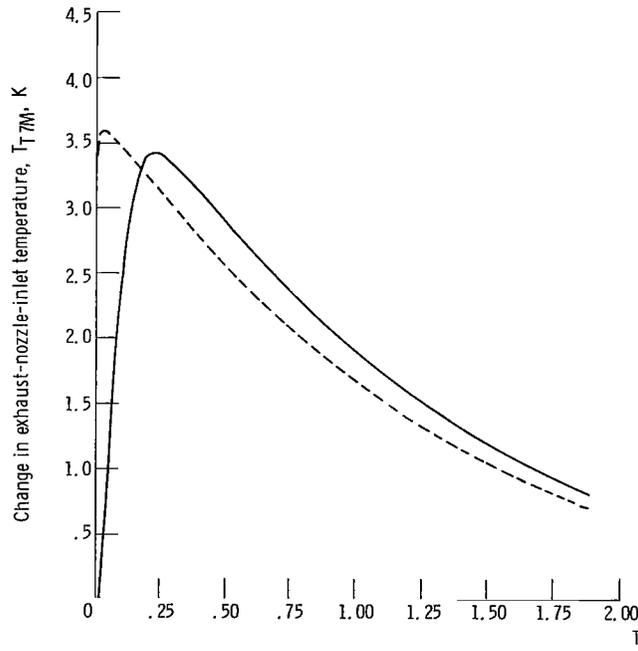
(g) Exhaust-nozzle-inlet temperature.

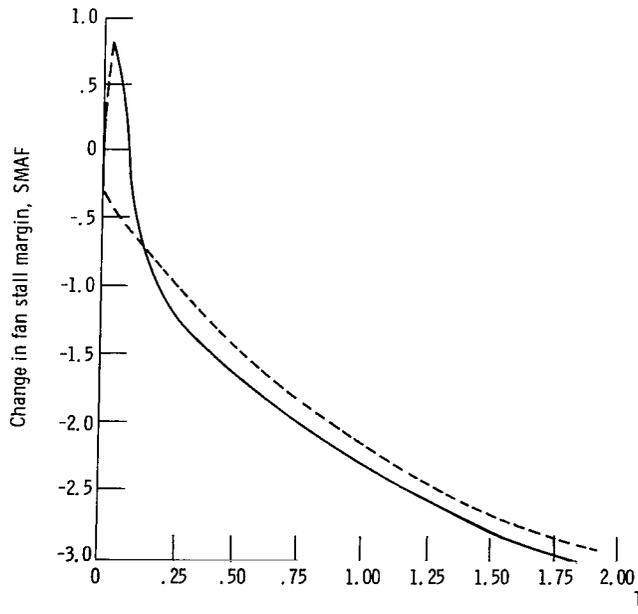(h) Total engine airflow.

Figure 12. - Continued.
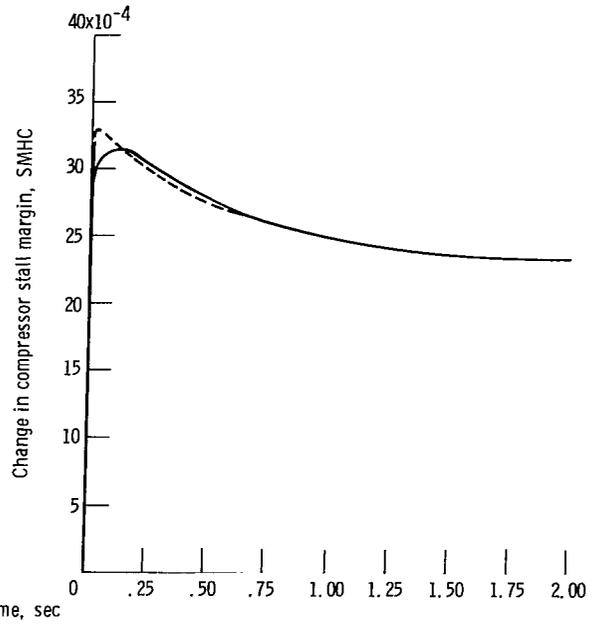
85

Full-state model
Reduced-order model

(i) Burner-exit temperature.

(j) Fan stall margin.

(k) Compressor stall margin.
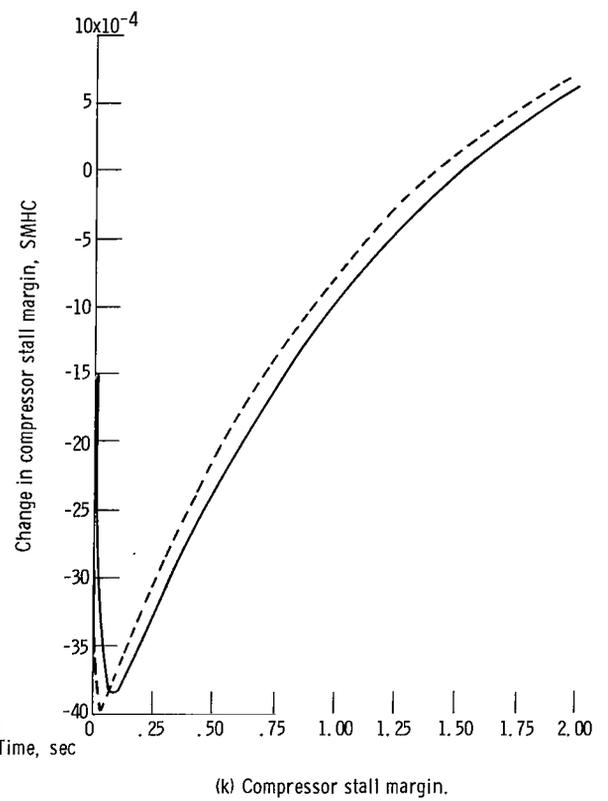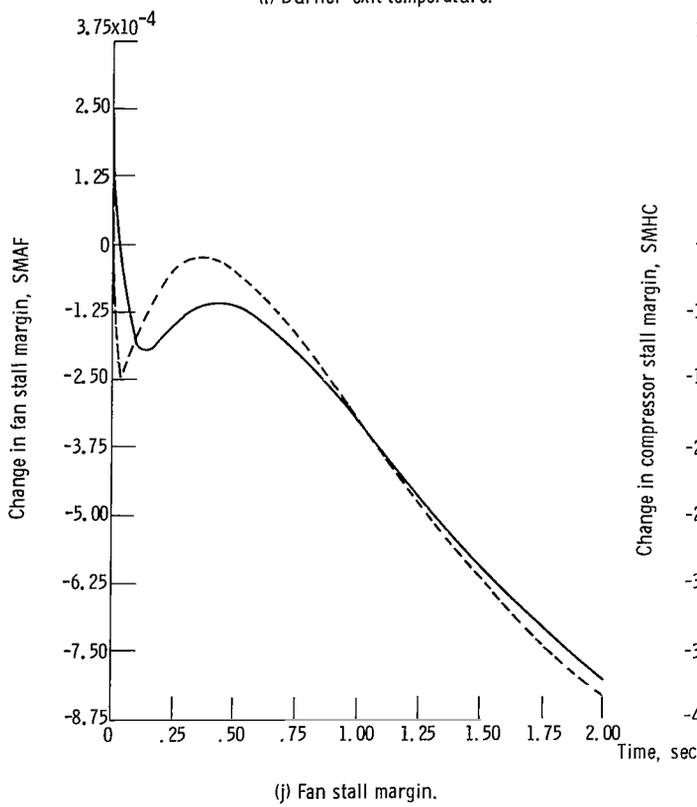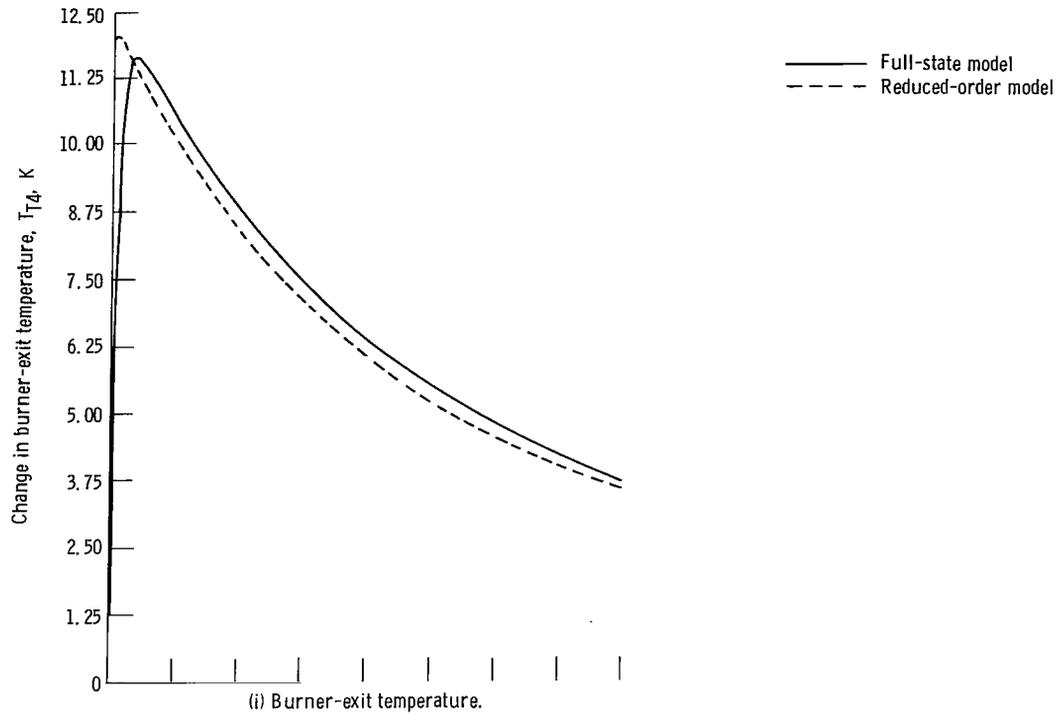
Figure 12. - Continued.
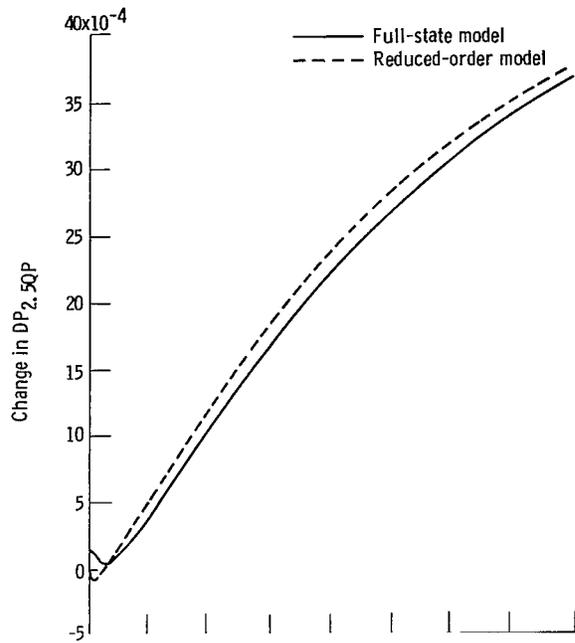
(ℓ) Empirical fan-exit $\Delta P/P$ parameter.
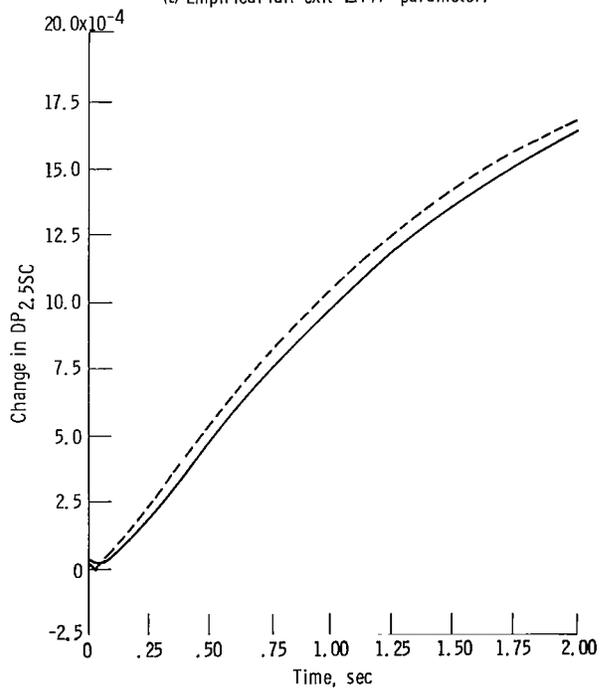
(m) Theoretical fan-exit $\Delta P/P$ parameter.

Figure 12. – Concluded.

(a) Fan inside-diameter discharge temperature.

(b) Duct temperature.

(c) Compressor-discharge temperature.

(d) Burner-exit temperature.
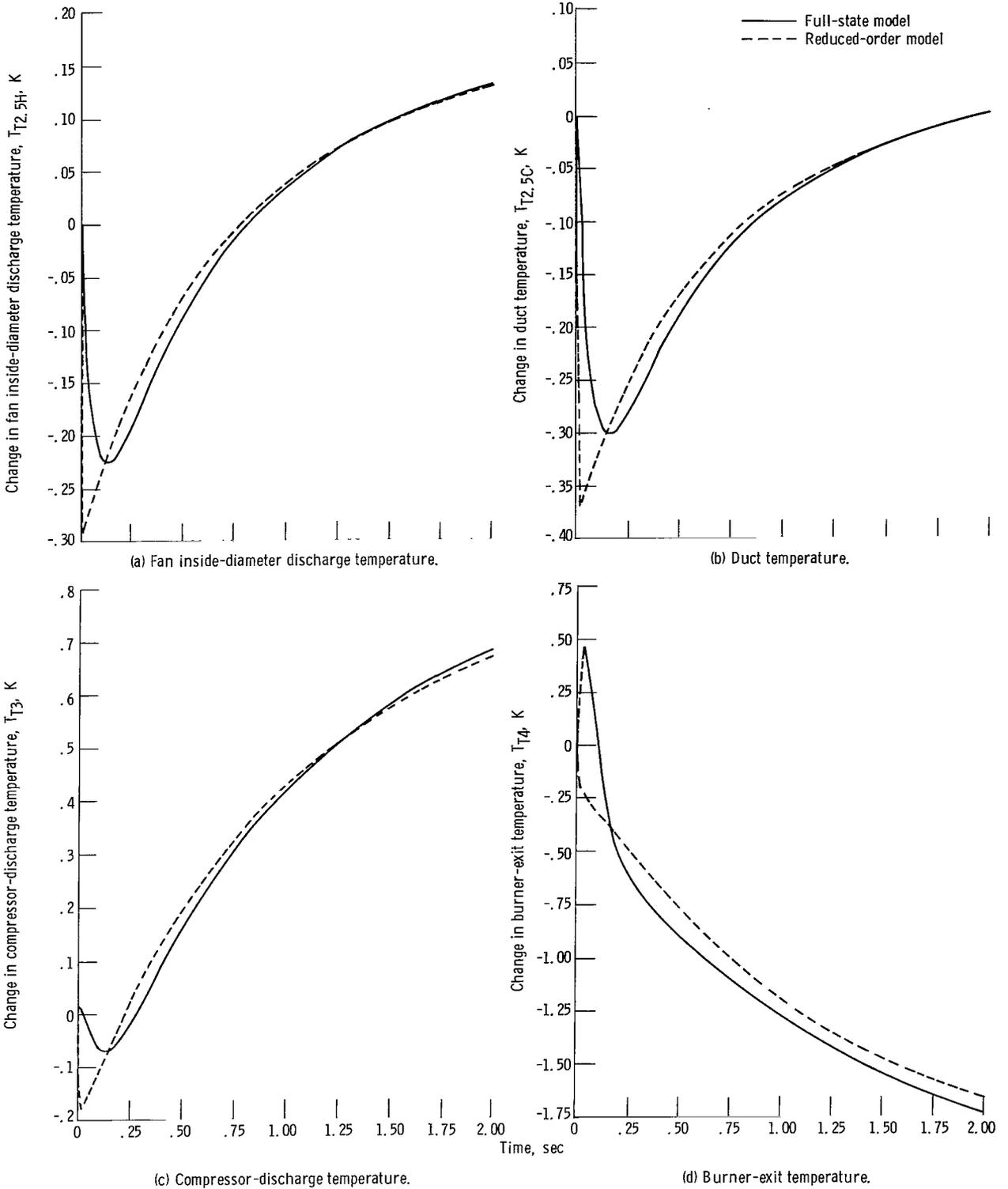
Figure 13. - Comparison of full-state and reduced-order (4th) linear-model responses to a +3 percent step in nozzle area; sea-level-static-idle operating point.

88
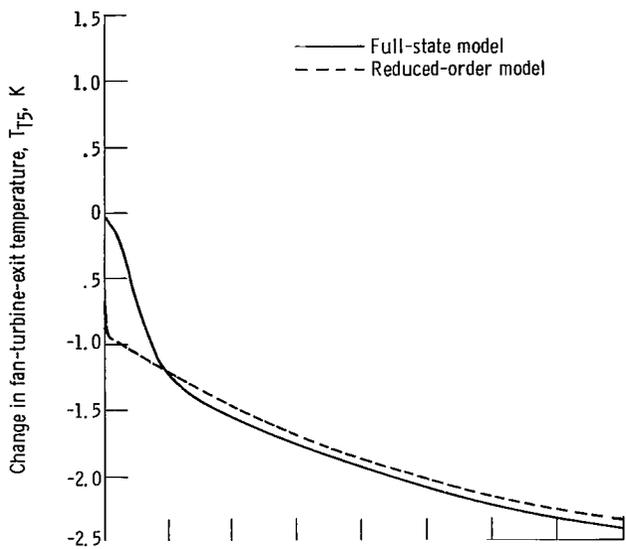
(e) Fan-turbine-exit temperature.

(f) Duct exit temperature.

(g) Exhaust-nozzle-inlet temperature.

(h) Total engine airflow.

Figure 13. – Continued.

89
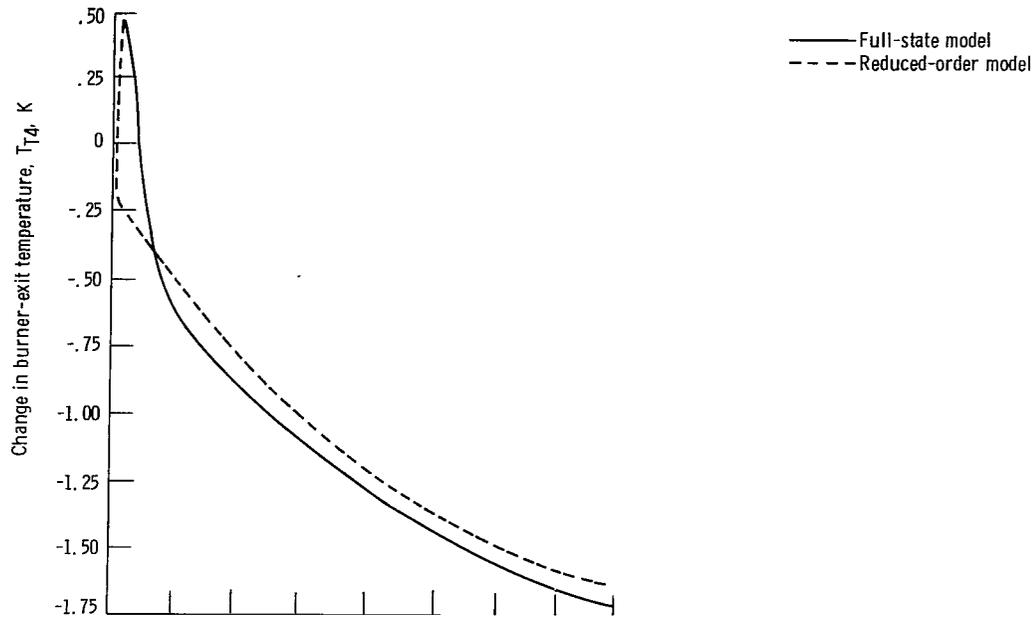
(i) Burner-exit temperature.

(j) Fan stall margin.

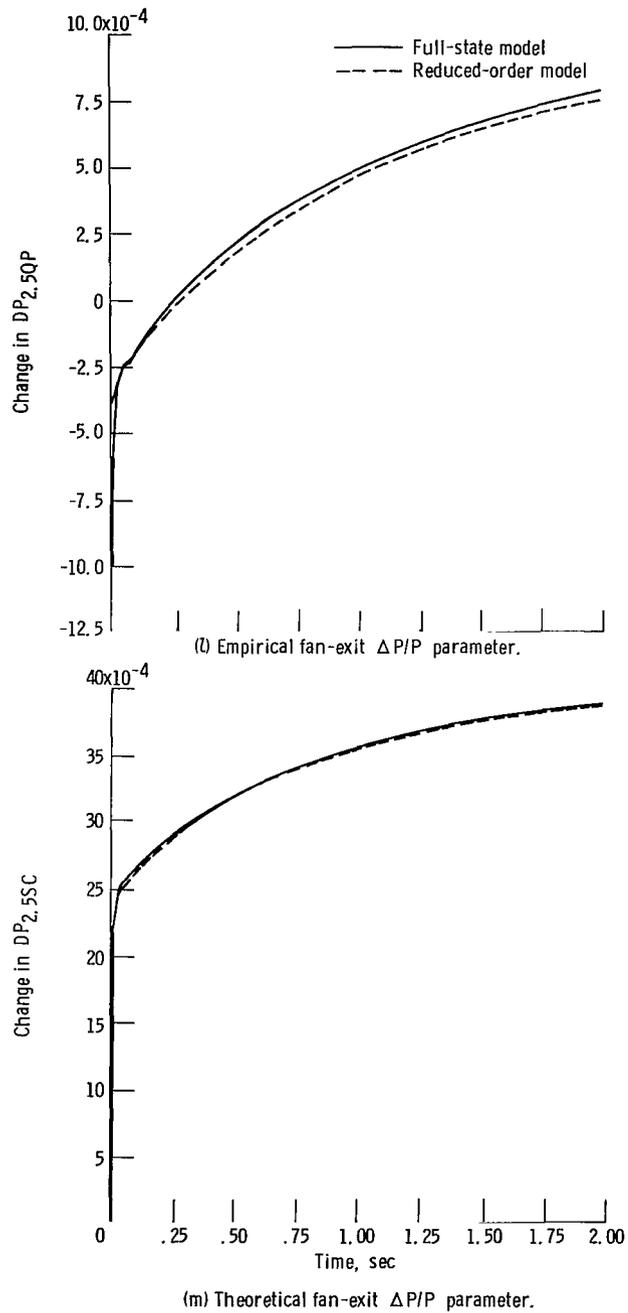(k) Compressor stall margin.

Figure 13. – Continued.

(l) Empirical fan-exit $\Delta P/P$ parameter.

(m) Theoretical fan-exit $\Delta P/P$ parameter.

Figure 13. – Concluded.

1. Report No. NASA TP-1388	2. Government Accession No.	3. Recipient's Catalog No.
4. Title and Subtitle GENERATION OF LINEAR DYNAMIC MODELS FROM A DIGITAL NONLINEAR SIMULATION		5. Report Date February 1979
		6. Performing Organization Code
7. Author(s) Carl J. Daniele and Susan M. Krosel		8. Performing Organization Report No. E-9490
		10. Work Unit No. 505-05
9. Performing Organization Name and Address National Aeronautics and Space Administration Lewis Research Center Cleveland, Ohio 44135		11. Contract or Grant No.
		13. Type of Report and Period Covered Technical Paper
12. Sponsoring Agency Name and Address National Aeronautics and Space Administration Washington, D.C. 20546		14. Sponsoring Agency Code

15. Supplementary Notes

16. Abstract

Presented are the results and methodology used to derive linear models from a nonlinear simulation. It is shown that averaged positive and negative perturbations in the state variables can reduce numerical errors in finite-difference, partial-derivative approximations and, in the control inputs, can better approximate the system response in both directions about the operating point. Both explicit and implicit formulations are addressed. Linear models are derived for the F100 engine, and comparisons of transients are made with the nonlinear simulation. The problem of startup transients in the nonlinear simulation in making these comparisons is addressed. Also, reduction of the linear models is investigated using the modal and normal techniques. Reduced-order models of the F100 are derived and compared with the full-state models.

17. Key Words (Suggested by Author(s)) Linearization Full state linear model F100 engine Reduced order model Startup transient	18. Distribution Statement Unclassified - unlimited STAR Category 01		
19. Security Classif. (of this report) Unclassified	20. Security Classif. (of this page) Unclassified	21. No. of Pages 94	22. Price* A05

```
   3    1 1U,A,          012779 S00903DS
DEPT OF THE AIR FORCE
AF WEAPONS LABORATORY
ATTN: TECHNICAL LIBRARY  (SUL)
KIRTLAND AFB NM 87117
```

NASA